CHALMERS
UNIVERSITY OF TECHNOLOGY

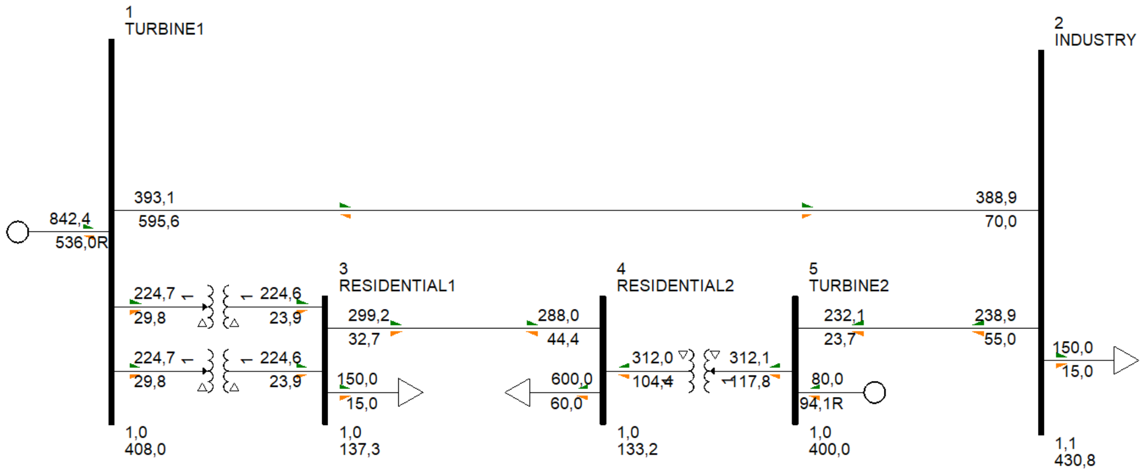

Integration of Electric Vehicles (EVs) in Future Renewable Energy Based Power Grid

Master Thesis in Electric Power Engineering

HAFIZ M ABU BAKAR KHAN
HAIDER ALI

Department of Energy and Environment
CHALMERS UNIVERSITY OF TECHNOLOGY
Gothenburg, Sweden 2020

MASTER THESIS 2020

Integration of Electric Vehicles (EVs) in Future Renewable Energy Based Power Grid

HAFIZ M ABU BAKAR KHAN
HAIDER ALI

CHALMERS
UNIVERSITY OF TECHNOLOGY

Department of Energy and Environment
Division of Electric Power Engineering
CHALMERS UNIVERSITY OF TECHNOLOGY
Gothenburg, Sweden 2020

Integration of Electric Vehicles (EVs) in Future Renewable Energy Based Power Grid

Examiner: Ola Carlson, Division of Electric Power Engineering

Master Thesis 2020
Department of Energy and Environment
Division of Electric Power Engineering
Chalmers University of Technology
SE-412 96 Gothenburg
Telephone +46 31 772 1000

Typeset in LaTeX
Printed by Chalmers Reproservice
Gothenburg, Sweden 2020

Integration of Electric Vehicles in Future Renewable Energy Based Power Grid
Department of Electric Power Engineering
Chalmers University of Technology

Abstract

The future Swedish Electric Power System (EPS) is expected to be based heavily on Renewable Energy Sources (RES) of electricity such as Hydro, Wind and Solar Energy. It is expected that by the year 2040 the Wind Turbines installed capacity will increase by $300 - 400\%$. But with the addition of number of Wind Turbines − based on Doubly-Fed Induction Generator − into the power system, the inertia of the system is expected to decrease, if simultaneously Nuclear Energy is *phased-out*, creating an issue of stability for the Electric Power System (EPS). It is also expected that the Electric Vehicle (EVs) will rise in the future with almost all the current combustion-engine based transport being replaced by Electric Vehicles (EVs). Due to this rise in e-mobility application and the diverse charging requirement of the Electric Vehicle (EVs) owners, it can overburden the Electric Power System and the energy balance will also be significantly affected, if not controlled through different charging strategies.

The aim of the thesis was the investigate whether the future Swedish Electric Power System (EPS) based on Renewable Energy Sources (RES) is able to have energy balance between supply and demand, as well as maintain stability during the transient conditions. Another aim was to develop some *Demand Side Management* techniques to integrate the Electric Vehicle (EVs) charging into the Electric Power System (EPS) based intermittent sources of electricity production.

The results indicated that for future Swedish Electric Power System (EPS), the hourly energy balance between demand and supply will have more mismatches due to high penetration of Wind in the system. The results indicated that in 2019, almost $24TWh$ was exported and $2TWh$ was imported to maintain the energy balance while it is expected that in future *Wind Scenario 2040*, the export of electricity will be reduced to $10TWh$ and a considerable increase in import of electricity of $16TWh$ will be required to maintain the energy balance. However, based on *Fast Fourier Transform (FFT)* analysis of electricity production from Wind in Sweden, indicates peak generation after every three-days and $24 - hrs$ intervals. Therefore diversified load such as Electric Vehicle (EVs) can be charged during these peaks to reduce the mismatch energy balance. The future Swedish Electric Power System (EPS) due to reduced inertia, will become less stable in terms of system frequency response, with higher frequency variations and reduced ability to recover frequency stability after large disturbances. It is expected for future Swedish Electric Power System (EPS), system frequency variations for hourly load variations will be increased to $\pm 1\%$, i.e. outside current *frequency deadband* of $\pm 0.2\%$ for primary frequency control. However with additional control algorithms for inertial support in Wind Turbines, there is huge potential to mitigate system frequency stability issues.

Acknowledgements

The authors would like to first and foremost thank their supervisor at Chalmers University of Technology, Ola Carlson for his kind guidance as well as offer gratitude to Hannes Hagmar and David Steen, at Chalmers University of Technology, for sharing with the authors of this thesis their ideas, data and ways to make this thesis a success.

The authors would like to show their utmost gratitude to God for showing the way and providing with all the blessings in this life and then also offer gratitude to their parents, brothers, sisters, friends and colleague for their continued support.

”Verily, to God we belong and to Him we shall return” (Quran 2:156)

Hafiz and Haider, Gothenburg, 2020

Contents

List of Figures

1
Introduction

The modern world is facing an ever increasing energy demands and it is one of the most important and critical challenge for this generation that needs to be solved efficiently. The challenge lies not only in meeting these growing energy needs but to meet them in a sustainable way. This implies the use of renewable energy resources to act as replacement for the fossil fuels currently dominating the energy markets. This implies also a revamping of the whole infrastructure that we have today whether it is the transportation sector or the electricity networks. As it has been concluded over the years that the use of fossil fuels to meet the energy needs affect the climate in general and the society and living being in particular; so the focus has been shifting towards finding sustainable ways to provide for the growing energy needs.

Several steps have been taken in the recent past decades such as government and corporations funding research into renewable energy as well as coming up with innovative policies to curb the emissions from the transportation sector and the electricity generation units. It has also been concluded from several studies that the temperature of the Earth is rising every year and that is affecting the glaciers which in turn making the sea level to rise, making it dangerous for the communities who have been living around water. It is also creating many social challenges for the governments, as the people who are being affected are migrating to other lands in order to sustain themselves thus making it difficult for local governments and countries to support them. A recent survey by United States Energy Information Administration reveals that the world's energy consumption will increase up to 56 percent in between time frame from 2010 until 2040 [1]. With the current types of fuels we are using and the future projections of the high consumption of energy would result in drastic increase in the emission of carbon dioxide and other greenhouses gases that ultimately will raise the temperature of Earth beyond the limits of 2 °C prescribed by the Paris Agreements [2].

One of the areas where there is a lot of potential to reduce the carbon emissions is the transportation sector. By electrifying the vehicles using energy storage batteries that are rechargeable will significantly reduce the emissions from the vehicles. In 2018, almost 5 million electric cars were sold to the customers with around half of them in China [3]. It is also estimated that the sales of rechargeable vehicles - or *Plug-In Hybrids* - will rise in the future due to many factors such as lower operating and maintenance costs; less fluctuation and cheap prices of the electricity [3].

Plug-in electric vehicles has many advantages over the conventional vehicles as mentioned earlier but the charging infrastructure for the vehicles needs more investment and development. Another area that demands more research is the charging station's interaction with the future power grid that is highly reliant on intermittent sources of energy such as wind and solar that depend on weather conditions. The electricity demand and supply must be equal at all the times. During the times of low generation from these sources and high demand from the user, a mismatch would be produced, making the power grid unreliable. Several techniques are being studied to tackle this such as Demand Side Management (DSM) that will be discussed in this thesis.

1.1 Background

While the renewable energy based power production technologies are cheap and produces no CO_2 emissions, it on the other hand poses some challenging task for the network. First is, being intermittent source of energy, meaning that the production depends on the weather condition. There is always an underlying need for a conventional power production available to support the network's electricity needs during the time of low production from electricity produced from *RES*. This underlines the importance Hydro or Fossil Fuel based technologies, which acts quickly to fill in the electricity need during Peak Load conditions. But a huge amount of addition of the renewable energy sources in the network will also have a downgrading effect, and may result into low inertia of the system against disturbances. A rotating mass adds inertia into the system, that help support the power grid during any disturbance in the system. Solar Energy has zero rotating mass while Wind Turbine inertia from its rotating mass is detached from the power system due to power electronic interface. Due to this, Wind Turbine can provide a very marginal support to the power system during the transients such as during under or over frequency events. Furthermore the cheapness of these resource may out compete the existing generating units resulting in costly generation of electricity in the peak loads.

Nowadays there is a rapid increase of plug in electric vehicle (EVs) i.e battery electric vehicles and plug in hybrid electric vehicles. A study reveals that in Norway the number of plug in hybrid electric vehicles was 4700 in year 2012. In 2020 the number was gone up to 200,000 which is expected to be more in the coming years [4]. So it is imperative that the power system based on renewable energy sources (RES) is able to support the charging of these electric vehicles. Due to the rise of plug-in electric vehicles (EVs) and other applications of electric power, the load is getting increasingly diversified. This diversified load can have its impact on such a weak system hence resulting in unfavourable cost and decreased system reliability. But with well planned control of charging the problem can be minimized.

1.2 Purpose

The purpose of this thesis mainly highlights and focuses on the impacts of charging of electrical vehicles (EVs) on the power systems in which renewable energy resources are the main contributors of power generation. The thesis is based on one of the future scenario of the Swedish Energy Agency (Energimyndigheten) where the nuclear plants will be phased out and the only contributors to the power production will be huge penetration of wind turbines combined with hydro power generation. It will focus on Demand Side Management for efficient charging of Electric Vehicles (EVs). The thesis will also focus on the stability of the power grid during the load variations and will delve into the question that whether a system based solely on renewable energy sources is able to support future load demand of the electricity network. A focus specifically focusing on voltage and frequency stability of power system will be studied in case of highly time diversified plug in hybrid vehicle (EVs) charging. For this purpose, PSS/E software tool will be used for the simulations of voltage and frequency stability. Some other important parameters for the wind turbines will also be looked at and a conclusion will be drawn based on the results.

1.3 Scope and Limitations

The thesis will be based on an imaginary 5-bus power system with one hydro power plant and a large amount of wind turbines modeled as a single wind turbine serving a balanced load. The load is also modeled as linear constant power load. All the non-linearities in the actual loads are not modeled in this thesis. Consequently, the effect of unbalanced and non-linear loads on the rotating machines such as temperature rise in the windings does not come under the scope of this thesis. That also means that it will not perfectly model how the power system will behave in its entirety as there are many components in the real power system that combine to produce a certain response. Secondly the transmission lines are modeled in a very simple way to simplify the analysis. The transmission lines are taken to be less than *80 km* and therefore are only limited by the thermal capacities and not limited by voltage drops along the line. As in the case of real power system, when the voltage drops at the bus, capacitor banks and other solution are used to boost up the voltage at the bus. But in this thesis, no solutions are used for this and the voltage drops are calculated on each bus without any implementation of boosting it to the nominal values.

1.4 Social, Ethical and Ecological Aspects

This thesis will take into consideration the sustainability and ethical aspect of solving the engineering problem being put forward. The sustainability aspect of designing the electric power network consists of investigating how the material, energy sources and different components will have its impact on the environment.

The aim of this thesis is to investigate how the electric vehicles are efficiently integrated into the future electricity network based on renewable energy sources. When it comes to the technologies used for the thesis, we have made use of hydro power plants and wind turbine. So for this case, no fossil fuel based technologies are being investigated. This will help in better understanding the sustainable technologies of the future and therefore the thesis is helpful in terms of ethical aspect. Also the goal of this thesis is the optimum utilization of the energy and promoting the use of wind turbines, therefore an analysis regarding the efficient use of the available turbines will lead to less mining of iron and copper used as primary materials used in the manufacturing of wind turbines. The thesis uses Doubly-Fed Induction Generator ($DFIG$) wind turbines which does not use any rare earth material during its manufacturing like in the case of permanent magnet based synchronous machines. With the maximum utilization of energy from the wind turbines using Demand Side Management techniques, briefly touched in this thesis, there will be a efficient use of energy during peak demand and therefore less fossil fuel based power generation, with quick response, will be used. This will help in reducing the greenhouse gas emissions and will demotivate the use of fossil fuels based technologies.

There are two basic ethical codes being set by IEEE.

1) The first code of ethics is ‘To be honest and realistic in stating claims or estimates based on available data‘. In order to report this aspect a detailed research has to be carried out on the behaviour of grid when electric vehicles will be charged and any negative effect will be presented without any hesitation, so as to honestly report the benefits as well as the technical problem that may arise during its integration.

2) The second code of ethics is to ‘Improve the understanding of technology, its appropriate application, and potential consequences’. Before designing the grid, a detailed research will be carried out regrading the technology. In this way a better understanding of the grid model will be achieved and it will give the chance to know what to change and how to improve the model later.

The production and consumption of electricity may lead to environmental impacts which should be kept in consideration while making decisions and before making any new energy policy. The key to moving towards sustainable energy developments lies in finding the balance between the environmental, economic and social goals of society and integrating them efficiently at the earliest stage of project planning, program development and policy making.

2

Background

2.1 Renewable Energy Sources (RES)

Renewable sources of energy are defined as the sources that is naturally replenishing, inexhaustible in duration but limited in flow of energy per unit time. Using renewable sources, there are no harmful emissions produced during the process of electricity generation. Every year new technologies are being researched by universities and companies around the world and relatively more mature technologies such as Solar Energy, Wind Turbines, are continuously being refined. Due to this the capital cost for the infrastructure as well as electricity price per unit MWh are continuously decreasing.

Besides that, an investment into the RES can be financially beneficial for individuals as well as countries. For a private individual, the excess electricity produced during low consumption at home, can be sold to the national grid. Similarly, if the power system between the countries and regions are interconnected through transmission lines, excess electricity can be sold to other countries during high production. While during high consumption and peak demand, electricity from other regions and countries can be imported. There is a huge potential for the collaboration between countries and regions to come together to produce clean and carbon-free electricity. Some of the various sources of electricity generation from renewable sources available today are mentioned below.

- Solar Plants
- Hydro Plants
- Wind Turbines
- Geothermal Plants

Compared to clean electricity generation technologies listed above, other conventional fossil fuel based energy produces a lot of emissions. In the process of coal fired power plants, the overall emissions of CO_2 combining the emission from combustion of fuel and emission during manufacturing of equipment; it sums up to a substantial level in the range of 943g-CO2/kWh [5].

Figure 2.1 shows various type of generation technologies and its respective emissions

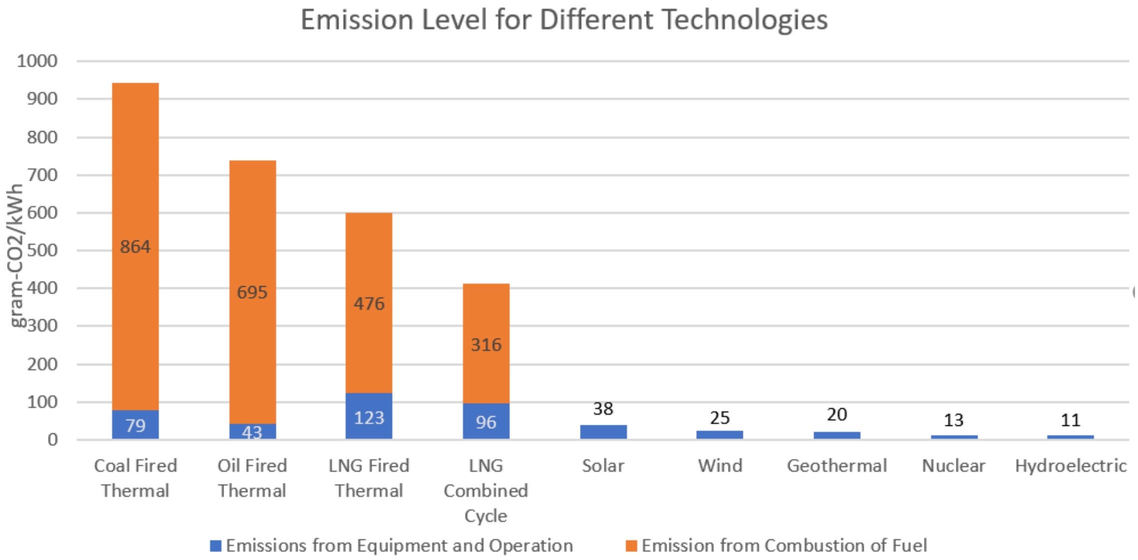

Figure 2.1: Emission Of Carbon Dioxide per kWh of Consumption [5]

2.2 Current And Future RES Trends in the World

In order to get a perspective on how much the renewable energy sources (RES) contribute towards meeting the energy demand of the world, it is necessary to look at the overall picture. As of 2017, according to the gathered data, the total world energy demand stands around a staggering *150,000 TWh*. In order to meet the demands; coal, oil and natural gas are the three most used sources of energy. The Figure 2.2 shows this, based on the report by BP Statistical Review of World Energy [6].

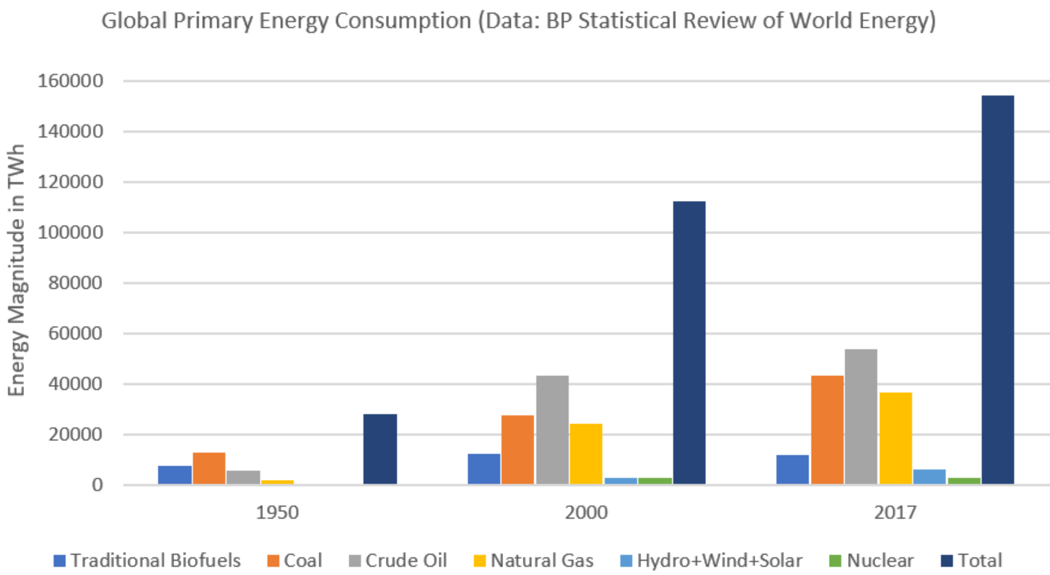

Figure 2.2: Global Energy Consumption, 2017

As it can be seen in Figure 2.2 that major contributors to meet the energy demands are coal, crude oil and natural gas while contribution from other sources such as bio-fuels, nuclear, hydro, wind and solar are minimal. Although there has been a continuous increase towards the investments in solar and wind energy in the recent decades, but it is minute compared to increase in fossil fuel based energy. This is an alarming situation that demands more investments towards the renewable energy sources (RES), if we are to fight the climate change and reduce the emissions and greenhouse gases. As it can be seen in the Figure 2.3, since the turn of *20th* Century, the total greenhouse and CO_2 emissions are increasing at a fast pace and average Earth temperature is following the same trend shown in Figure 2.4 below [7].

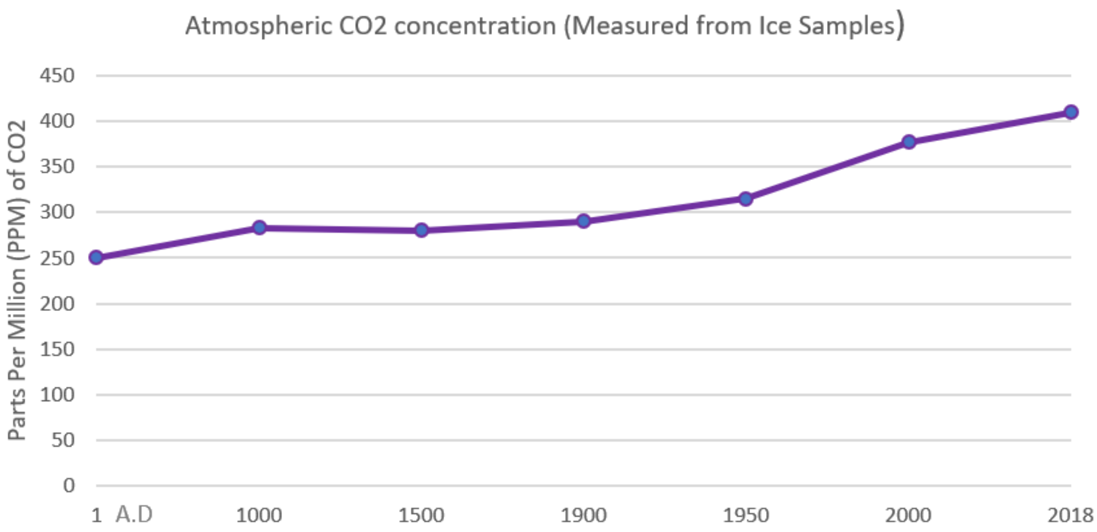

Figure 2.3: Greenhouse and CO_2 Emissions, A Historical Data

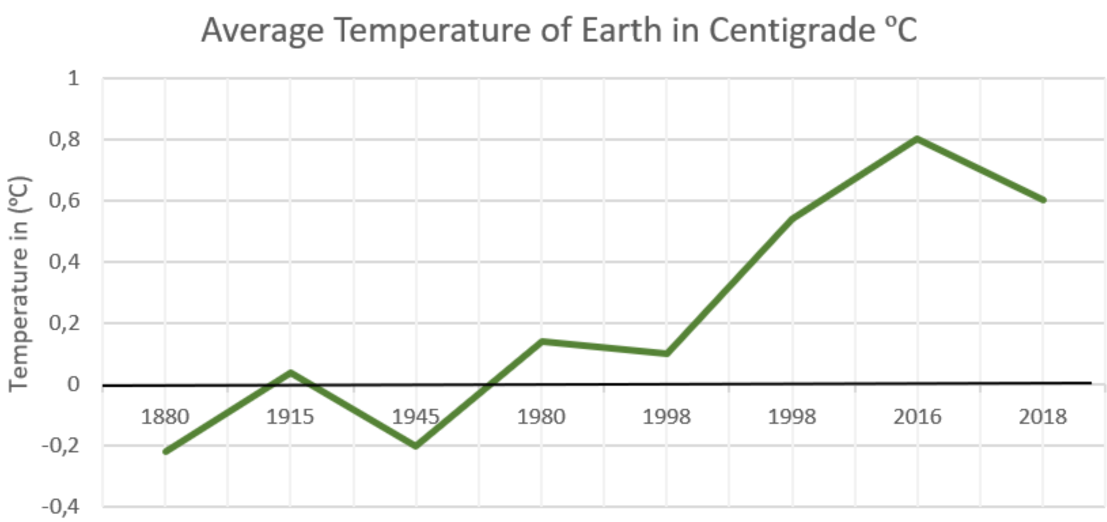

Figure 2.4: Average Temperature of the Earth

Currently at least 30 nations around the world have renewable energy contributing more the 20 percent of energy supply, the latest survey in 2017 accounted that renewable technologies amounted to more than 279.8 billion US dollars [9]. With large contribution from China, worth of 126.6 billion US dollars making it the largest investor of the renewable technologies with 45 percent of the global investment, these renewable energy sources are often large scale energy projects and many rural and under developed countries gets nourished with the benefits available from these technologies in the market [10].

Based on the predicted scenarios for the future energy mix, more investment will be made in the energy sources which has less impact on the environment and has less carbon footprint, such as natural gas. There are many justifications for natural gas to surge nearly 50%, mainly due to the cheap shale gas production as well as providing flexibility to the grid owner during peak loads. It is also expected that most countries around the world will phase out the nuclear plants while investing more in the renewable based energy sources such as wind turbines, hydro power plants and solar energy. It is expected that in future, the renewable energy sources will be the biggest contributors of electricity production when combined, with solar energy taking the lead and crossing the coal and gas in terms of electricity supply. The Figure 2.5 is taken from International Energy Agency (IEA) World Energy Outlook 2019 report and looks at the future power mix based on the Stated Policies 2040 [11].

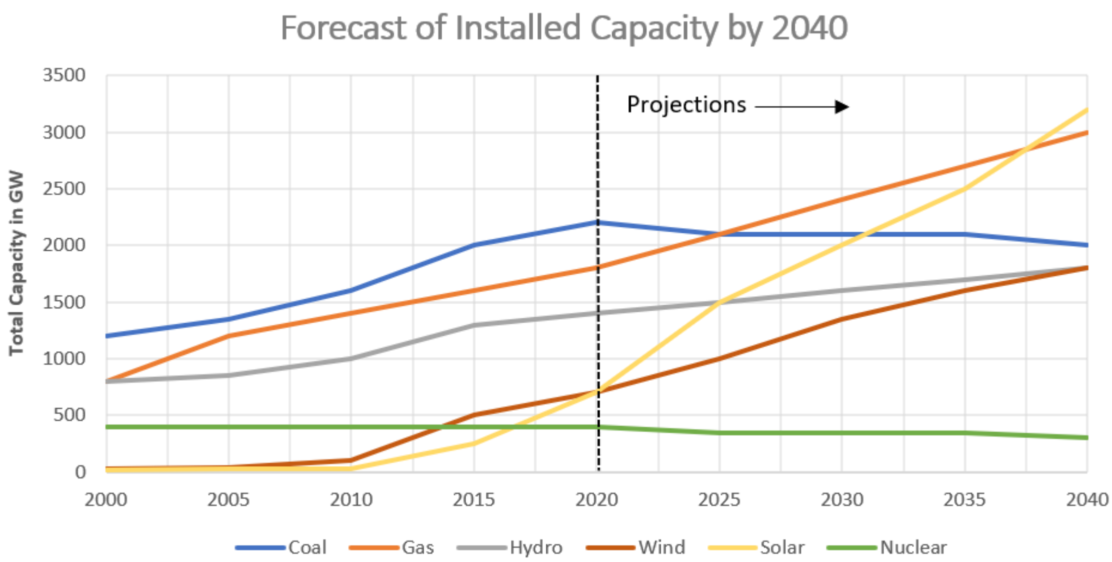

Figure 2.5: World Energy Outlook Report 2019

As it can be seen in the Figure 2.5, the future grid will have a lot of renewable energy based electricity supply. This will without a doubt, reduce the impact on the environment in terms of carbon emissions and greenhouse gases but will also come with its own perils. As renewable sources such as wind and solar are intermittent sources of electricity, so there is always a need to manage the demand and supply at all time. Different Demand Side Management are being studied around the world currently. Besides this, solar and wind turbines in its most basic form does not have a stable inertial support for the Electric Power System (EPS). Therefore many techniques are currently being discussed such as battery storage to support system frequency dips, synthetic inertia; that use power electronics and control schemes to help in maintaining the inertia in the system by improving system frequency lowest value during frequency dip − commonly known as *nadir* − as well as improving the rate of change of frequency (ROCOF).

2.3 Current RES Trend in Sweden

The Swedish Electric Power System (EPS) has one of the least dependence on fossil fuels for the generation of electricity to meet the demands of its end-user consumption by industrial and residential sector. In 2019, a total of $165TWh$ of electricity was supplied, including the transmission and distribution losses, which accounts for the consumption of $139TWh$ by the end-user [12]. The rest of electricity was exported to neighbouring countries. The major source of electricity supply in TWh comes from Hydro Power, Nuclear Energy and Wind Turbines. The Figure 2.6 shows the share of electricity production from different technologies [13]. As it can be seen, a combined total of 50% electricity was generated from renewable sources of energy, *vis-a-vis*, Wind Turbines and Hydro Power Plants.

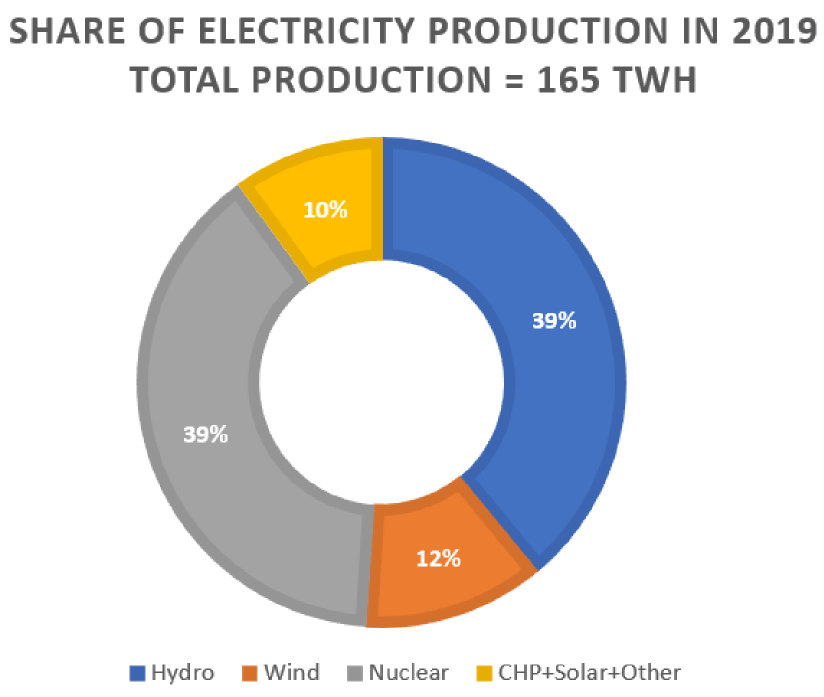

Figure 2.6: Electricity Production in TWh of Different Technologies in 2019 Based on data from Swedish Energy Agency [12]

At present, there is a diverse portfolio of generation technologies available in Sweden. Ranging from Nuclear Power Plants to Combined Heat and Power to Solar Energy and Gas Turbines. In the North of Sweden, many hydro power plants are situated and most of the load is naturally in the South of Sweden having more industries and higher population density. The Figure 2.7 gives an estimate of different technologies as installed capacity currently available for the production of electricity in Sweden and the total capacity amounts up to $40GW$.

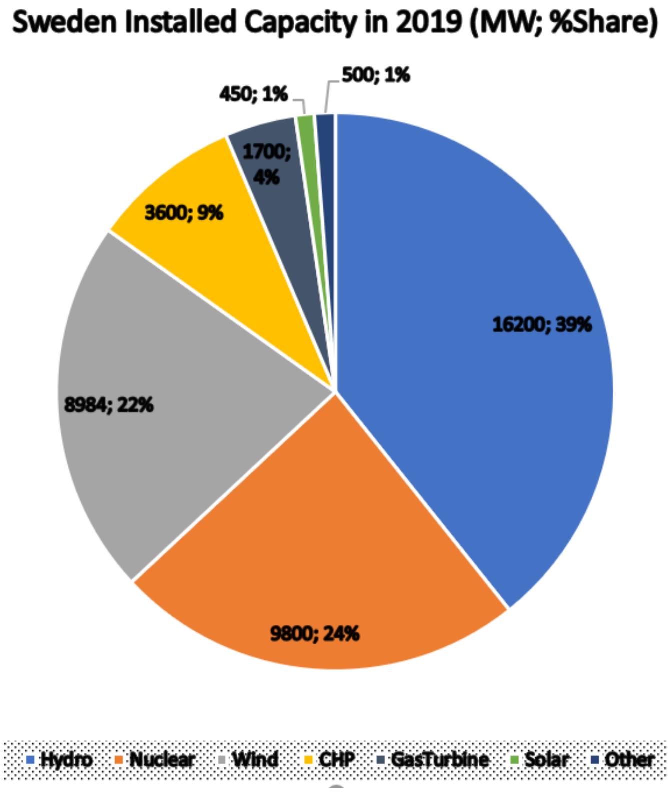

Figure 2.7: Installed Capacity of Different Technologies in Sweden, Total Installed Capacity, $40GW$

2.3.1 Hourly Energy Balance In 2019

The electricity generation and consumption data for the year 2019 taken from *Svenska Kraftnät* or SvK, shown in Figure 2.8, suggested a power system that was sufficient to provide for the national consumption of electricity but also had a high export of electricity to other countries. This high export can be attributed to a relatively high wind energy production during the year when the load demand is less compared to the total electricity generated from all the available technologies. Some of these electricity production technologies, such as Nuclear Power Plants having high cycling cost, are therefore not disconnected from the power system during short-lived demand dips, and therefore becomes a facilitator in the export of electricity. Cycling cost refers to the cost of operation of electric generating units at varying load levels, including on/off, load following, and minimum load operation, in response to changes in system load requirements [14].

In the Figure 2.8, it can also be seen that there is a very high mismatch of generation and consumption during the months of summer. This can better understood from the Figure 2.9, where hourly electricity generation of different technologies is shown. The total generation is very high compared to the total consumption, especially during the hours *3690h - 4230h*, which comes during the months of May and June. As can be noted during these months, the Nuclear Power Plants were running at their maximum capacities in order to make up for the low generation from the Hydro Power Plants. This can be explained due less precipitation of rain in the months of May and June in 2019 and therefore less generation from Hydro Power Plants [15].

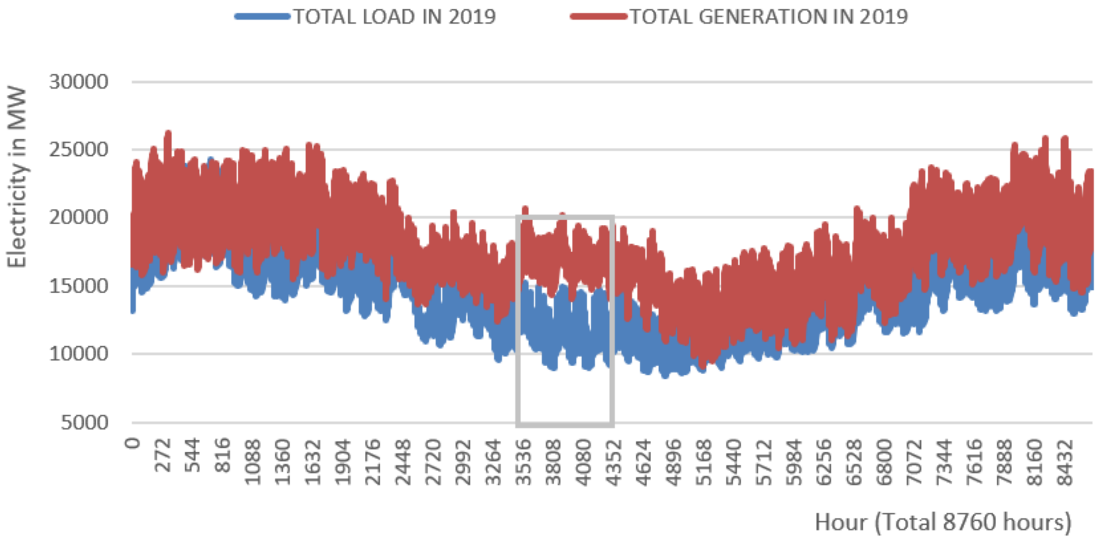

Figure 2.8: Total Generation and Load Consumption, 2019

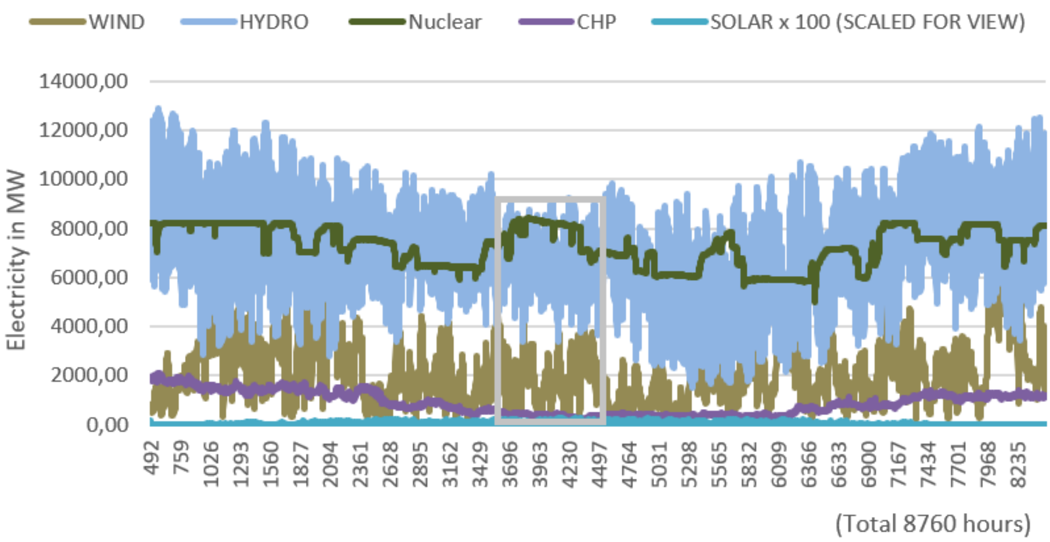

Figure 2.9: Electricity Generation from Different Technologies, 2019

2.3.2 Hourly Trade of Electricity in 2019

The Figure 2.10 shows the exported and imported electricity for the year 2019 according to SvK. As it can be seen that for most of the time, electricity has been exported, most notably with Norway and Denmark and for only few occasions, electricity was imported, most notably from Norway and Finland [16]. The high export to other countries, is due to the high capacity factor of Nuclear Power Plants as well as high electrical generated from the Wind Turbines, equivalent to 12% of total generation or $20TWh$, based on the data mentioned in Figure 2.6.

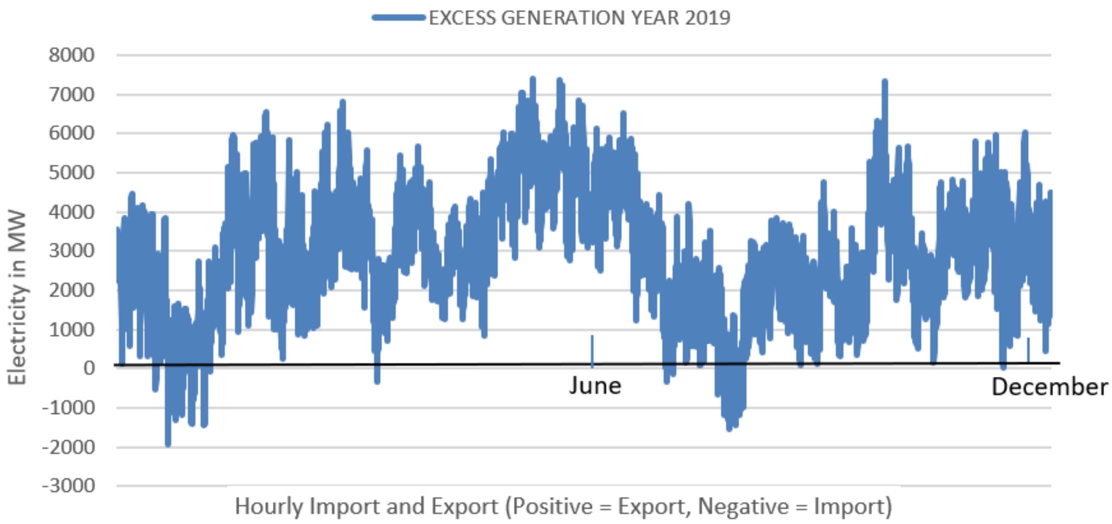

Figure 2.10: Excess Generation in Sweden, Import and Export in 2019

2.4 Future RES Trend in Sweden

According to Swedish Energy Agency's 2030 goals, share of renewable energy shall be at least 32% of the total energy use and 14% of the energy supplied to the transport sector shall come from renewable source [13]. The 2040 goals are even more demanding, with share of renewable to be 100% for the total electricity consumption [13]. In order to achieve the targets of having all the electricity generated from renewable in the future, large investments are being done in the renewable energy sector. In the recent decades, the wind energy share in the Swedish national grid is increasing with an average of of 10% *year-on-year* increase for the installed capacity. The investment in Wind Energy in Sweden is the biggest compared to the other renewable technologies such as Solar Energy. This is due to the geographical location of Sweden, which has more potential for wind energy compared to the solar energy, based on current technology available in the market.

2.4.1 Wind Energy Increase, A Forecast

The Figure 2.11 is taken from the forecast data published by *Svensk Vindenergi*, or the Swedish Wind Association, that predicts the potential increase in wind capacity until 2040. As shown, according to the estimates by Swedish Wind Association, the investment in the Wind Energy will lead to almost $45TWh$ of electricity added into the Swedish national grid by 2023 and a substantial $100TWh$ by 2040 [18]. This will lead to a power system heavily dominated by Hydro Power Plants and Wind Turbines. However, it is not the only likely scenario that can happen in future, there are various other scenario that are currently being debated at large by the public and private institutions in Sweden.

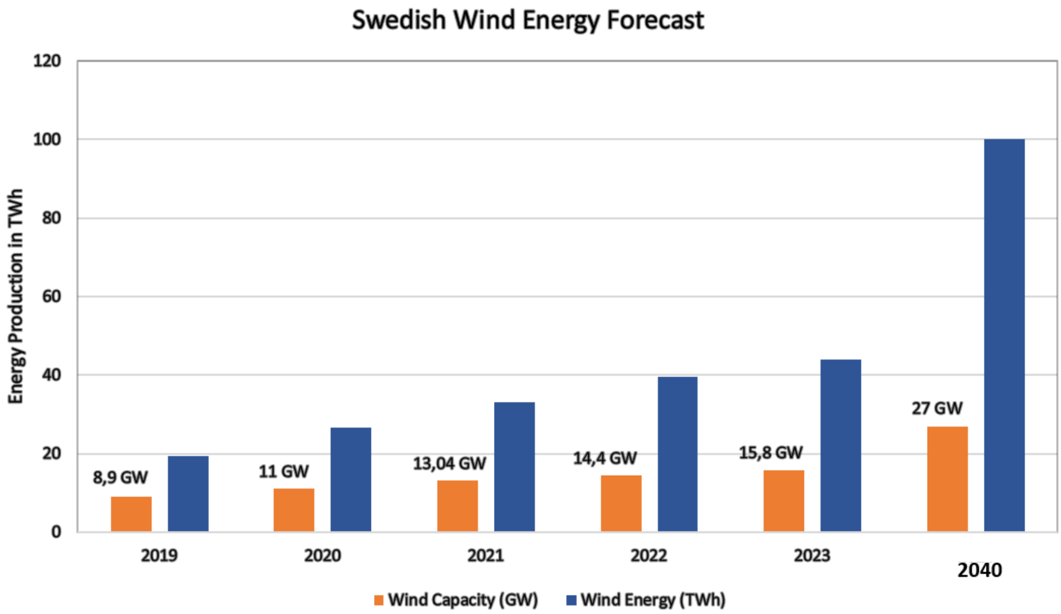

Figure 2.11: Predicted Wind Capacity and Energy Increase, Swedish Energy Agency [17]

2.4.2 Three Different Energy Scenarios, A Forecast

According to the estimates and predictions, the future Swedish power system is moving towards being heavily based on the renewable energy. The Figure 2.12 shows three different future scenarios based on the report by *Energimyndigheten*, the Swedish Energy Agency [19]. It shows that by the year 2040, Nuclear Power Plants will be completely *phased-out* from the Swedish power system and its vacant position will be filled by either one of the three technologies, *vis-a-vis*, Wind, Solar or Combined Heat and Power (CHP). These scenarios are drawn by Swedish Energy Agency based on current and predicted future trends, current research focus in different technologies as well as the possible political choices.

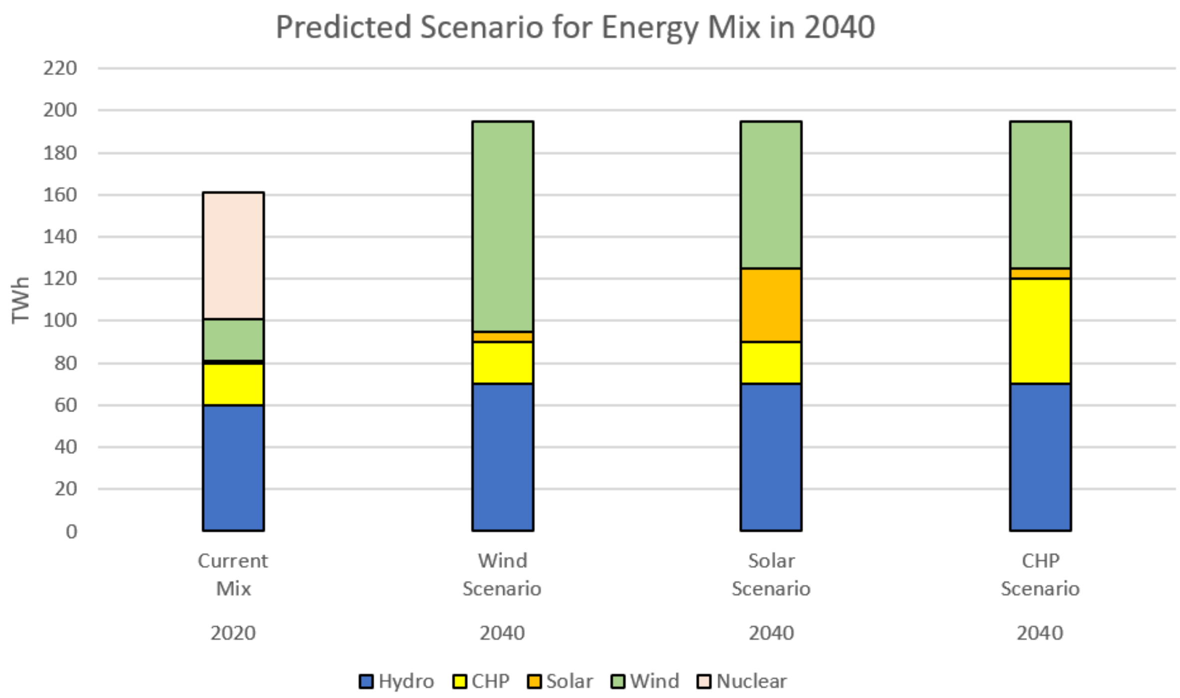

Figure 2.12: Four Predicted Energy Production Scenario in 2040

Besides these three scenarios laid down by Swedish Energy Agency for 2040, there is an equal chance of Nuclear Power Plants still being kept into the system. This is due to the current legislation, that older Nuclear Power Plants are to be replaced with next generation nuclear power plant technologies in the future, that has increased safety of operation and more environment friendly. Based on the Figure 2.12 and the conclusions drawn from the Figure 2.11, the most likely scenario that can happen is the *Wind Scenario 2040*, and will be the only scenario that comes under scope of this thesis, where maximum $100TWh$ of the electricity will be generated from Wind and the remaining from the Hydro Power Plants, Solar and CHP combined with import from other countries.

2.4.3 Energy Balance Analysis of Wind Scenario 2040

Based on the hourly electricity generation and consumption data from SvK in 2019 shown in Figure 2.8, it is possible to perform a very basic simulation for the power system energy balance in 2040. In the following analysis, certain assumption have been made. The hourly generation and consumption data in MW for 2019 as shown in Figure 2.8 and Figure 2.9 is used and multiplied by a scaling-factor and the results are plotted in Figure 2.15 and 2.14. Based on *Wind Scenario 2040* and the conclusions from Figure 2.11 and Figure 2.12, scaling factors as shown in Figure 2.13 are used and shown in a graphical form. It can be noted that in 2040, it is assumed that Nuclear Power Plants will be completely *phased-out* from the power system. Wind installed capacity will be increased three-folds, while other technologies will change with only a marginal increase of $10 - 20\%$ and load is assumed to have increased by 10% by 2040.

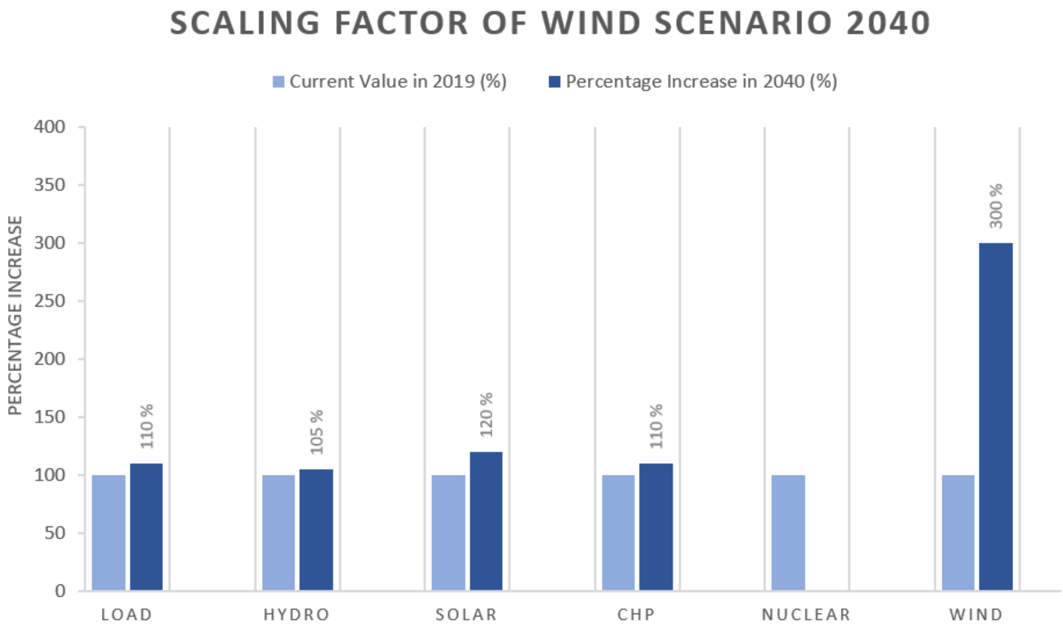

Figure 2.13: Scaling Factor Based on Wind Scenario 2040

In the analysis it is also assumed that in 2040, the month-wise precipitation in *mm* is exactly similar as in 2019 and the Hydro Power Plants are turned on and off to generate electricity at exactly the same instants and only the total installed capacity of Hydro Power Plants is scaled by 5%. Also it is assumed that the wind speed received by all the available Wind Turbines in 2040 has exactly similar pattern in time and magnitude as in 2019 and only the total installed capacity of Wind Turbine is scaled by 300%. It should be noted that no other additional factors are included in the energy balance analysis besides the scaling factor implementation and therefore results are very rudimentary in nature and conclusions drawn from the results are cautious and conservative in nature.

2.4.4 Hourly Energy Balance in 2040, A Forecast

Based on the Figures 2.15 and 2.14, it can be noted that the total electricity production from all the available technologies has a lot of variations. At some instants, there is a very high production of electricity compared to the load, while at other times, the production falls short of the total consumption. The total electricity production falling short of the total demand is seen to be more frequent. When compared with Figure 2.8, the power system in 2019 is more stabilized by a constant source of electricity generated by Nuclear Energy. However in *Wind Scenario 2040*, the power system becomes more dependent on the availability of wind received in 2040. This is based on the assumption that the wind has similar pattern in time and magnitude as it was in 2019. It is also worth-mentioning that the wind has high energy during winter months compared to the summer months.

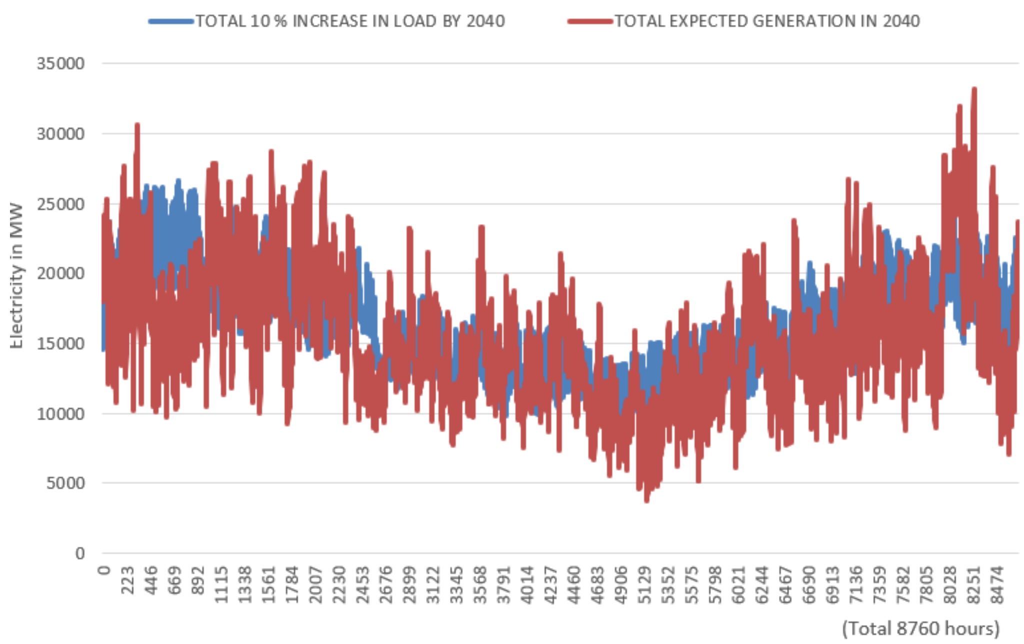

Figure 2.14: Total Expected Generation and Load Consumption, 2040

As can be noted earlier, due to less electricity generation from wind the the warmer months, there is however an opportunity for Solar Energy to fill the position of supply a sustained source of electricity. Due to longer summer days in Sweden and higher energy density of sunshine in the warmer months, there is a huge potential to invest in the Solar Energy to increase the installed capacity. In the *Wind Scenario 2040*, only 20% increase in electricity from Solar Energy is implemented as shown in Figure 2.13. However, with a similar 300% increase in installed capacity of Solar Panels, the total electricity production during the warmer months can be significantly increased.

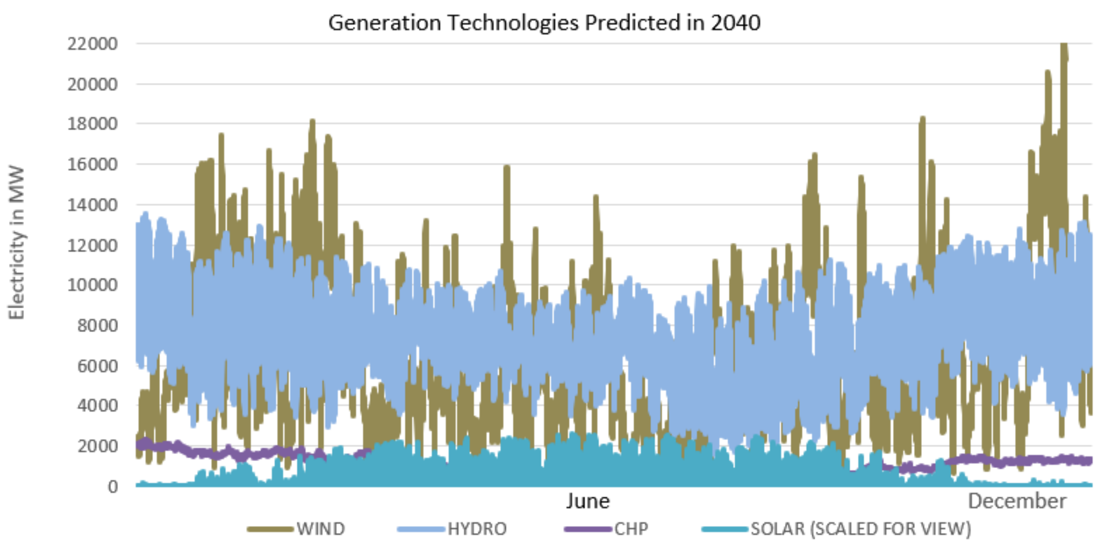

Figure 2.15: Electricity Expected Generation from Different Technologies, 2040

2.4.5 Hourly Electricity Trade in 2040, A Forecast

However, at times when production is very high compared to the load, the additional electricity is exported to other countries. The Figure 2.16 shows the expected trade of electricity to neighbouring countries. As it can be noted, there is a high import dependency. But at the same time the maximum hourly peaks of around $10,000MW$ is seen and comparing to Figure 2.10 from 2019, where it was around $7000MW$. Due to many occasion where the total electricity generated is lower than the demand, it will lead to a many instance of under-frequency of the power, if import is not available. As the Nuclear Power Plants will be *phased-out* from the system, that will reduce the inertia of the system, leading to unstable power system, that will be discussed in detail in the later chapters.

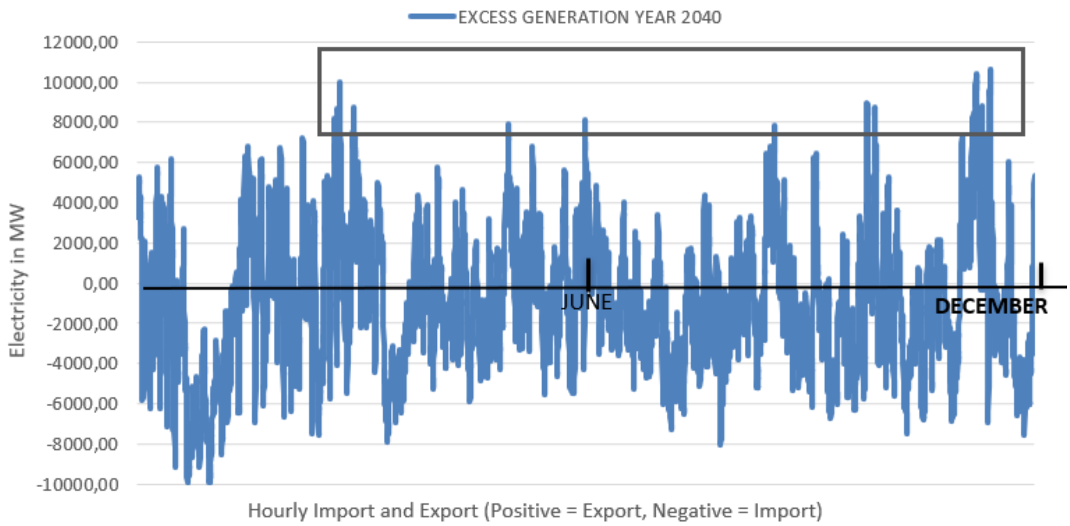

Figure 2.16: Expected Excess Generation in Sweden, Import and Export in 2040

2.5 Correlation of Export with Generation Technologies

In order to analyze which technology has the most effect on the export of electricity, it is possible to use *Pearsons Coefficient* to calculate the dependence of export of electricity with each individual technology. In simpler terms, it means to calculate when electricity generation is higher than the demand and exported to neighbouring countries, which of generation technologies are producing more electricity and connected to the power system and which of generation technologies are producing less electricity or *turned-off*.

Pearson Product-Moment Correlation Coefficient can be calculated using $MATLAB$ and it is a measure of the linear correlation between two variables or data series A and B in the Figure 2.17 shown below. According to the *Cauchy–Schwarz* inequality it has a value between $\rho = +1$ and $\rho = -1$

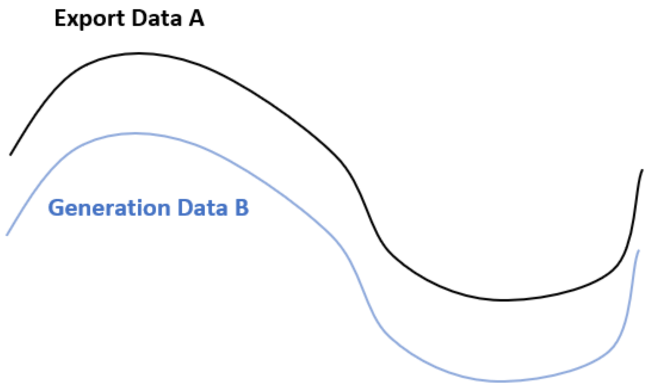

Figure 2.17: Correlation Coefficient Between Two Signal Series A and B

$$\rho(A,B) = \frac{1}{N-1}\sum_{i=1}^{N=8760}\left(\frac{A_i-\mu_A}{\sigma_A}\right)\left(\frac{B_i-\mu_B}{\sigma_B}\right) \tag{2.1}$$

where, ρ is correlation coefficient between A and B, μ_A and μ_B is the mean value of the data series A and B respectively and σ_A and σ_B is the standard deviation for A and B respectively.

- $\rho = +1$ is highest positive linear correlation which means two signals are exactly similar in shape and when one increases the other increases as well
- $\rho = 0$ is no linear correlation and there is no relation between two signals
- $\rho = -1$ is highest negative linear correlation which means two signals are exactly similar in shape but when one increases the other decreases similarly in strength

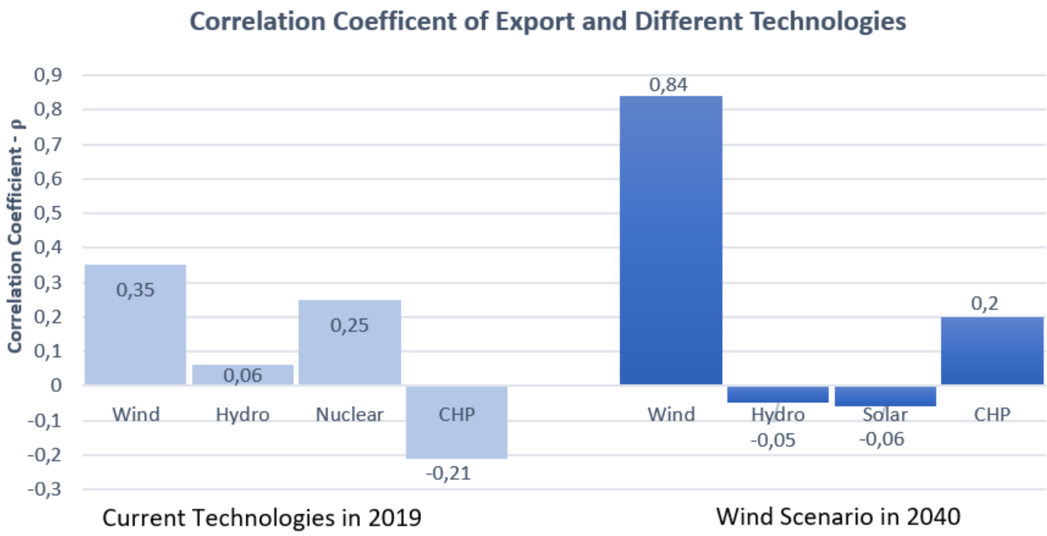

Figure 2.18: Correlation Coefficient of Export and Technologies

2.5.1 Correlation Coefficient in 2019

As can be noted from the above Figure 2.18 that in 2019, the export of electricity to neighbouring countries has a stronger correlation with electricity generation from Wind and Nuclear Power Plants, with its correlation of electricity generated from Wind being highest, equal to $\rho = 0.35$. Export has lower dependence on electricity generation from Hydro Power Plants due to a relatively dry summer in 2019 and water was saved only for supplying electricity during peak demand. It also explains that during the months of May and June, around $3690h - 4360h$, export is at its highest due to Nuclear Power Plants running close to it maximum capacity. Similarly it can be noted that in 2019 the exported electricity and CHP has an negative correlation. When electricity is exported to other countries increases, the electricity generated from CHP reduces and CHP are *turned-off* and disconnected from power system to save the bio-fuels.

2.5.2 Correlation Coefficient in 2040

Based on Figure 2.18, it can be concluded that the export of electricity will be heavily dependent on the electricity generated from only Wind as $\rho = 0.84 \approx 1$, where $\rho = 0.84$ means almost similar shape of curves for export and electricity generation from Wind. Based on the analysis, there is almost no correlation between the generation of electricity from Solar Energy and Hydro Power Plants as for both $\rho \approx 0$. In conclusion, it can be said that in 2040 when the electricity generated from Wind is high, the export will also be high. Due to a high dependence of exports of electricity on the variation of wind, it is also possible to use this additional information about the correlation of excess electricity production and subsequent export and the electricity generation from Wind, for the purpose of scheduling the charging of the Electric Vehicles (EVs) only during the high wind conditions. This subject will be discussed in detail in the subsequent chapters.

2.6 Total Additional Energy to Export in 2019 and 2040

The total exported electricity during peak production can also be used for Pumped Hydro Storage or battery storage to support the power system instead during peak demand, instead of importing the electricity from other countries. As discussed earlier, the exported electricity can also be used for charging the Electric Vehicles (EVs) to fulfil the Swedish Energy Agency goals of supplying $15\% - 30\%$ of the total energy consumption by transport sector from the renewable energy. The charging of Electric Vehicles (EVs) based on weekly and daily peaks of electricity generated from Wind Turbines will be discussed in the subsequent chapters. But here, it is possible to calculate total available electricity to export in 2019 and 2040

$$E_{\text{exported}} = \sum_{i=1}^{n=8760} (x_i \times h) \qquad \text{if and only if, } x \in x_+ \tag{2.2}$$

$$E_{\text{imported}} = \sum_{i=1}^{n=8760} (x_i \times h) \qquad \text{if and only if, } x \in x_- \tag{2.3}$$

In the Equations (2.2) and (2.3), h is *1-hour* interval, x_+ represent only positive integers i.e. export in MW for Figure 2.10 and Figure 2.16 and x_- represent only negative integers i.e. import in MW for Figure 2.10 and Figure 2.16.

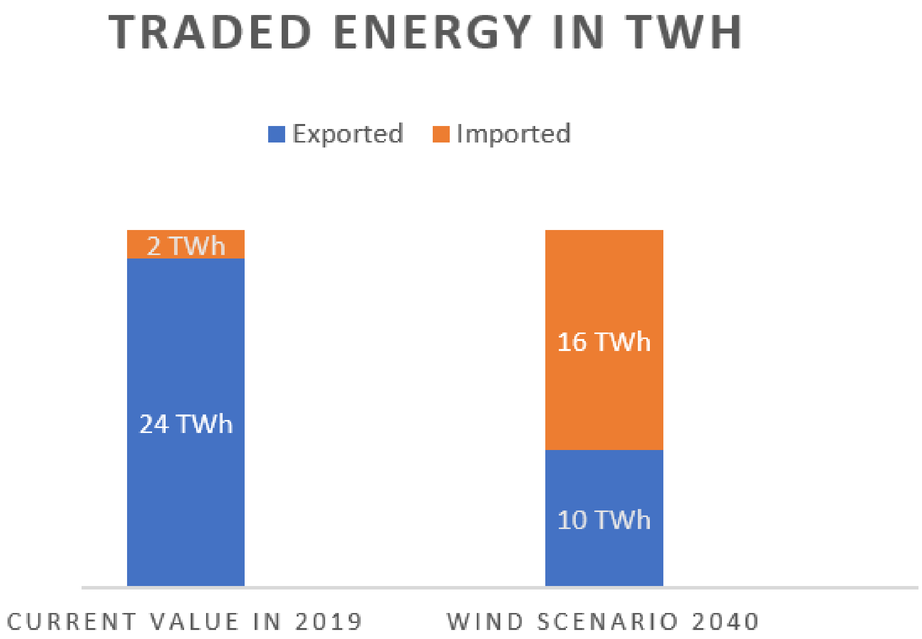

Figure 2.19: Imported and Exported Energy in 2019 and Wind Scenario 2040

Based on the earlier assumptions and analysis, the power system achieves a near 100% renewable electricity generation in 2040 but makes the power system more dependent on the import. In this case, almost $16TWh$ in 2040 is imported from neighbouring countries to fulfil the electricity demand compared to only $2TWh$ in 2019. And there is a possibility to export or use for storage purposes of only $10TWh$ in 2040 compared to a substantial $24TWh$ that was exported in 2019. This generates a *corollary* based on the analysis, that power system in 2019 is in a better position to carry additional load from PEVs to charge with $24TWh$ than for *Wind Scenario 2040* when only $10TWh$ is available to either supply for additional demand of electricity for PEVs charging or exporting to other countries. Using $MATLAB$, it can be calculated for how many hours $x \in x_+$ and electricity was exported to other countries. The results are shown below.

$$\text{Total Export Hours in 2019} = 8497h \tag{2.4}$$

$$\text{Total Export Hours in 2040} = 3227h \tag{2.5}$$

2.7 Vehicles Different Drivetrain Variations

There are various types of vehicles currently in the market today. It range from a ICE (Internal Combustion Engine) to a Mild Hybrid and from Full Battery Electric Vehicles to a Plug-In Battery Electric Vehicles. Due to the environmental and fuel price fluctuation concerns, consumer demand is shifting toward either Hybrid Electric Vehicles or Full Electric Vehicles. But the major concern regarding the Electric Vehicles are range and price. Due to current advancements in technology and reduced *Cost/kWh*. Electric cars sales has been rising in the recent decade, with the total number of electric cars standing at 5 million in 2018, an increase of 63% compared to 2017. Around 45% of electric cars on the road in 2018 were in China. Europe accounts for 24%, and the United States accounts for 22% of global Electric Vehicles (EVs) [20]. There are mainly three broad categories in which Electric Vehicles are divided. They are Hybrid Electric Vehicle (HEV), Plug-In Hybrid Electric Vehicles (PHEV) and Plug-In Battery Electric Vehicles (PEV).

2.7.1 Hybrid Electric Vehicles (HEV)

A Hybrid Electric Vehicle uses ICE (Internal Combustion Engine) as well as battery storage that drives the electric motor for the propulsion of vehicles. This type of configuration makes use of the different efficiency of propulsion types at different speed. The electric motor has more efficiency at lower speed while the ICE engine has more efficiency when higher speed are maintained. The electric motor turns into an electric generator during deceleration and starts to charge the battery storage again through a technique called as *Regenerative Braking*. At lower speed and with many breaks during the city driving, the electric motor is responsible for the propulsion of vehicle. The Figure 2.20 explain the propulsion mechanism of HEV. This interchange of propulsion type at different speed makes the Hybrid Electric Vehicle (HEV) more efficient than the ICE based vehicle. Exmaples of Hybrid Electric Vehicle (HEV) include *Japanese Railway E300*, *Toyota Prius* and *Honda Insight*.

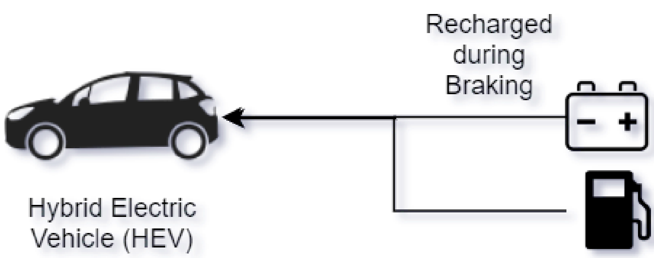

Figure 2.20: Hybrid Electric Vehicle (HEV) Drivetrain Scheme

2.7.2 Plug-In Hybrid Electric Vehicle (PHEV)

A Plug-In Hybrid Electric Vehicle (PHEV) has ICE engine combined with a battery storage as shown in Figure 2.21. The battery storage in PHEV can be recharged externally by connecting it to power supply from the grid. In terms of fuel efficiency, it is higher than a Hybrid Electric Vehicles (HEV) as in Plug-In Hybrid Electric Vehicle (PHEV) case, the battery can be charged from the wall outlet or from a charging station or through regenerative braking. The charging of the vehicle can be completely external and based on DC current or on-board charging based on AC-DC current conversion that takes the AC current and converts it to DC for charging the traction battery, while also monitoring characteristics such as voltage, temperature and state of charge SOC, among others. Mostly Lithium-Ion (Li-Ion) type batteries are used in Plug-In Hybrid Electric Vehicles (PHEVs). PHEVs typically require deeper battery charging and discharging cycles than conventional hybrids. PHEVs can save around $40 - 50\%$ in energy cost but due to the large and heavy battery packs, it becomes more heavier and has a higher price tag than Hybrid Electric Vehicles (HEVs). The drivetrain for Plug-In Hybrid Electric Vehicle (PHEV) is shown in Figure 2.21. Examples include *Mitsubishi Outlander*, *Chevrolte Volt*.

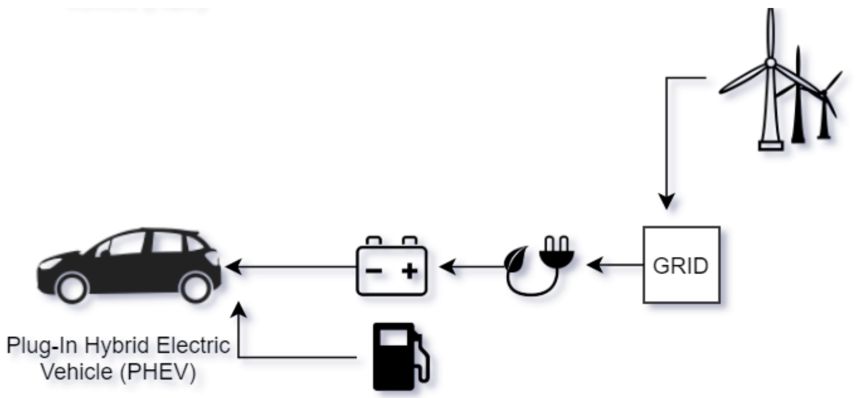

Figure 2.21: Plug-In Hybrid Electric Vehicle (PHEV) Drivetrain

2.7.3 Plug-In Battery Electric Vehicle (PEVs)

Plug-In Battery Electric Vehicle as shown in Figure 2.22 − that is the topic of thesis discussions − is a pure Electric Vehicle that uses only the rechargeable high voltage battery packs ($300 - 450V$)) as a source of propulsion and has no secondary source of propulsion. The most common battery packs are based on Lithium-Ion. They use only a traction battery connected to the electric motor though a high speed gearbox and connected through controllers and power electronics. The electric motors are mostly based on Permanent Magnet Synchronous Machines (PMSM), Switched Reluctance Motors (SRM) or Induction Motors. The electric motors are responsible for the propulsion during acceleration as well as for charging the battery in the regenerative braking mode. The drivetrain for PEVs is simpler compared to PHEV and HEV and is shown in Figure 2.22.

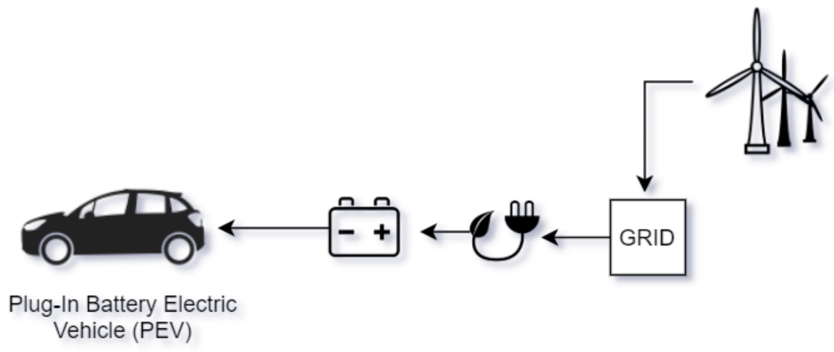

Figure 2.22: Battery Electric Vehicle (PEV) Drivetrain

The PEVs has substantially less moving parts as compared to either HEV or PHEV or ICE. Due to this the efficiency of this type of drivetrain is the highest as the friction losses and mechanical losses are significantly reduced. The PEVs are not limited to passenger cars but busses, trains, trucks as well. On a single charge, the PEVs can travel around $300 - 400km$. As it is only based on traction batteries so there are no emissions during the driving, although the manufacturing of PEVs and its individual components can involves emissions. Major concerns regarding PEVs include price, short range, low power density and access to charging infrastructure but it is constantly being expanded by energy supply company in collaboration with the car and truck manufacturers [21]. However, the effect of PEVs on the Swedish electric power system needs to be investigated further and will be a topic of this thesis. Based on the studies, there are three types of control schemes for charging of electric vehicles.

- Uncontrolled Strategy: The charging is done immediately after journey
- Loss Optimal Strategy: The charging is done to minimize the impact on Distribution System
- Price Optimal: The charging is done to minimize the electricity cost to consumers

Based on results from [22], if all vehicles in future were PEVs and charged uncontrolled, peak demand would increase by between $21 - 35\%$ in the residential area and by between $1 - 3\%$ in the commercial area. If customers would charge according to the price-optimal control strategy, peak power would increase by 78% for the residential area and 14% for the commercial area. If the charging were controlled using Loss Optimal Strategy, then charging would be conducted during off-peak hours even if all vehicles were PEVs, peak demand would be reduced by almost 10%. The *Loss Optimal Strategy* is only one of the techniques to reduce the burden on the Swedish power system. In the subsequent chapter, we will further investigate different *Demand Side Management* techniques such as the one based on electricity production from Wind and charging done only during peak productions.

2.8 PEVs Energy Demand and Its Integration

According to the report published in 2019 by Swedish Energy Agency, there is a total of $126TWh$ of energy consumption in the transportation sector in Sweden. $88TWh$ of it is consumed by the domestic transport inside Sweden, while $38TWh$ is consumed by international transport going out of Sweden, as shown in Figure 2.23 [13]. A total of $108TWh$ is supplied by the petroleum products and remaining comes from the combination of electrical network and bio-fuels. When it comes to the domestic energy consumption of transportation sector in Sweden, equivalent to $88TWh$, of which around $18TWh$ is supplied by combination of electrical network and bio-fuels while remaining $70TWh$ is supplied by petroleum and diesel products.

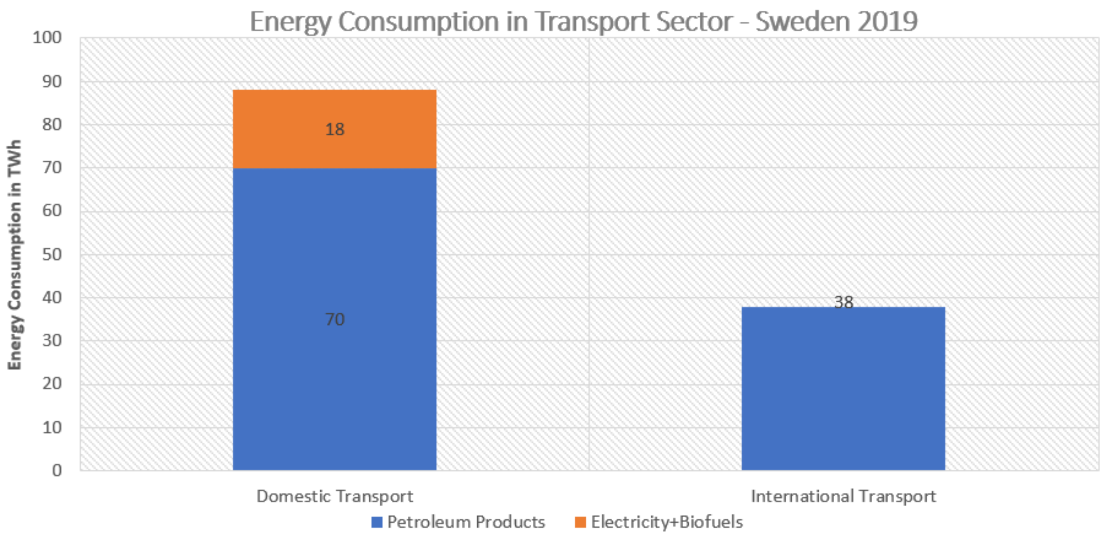

Figure 2.23: Total Energy Consumption by Transportation Sector in 2019

However theoretically, if all the vehicles based on petroleum products – a total consumption of around $70TWh$ – are replaced by the electric vehicles then the requirement of energy supplied by the electrical network to charge these electric vehicles reduces substantially as electric vehicles has more efficient drive-train compared to the the combustion engines [24]. According to other studies, for highway driving the electric motors has energy conversion efficiency of 80% compared to the 20% energy conversion efficiency of combustion engine. During city driving, electric motors have 70% energy conversion efficiency compared to only 10% conversion of combustion engines [23]. The Figure 2.24 converts the consumption equal to $70TWh$ for transport sector based on petroleum products to its equivalent consumption if the combustion engines are replaced by electric vehicles (EVs). The equivalent energy consumption is calculated based on the efficiency of the electric motor which can be approximated as the efficiency of the complete electric drive-train.

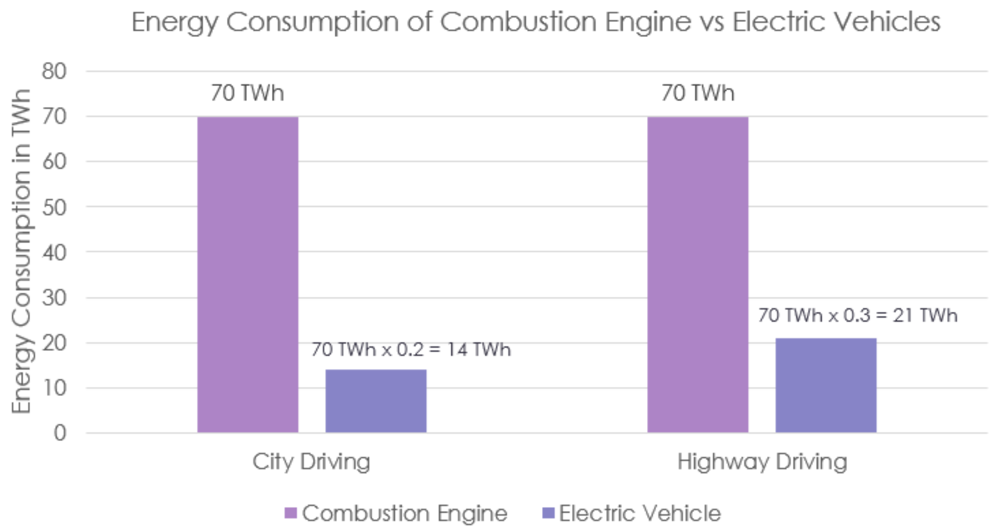

Figure 2.24: Total Energy Consumption by Transportation Sector in 2019

2.8.1 PEV Integration in Power System for 2019

Based on the analysis in Chapter 2.6, the additional electricity is calculated based on certain assumption. In case of 2019, a total of $24TWh$ of electricity was exported to neighboring countries. However, this additional electricity can be used to supply electricity to the transport sector. As calculated in Equation (2.4) for the 2019, the electricity was exported to other countries for $8497hrs$. Therefore to calculate the electric vehicle (PEVs) load that can be additionally integrated on an *hourly-basis* currently into the power system of 2019 is shown in Figure 2.25

$$P_{MW/hr} = \frac{24\text{TWh}}{8497\text{h}} \approx 2800\text{MW/hour for 8497-hrs} \tag{2.6}$$

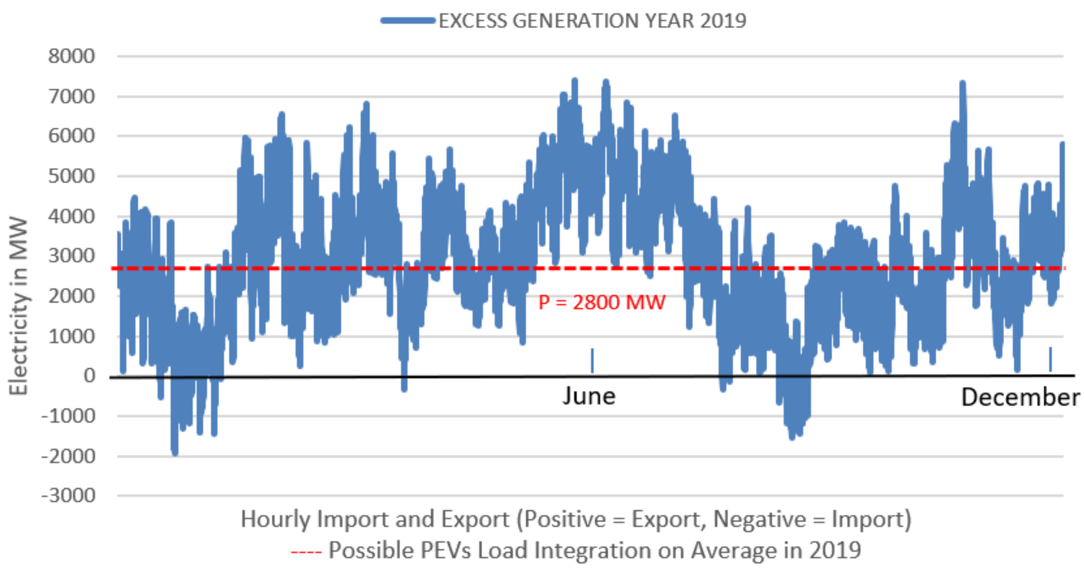

Figure 2.25: Possible PEVs Integration in 2019

2.8.2 PEV Integration in Power System for 2040

In case of power system based on *Wind Scenario 2040*, a total of $10TWh$ of electricity will be exported to neighboring countries based on analysis and conclusion from Figure 2.19. This additional electricity can be used to supply electricity for charging of vehicles in domestic transport sector. It is assumed that if the total domestic transport sector consumers rises by 10% by 2040, then the energy demand will also be increased linearly.

Expected Consumption for Domestic Transport in 2040 = 110% × Consumption for Domestic Transport in 2019

$$= 1.1 \times (E_{CombustionEngine} + E_{ElectricVehicles})$$
$$= 1.1 \times (70\text{ TWh}+18\text{ TWh})$$
$$= 1.1 \times (88\text{ TWh})$$
$$= 97\text{ TWh}$$

The above calculation is based on current energy conversion efficiency of the transport sector which stands around $10 - 20\%$ but as predicted, the future transport sector will be electrified, that has the conversion efficiency of around $70 - 80\%$ [23] as shown in a graphical form in Figure 2.26.

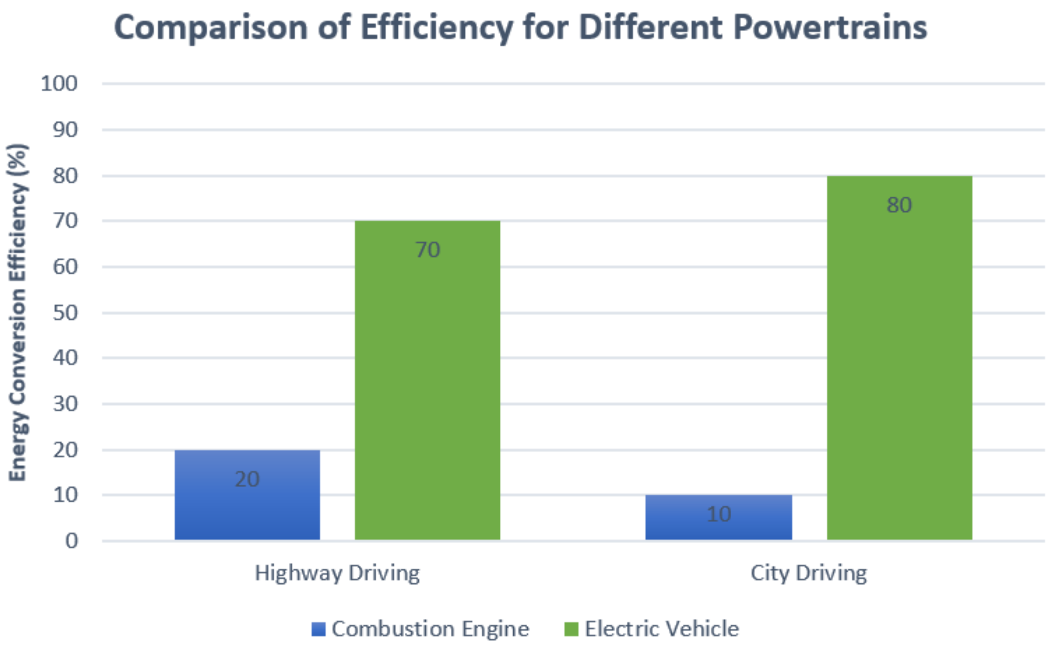

Figure 2.26: Efficiency Comparison for Different Powertrains [23]

$$\text{ICE Engines When Electrified} = (1 - \frac{HighwayEfficiency + CityEfficiency}{2}) \times 1.1 \times 70\text{ TWh}$$

$$= (1 - 0.75) \times (1.1 \times 70\text{ TWh})$$
$$= 0.25 \times 77\text{ TWh}$$
$$= 19\text{ TWh}$$

Based on the results from *Wind Scenario 2040* in Figure 2.19, $10TWh$ is additional electricity that will either be exported or can be used to supply electricity for charging of Electric Vehicles (EVs). As noted above, if the transport sector is 100% *electrified*, the the electricity demand for the transport is only additional $19TWh$ and energy saving of almost 75% will be achieved. As calculated, $10TWh$ of it is possible if *Wind Scenario 2040* is implemented with the scaling factor as defined in Figure 2.13, with almost 300% increase in installed capacity of Wind Turbines. However, there is a huge potential to invest in Solar Energy to supply the remaining $9TWh$ of electricity for charging of EVs. But with a Nuclear Power Plants *phased-out* and with a high penetration of RES based technologies such as Solar and Wind Turbine, the power system will have its own challenge when it comes to voltage and frequency stability that will be investigated in the subsequent chapters. As calculated in Equation (2.5) for the 2040, the electricity was exported to other countries for total $3227hrs$. Therefore to calculate the electric vehicle (PEVs) load in MW on an *hourly-basis* that will be integrated into the power system only during the export conditions, is shown in Figure 2.27

$$P_{MW/hr} \approx \frac{10\text{TWh}}{3227\text{h}} \approx 3100\text{MW/hour for 3227-hrs} \tag{2.7}$$

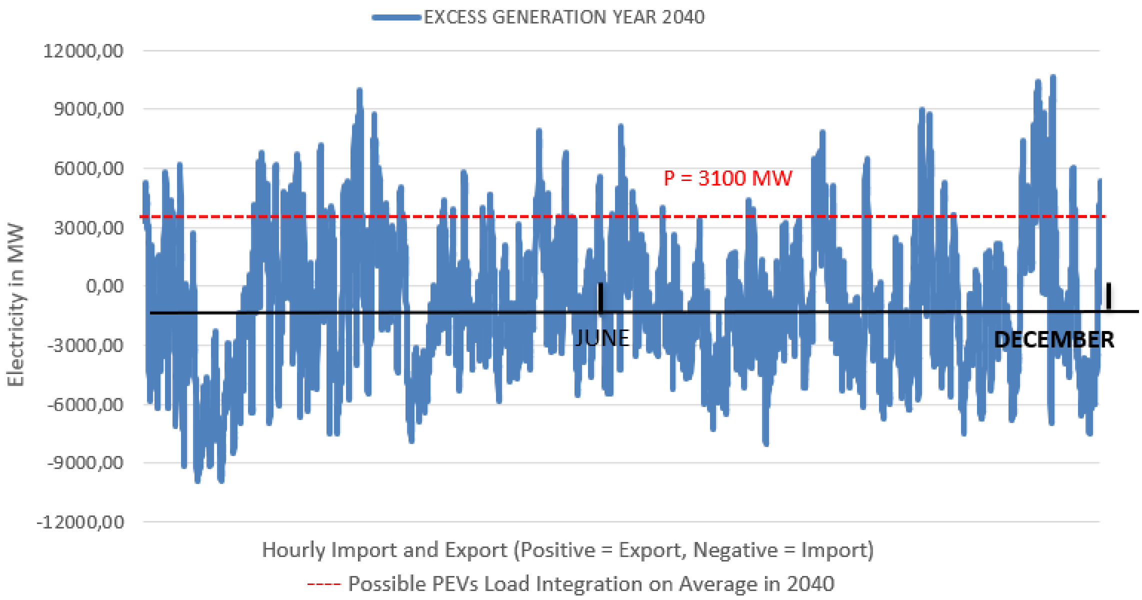

Figure 2.27: Possible PEVs Integration in 2040

2.9 Charging of PEVs for Wind Scenario 2040

As seen in the earlier chapters, the most likely scenario for the future Swedish electric power system is the *Wind Scenario 2040*. Based on the assumptions, it can concluded that in 2040, the installed wind capacity will be increased *three-folds*. Wind Energy is an intermittent source and electricity generation increase based on the occurrence and magnitude of wind.

The plot for electricity production from Wind Turbines is shown in Figure 2.28. Note that it has the same characteristic in time and magnitude as the electricity production in *2019* but the hourly electricity production is scaled by 300%, i.e. from current value of $9GW$ to expected $27GW$. Based on the analysis, at those instants where the electricity production from all the aggregate technologies becomes higher than the electricity demand, the remaining difference would be used for providing electricity for charging of Electric Vehicles (PEVs). It is also concluded that there is a $10TWh$ of potential to charge the electric vehicles (PEVs), based on the scaling factors shown in Figure 2.13. However, it is expected that around $19TWh$ will be the total electricity demand for charging of the Electric Vehicles (PEVs) by 2040. Hence, based on the assumptions, $27GW$ of installed capacity of Wind Turbines in 2040, will not be enough to charge all the Electric Vehicles if only $60TWh$ of electricity is produced from Wind i.e. three times the electricity production from Wind in *2019* equal to $20TWh$, as shown in Figure 2.7.

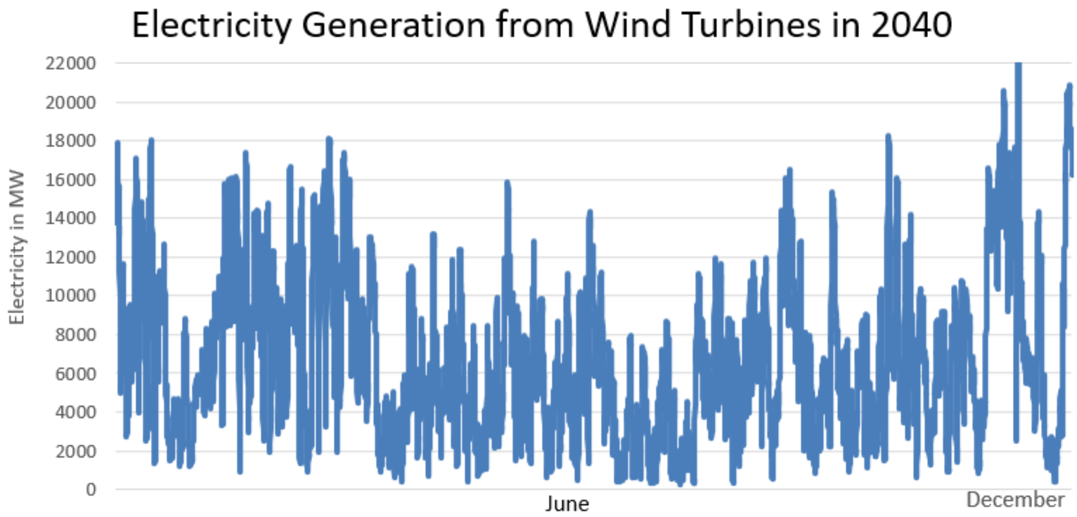

Figure 2.28: Expected Electricity Generation from Wind in 2040

The electric vehicles (PEVs) owner has different possibilities with charging at different locations and at different times. This can be done at home, at work or at any location between these two locations such as shopping malls or on through the charging stations at highway. Some results show that if the charging of the electric vehicles is uncontrolled in future and is done based on assumption that that the Swedish electric power will remain the same, then it could negatively affect the distribution system [22]. Based on this study, If the penetration of electric vehicles (PEVs) is very high then it could lead to the overloading of the transformers at the distribution level. Also in the residential areas, voltage drop issue might also be experienced due to uncontrolled electric vehicles (PEVs). This would mean that if all electric vehicles (PEVs) owner charge at the same time, for example during night time or at work, then it could affect the stability of power system. To avoid this, and many $(N-1)$ contingency planning will need to be done for the future Swedish electric power system, leading to high fixed and variable cost for operation.

2.9.1 Demand Side Management, FFT Approach

Based on the concept of *Demand Side Management*, if the charging of Electric Vehicles (PEVs) are done only during the time when there is a peak of electricity production, then the electricity production from intermittent sources of electricity such as Wind, can be efficiently and effectively used. Based on this, the Electric Vehicles (PEVs) will be charged at time when there is a high production of electricity rather than in an uncontrolled fashion, that can affect the stability of the power system. However, as Wind Energy is a natural and variable source of energy based on weather conditions, so electricity production from Wind Energy is also variable and unknown quantity for coming hours and days. Due to this, it can become very difficult for the power system owner for the planning of the power system and dispatch of electricity due to this variability. However − with a limited confidence interval − it is possible to predict when the peaks of electricity production from Wind arrives in the range of hours and days. Based on this knowledge the Electric Vehicles (PEVs) can be scheduled for charging. As electricity production from Wind has a low marginal cost of production, therefore charging of Electric Vehicles (PEVs) becomes very cost-effective for the owners.

2.9.2 FFT Analysis of Wind Scenario 2040

Using the Discrete Fourier Transform (DFT), the time-domain electricity production from Wind in 2040 can be transformed into its equivalent frequency domain sinusoidal components as shown in Figure 2.29. The DFT is a complex number with information regarding the magnitude and phase of each individual component that constructs the actual time domain signal when added together. Each component in the DFT has a certain period and the information regarding the period is very important in our analysis as this gives us information about the hours and days when a peak of electricity production from Wind 2040 returns with a certain magnitude. Using this knowledge about the period and the magnitude of that component, it is possible to perform the charging of Electric Vehicles (PEVs) during those instants in time.

In mathematical terms, Discrete Fourier Transform converts a finite sequence of equally-spaced samples of a signal into a same-length sequence of equally-spaced samples which is a complex number and is function of frequency. The interval at which the DTFT is sampled is the reciprocal of the duration of the input sequence. In the analysis, it is equal to *1-hour* interval in time domain and equal to *1-Hz* interval in the frequency domain. It is defined as

$$X_k = \sum_{n=0}^{N-1} (x_n \times e^{kn\frac{-i2\pi}{N}}) \tag{2.8}$$

$$X_k = \sum_{n=0}^{N-1} (x_n \times \left[\cos\frac{2\pi kn}{N} - i\sin\frac{2\pi kn}{N}\right]) \tag{2.9}$$

Here X_k is defined as Discrete Fourier Transform at *kth* frequency and is a combination of a real and imaginary number according to *Eulers Identity*. In this analysis, the magnitude of each individual component with a certain period is important as it gives the strength of electricity production from Wind *2040*.

$$X_k = Real\ No.\ A + Imaginary\ No.\ B$$

-

$$|X_k| = \sqrt{A^2 + B^2}$$

-

$$\text{Here, } X_k = X_0, X_1, ..., X_{N-2}, X_{N-1}$$

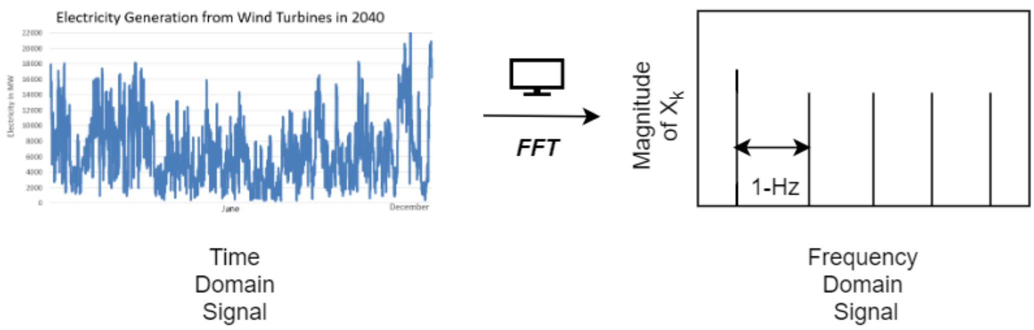

Figure 2.29: FFT Analysis on Electricity Production from Wind

If the total number of samples are very high, as in our case with *8760-hours*, it becomes more convenient computationally to use the *Fast Fourier Transform*, which is based on *Cooley-Tukey Algorithm* to calculate the value of X_k in the Equations (2.8) and (2.9), for Discrete Fourier Transform (DFT).

2.9.3 Results from FFT Analysis of Wind 2040

The results shown in Figure 2.30, the Discrete Fourier Transform of the electricity production from Wind. For convenience, the results are shown for a period of week. As can be noted, there are three major *Fourier Components*, $T1, T2, T3$, having a higher magnitude compared to other *Fourier Components*.

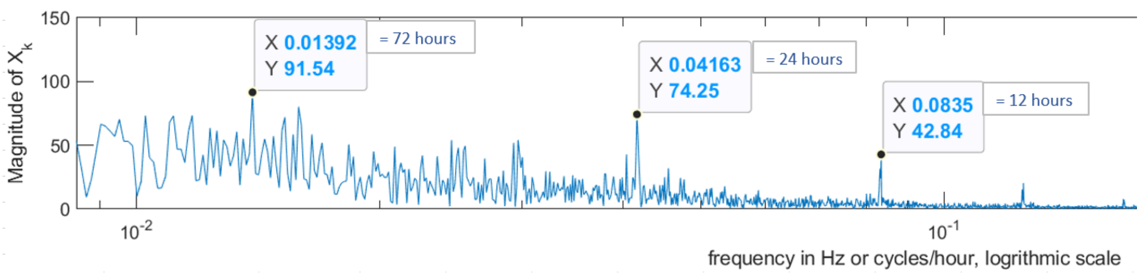

Figure 2.30: FFT Analysis on Electricity Production from Wind

The *Fourier Components* have a certain magnitude that defines which of the component contains more strength if the actual *time-domain* is to be reconstructed from its individual components. In this analysis, it means which component with a certain period, contains the highest electricity production from Wind. The period, as mentioned earlier is very important in the analysis as it gives the information regarding the occurrences of the peaks of electricity production from Wind. These are calculated below based on Figure 2.30.

$$\mathrm{T}_k = \frac{1}{f} \equiv \text{(Period of Fourier Component)}$$

-

$$\mathrm{T}_1 = \frac{1}{0.01392} \approx 72 - hours(3 - days)$$
$$\mathrm{T}_2 = \frac{1}{0.04163} \approx 24 - hours(1 - day)$$
$$\mathrm{T}_3 = \frac{1}{0.08355} \approx 12 - hours(1/2 - day)$$

-

Based on these results, there are three peaks of electricity production from Wind. It arrives after a three days period, one day period and every 12 hours, with the magnitude of strength decreasing gradually. In order to charge the Electric Vehicles (PEVs) and use the Wind Energy efficiently, it will become more cost-effective for the owners of Electric Vehicles (PEVs) during these times intervals. This will also lead to a much stable power system and overloading of transformer at distribution level can be reduced. However it should be noted that the *FFT* has been calculated for *1-hour* interval of electricity production from Wind and therefore more accuracy in the time periods $T1, T2, T3$ can be obtained if the sampling of electricity production data is increased to minutes or seconds intervals to increase the *confidence interval* of the results.

The results shown here is based on the assumption that the Wind in 2019 is similar in time and magnitude as Wind in 2040, which is not a very accurate representation but it gives a general pattern of wind variance with time based on data from earlier years. Therefore there are other prediction techniques and calculation methods based on *Auto Regressive (AR) and Artificial Neural Network (ANN)* [25]. These techniques relies less on the data from previous years, rather on the instantaneous wind variation and its expected pattern of wind variations based on probabilistic approach of predicting the wind for the next hours and days. These methods also comes under the *Demand Side Management* methods and can be used by the grid owners for planning and operation of the power system in the future to dispatch the electricity and by the consumers to schedule the charging of Electric Vehicles (PEVs). Based on the current technologies available, the total time for charging can vary from *15-minutes to 1-hour* based on 16 A, Single Phase and 32 A, Three Phase, respectively. This means that if all the (PEVs) are charged in a controlled and predictable manner by owners, it will become easier for the grid operator to prepare for high load demand and therefore other technologies such as *Gas Turbines* can be dispatched by grid owners to provide for sudden increase in demand, if the electricity production from Wind is not high enough.

3

Theory of Renewable Power Grid

From the discussion in Chapter 2, we have concluded that the future Swedish power system will be based on the most likely scenario known as *Wind Scenario 2040*. In the *Wind Scenario 2040*, electricity production from Wind and Hydro will have the highest share in the energy mix. The installed Wind Turbines capacity will stand at $27GW$ and installed Hydro Power Plant capacity around $18GW$. Based on the assumptions from Figure 2.13, the electricity consumption will be increased to $180TWh$ in 2040. Also based on the conclusions from Figure 2.19, $16TWh$ will be imported from other countries. It is concluded that the electricity generated in TWh from the combination of Wind and Hydro Power Plants will be able to fulfill 80% of Sweden total electricity demand, while other 7% supplied from a combination of Solar and CHP and 13% imported from other countries as shown in the Figure 3.1. Based on the scaling factors used in Figure 2.13 $-$ due to threefolds increase in wind capacity $-$ only $60TWh$ is produced compared to the $100TWh$ forecasted by Swedish Energy Agency. The difference could be explained by Swedish Energy Agency assumed forecast of investments and installation in *2040* of wind turbines in areas which receives higher wind for longer time resulting in higher wind capacity factor and could also be explained by technology and efficiency improvements of wind turbines by the year *2040*

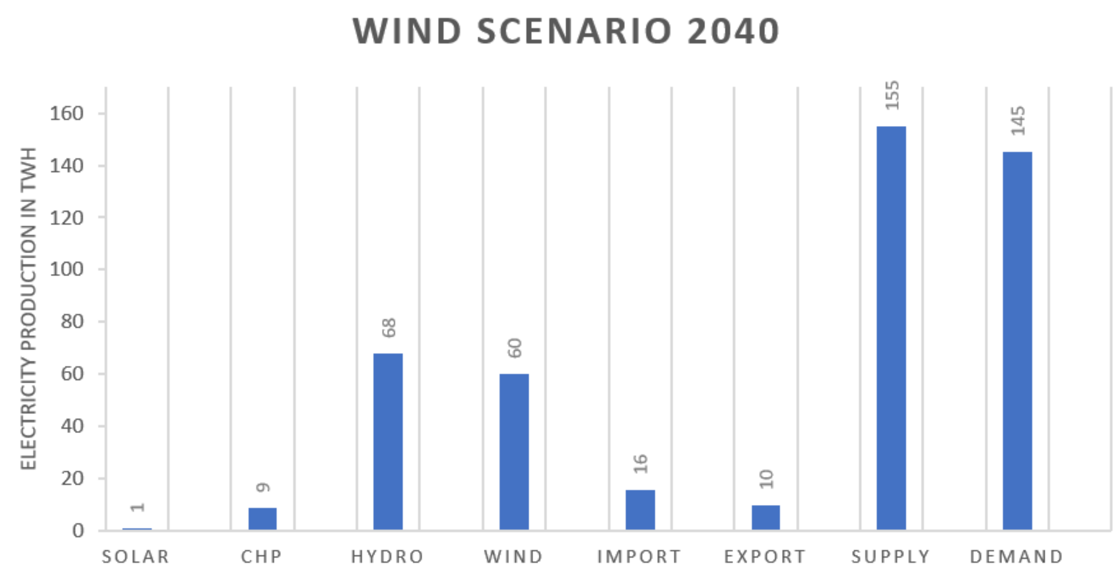

Figure 3.1: Electricity Production in TWh, Wind Scenario 2040

As shown in Figure 3.1, due to the major share of Wind and Hydro in the Swedish power system in 2040 and the *phasing-out* of Nuclear Power Plants, it is therefore important to see its effect on the stability of the system and whether it is a feasible. The Swedish power system in future based on *Wind Scenario 2040* will have a lot of fluctuations in terms of mismatch between supply and demand. This mismatch in supplied power and consumed power will have an effect on the frequency stability of the system. In order to deal with this subject and the simulation of the Swedish power system, some of the building blocks on which the simulation stands on will be discussed theoretically. This includes

- Wind Turbines, Mechanical Design
- Wind Turbines, Electrical Design
- Hydro Power Plants
- Inertia of Power System
- Power Flow Study
- Python Based PSS/E Simulations

3.1 Wind Turbines, Mechanical Design

The wind energy is used as a source of supplying emission-free electrical energy to the continuous growing demand in the world. Due to the wind being a naturally occurring clean source of energy, electricity production from wind has a very cheap marginal price for a *MW* of power. A study carried out by US Energy Information Administration in year 2008, revealed that 89% of the energy consumed in US is coming from non-renewable energy sources while only 11% is from renewable energy sources [26]. Therefore in many parts of the world, there is a huge potential to invest in the Wind Energy. In case of Sweden, a lot of future investments in the field of energy is towards Wind Energy. There are mainly two types of wind turbines, namely vertical axis and horizontal axis wind turbines.

3.1.1 Vertical-Axis Wind Turbine

The vertical axis wind turbine has the main rotor perpendicular to the the ground and its blades rotates around vertical axis to generate power. Due to its generator, gearbox and the power electronics close to the ground, it becomes easier in terms of repair and maintenance. They do not require much wind and it is regardless of the wind direction as compared to the horizontal wind turbine. They are permissible where higher structures are prohibited. The disadvantage associated with this type of wind turbine is mostly due to shorter lifetime with higher chances of breakdown due to less mechanically stable design, bending and cracking of blades. Due to this the maintenance costs is very high for this type of wind turbine and therefore are generally not preferred.

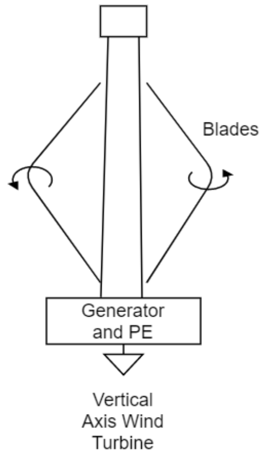

Figure 3.2: Vertical Axis Wind Turbine

3.1.2 Horizontal-Axis Wind Turbine

The horizontal axis wind turbine has the main rotor parallel to the the ground and its blades rotates around horizontal axis to generate power. It has highest efficiency, and require faster wind speed to produce sufficient power. These turbines are usually mounted at higher altitudes where there is not enough friction slowing down the velocity of wind. A gearbox between blades and the rotor of the generator increases the speed to produce sufficient electrical power from generator. The advantage of horizontal axis is that it can also have variable blade pitch and can adjust itself according to the magnitude and direction of the winds. At lower speed power output is proportional to the wind speed while higher speed it is almost constant adjusted by the blade pitch. The typical output from horizontal axis variable speed wind turbine is shown in Figure 3.4. This type of wind turbine is the most common and has highest advantages in terms of control of active and reactive power.

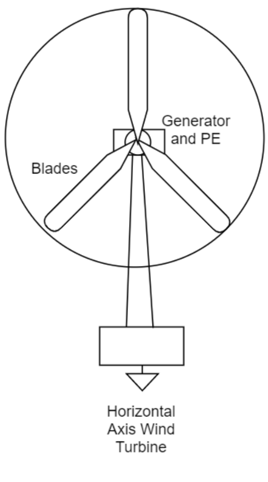

Figure 3.3: Horizontal Axis Wind Turbine

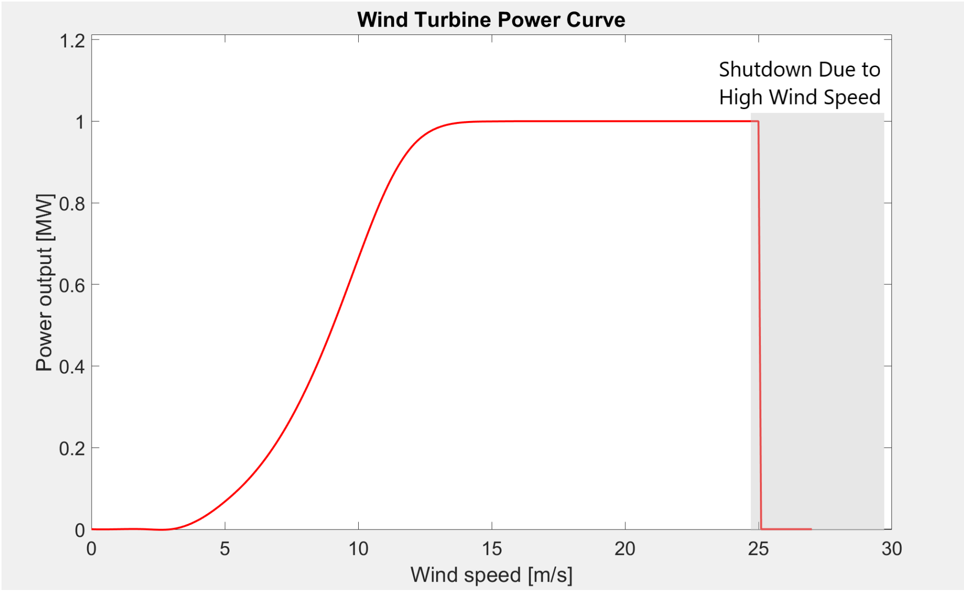

Figure 3.4: Typical Output of Horizontal Axis Wind Turbine

3.2 Wind Turbines, Electrical Design

Wind Turbines differs not only based on the physical structure but also in terms of electrical design and the power electronics involved between the shaft of the blades and the generator producing electrical energy. There are various schemes of the interconnection of the shaft of the blades, the generator and power electronic involved and some of these schemes are briefly discussed. Each has its own advantages and disadvantages over another. Due to its frequent use around the world and overall advantageous over other types, more emphasis will be on Doubly Fed Induction Generator ($DFIG$), and will be main topic of this thesis and the type of wind turbine used in the subsequent simulations.

3.2.1 Induction Generator With Soft Starters

A wind turbine can also supply less fluctuating electrical power to the grid using a soft starter. When a wind turbine based on the induction generators are connected to the grid, it absorbs a large reactive power to magnetise the core, this reactive power absorption is seen as a high *in-rush current* at the start. Soft-starter is switched on to reduce the fluctuation caused by the *in-rush current* at the time when it is being connected to grid. However due to no control of active and reactive power after the soft starter is switched off, there can be a lot of fluctuations based on wind speed injected into the grid unless more power electronic control scheme are introduced. It is an older technology mostly used in $1980 - 1990$ that has gone out of fashion as more requirement are put in place for the wind turbine from the grid owners to support the grid for frequency and voltage stability. However the idea is simple and requires low maintenance.

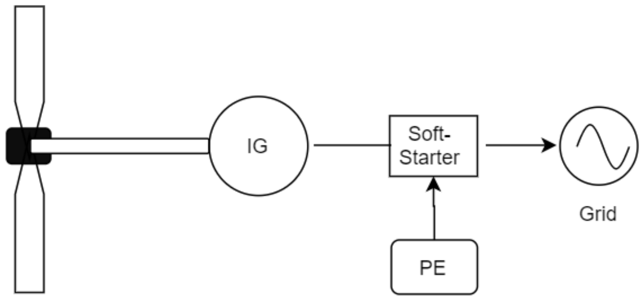

Figure 3.5: Induction Generator With Soft Starters

3.2.2 Controlled Rotor Resistances Based Wind Turbine

Due to the wind fluctuations, the speed of the shaft changes continuously and that can lead to a varying electrical torque generation in the generator leading to fluctuating electrical power delivered to the grid side. In order to control the torque speed curve and the control the output power, power electronics based extra three resistances are added to the rotor winding of the generator that can change the rotor current based on the fluctuation of the wind speed and therefore control the stator current and the electrical output from the generator. The higher the rotor resistances compared to the *nominal rotor resistance* R_r, the better the performance of the stator current and less the fluctuation seen on the grid side of the generator [27]. However due to extra resistances added to the rotor circuit of the generator, the copper losses increases and therefore the efficiency is reduced. But adding the rotor resistances leads to limited torque control but reduced speed variations.

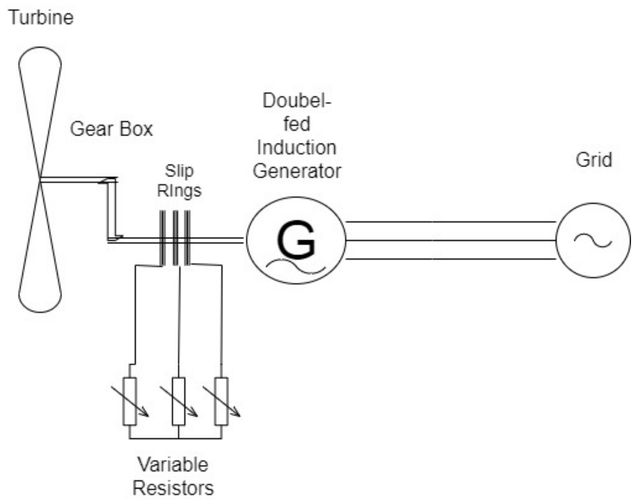

Figure 3.6: Controlled Rotor Resistance Based Wind Turbine

3.2.3 Full Power Converter Based Wind Turbine

Full Power Converter consists of two back-to-back converter topology and has a generator side converter (GSC) connected to either asynchronous or synchronous generator and a line side converter (LSC) with a DC-link capacitor separating them. This voltage source converter (VSC) topology is used for the generating electrical power at a nominal frequency such as $50Hz$ or $60Hz$ using PWM techniques. The generator side converter (GSC) part of the wind turbine is controlled using Direct Torque Control (DTC) to capture maximum kinetic energy generated from the blades. The Line side converter (LSC) helps in the supplying the active power and also controls the reactive power to support the grid stability. This type of electrical system works mostly with variable speed wind turbines. It has higher losses compared to other types but full control of active and reactive power. The electrical design is shown in Figure 3.7

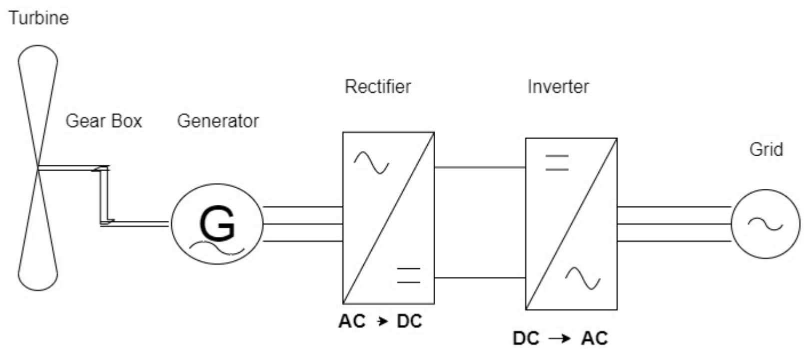

Figure 3.7: Full Power Converter Based Wind Turbine

3.2.4 Doubly Fed Induction Generator Based Wind Turbine

These days, Doubly Fed Induction Generators ($DFIG$) are the most widely used type of wind machines to produce electricity from wind turbines. It tackles all the limitation and shortcomings of earlier technologies and uses the strengths and advantages from each of the above mentioned wind turbines into one single package. This means it has the ability to control the rotor currents leading to control of speed variations and the advantages of full power converter of having a full control over the active and reactive power. Double fed induction generator have a number of advantages over other types of generators when used in wind turbines. Some of them are given below:

- Doubly-fed induction generators when used in wind turbines allow the amplitude and frequency of their output voltages to be maintained at a constant value. Resultantly, $DFIGs$ can be directly connected to the AC network and remain synchronized at all times.

- Its ability to control power factor, due to the fact that converter can control the reactive power flow in both directions; flowing into and out of the grid.

- Reduced inverter costs because the rating of the inverter is nearly *25%* of the system rating due to which it can be made smaller and can have up to *33%* speed variation above synchronous speed [28]

- It has good low voltage ride through (LVRT) capabilities that is essential for power system voltage stability.

This makes the doubly-fed induction generator more robust and effective compared to the other mentioned technologies available for wind turbine discussed earlier. Based on certain control techniques, it can also be used to help in primary and secondary frequency support [30].

3.2.5 Inertial Response of DFIG Connected Wind Turbine

A wind turbine in its simplest form produces an electrical power with a varying frequency due to the fluctuation of the wind speed. In order to mitigate this, there is always a need to use a power converter as discussed earlier to generate electrical power at a constant frequency. But due to the connection of wind turbine to the grid through power electronic interface, the inertia of the rotating mass of the wind turbine is decoupled from the grid. Also it is known that the frequency is related to the active power. If the electrical power can be increased during the frequency dip and electrical power reduced during frequency overshoot, then this can help to mitigate the effects of frequency variations. Using the techniques of *synthetic inertia*, where additional control loop in the $DFIG$ wind turbine sense the frequency dip or frequency rise, the wind turbine is directly connected to the grid and the kinetic energy stored in the rotating mass can be used to inject active power during the frequency dip.

3.2.6 Working Principle Of DFIG Connected Wind Turbine

Doubly-Fed Induction Generators are electric machines which have armature winding directly connected to the grid and the rotor windings also indirectly connected with grid through a back-to-back AC/DC voltage source converter, that controls both the rotor current and the reactive power flow using Direct Torque Control (DTC) control technique.

In this way, the active and reactive power flowing into the grid can be controlled through the rotor current controlled by the converter, independent of the rotation of the turbine. During the rotor winding connection, either slip rings or brush-less topology is used.

In normal operating conditions, $DFIG$ supply active power to the grid and can consumes or produce reactive power from or towards the grid, respectively. The electrical design of the ($DFIG$) is shown below.

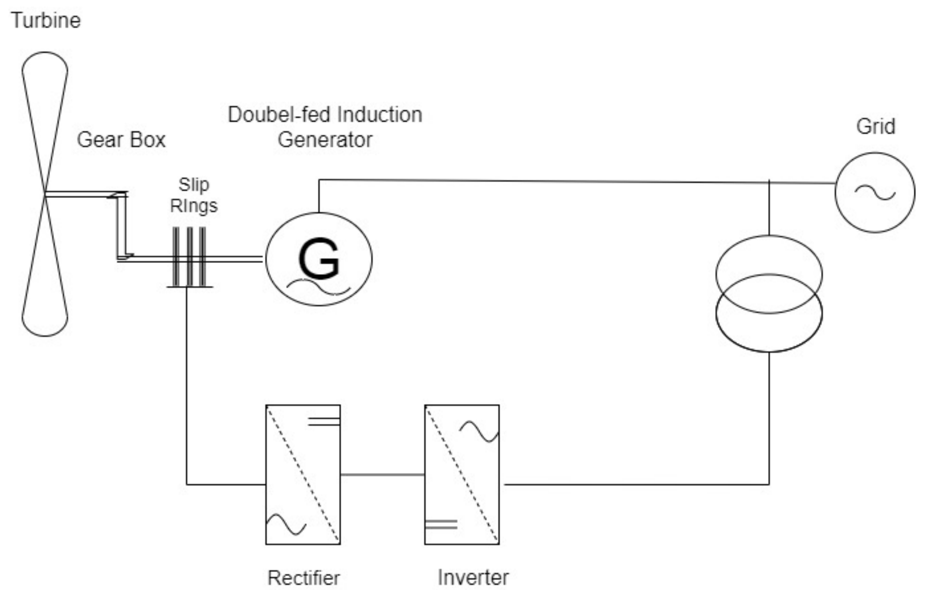

Figure 3.8: Doubly Fed Induction Generator

Using a Doubly-Fed Induction Generator, the wind turbines can also be made to run at speeds slightly higher than the nominal synchronous speed. This can be helpful for variable speed wind turbine where it is required for a short time to be able to withstand higher wind speeds. Although their principles of operation have been known for decades, currently doubly fed induction generators is one of the most widely accepted wind turbine technology due to its advantages over other type of wind turbine technologies.

3.2.7 Modeling of Doubly-Fed Induction Generator

In order to separately control the active and reactive in a *four-quadrant operation*, with active and reactive power flow to and from the grid, a dynamic model of the Doubly-Fed Induction Generators ($DFIG$) is needed. The stator and the rotor current in a stationary reference frame, referred to stator is given as,

$$V_{sj} = r_s * i_{sj} + \frac{\delta\psi_{sj}}{d_t} \quad j = 1, 2, 3 \tag{3.1}$$

,

$$V'_{Rj} = r'_R * i'_{Rj} + \frac{\delta\psi_{Rj}}{d_t} \quad j = 1, 2, 3 \tag{3.2}$$

The electrical torque generated by the Doubly-Fed Induction Generator is give as

$$T_{el} = \frac{p}{2} \sum_{j=1}^{3} i_j * \frac{d\psi_j}{dv} \quad j = 1, 2, 3 \tag{3.3}$$

Transforming the Equation (3.1) and (3.2) from *three-phases* into $\alpha\beta$ and then to dq transformation using the *Park and Clark Transformation*. Also as the vector is divided into a real part and an imaginary part. Therefore after *dq transformation*, the stator and rotor current can be written as

$$\underline{u} = u_d + j.u_q \tag{3.4}$$

$$\underline{V}_s = r_s * \underline{i}_s + \frac{d\underline{\psi}_s}{dt} + j * \omega_s * \underline{\psi}_s \tag{3.5}$$

$$v_{sd} = r_s * i_{sd} + \frac{d\psi_{sd}}{dt} - \omega_s * \psi_{sq} \tag{3.6}$$

$$v_{sq} = r_s * i_{sq} + \frac{d\psi_{sq}}{dt} + \omega_s * \psi_{sd} \tag{3.7}$$

Similarly, the rotor current referred to stator can be written as

$$\underline{V}'_R = r'_R * \underline{i}'_R + \frac{d\underline{\psi}'_R}{dt} + j * \omega_R * \underline{\psi}'_R \tag{3.8}$$

$$v'_{Rd} = r'_R * i_{sd} + \frac{d\psi_{sd}}{dt} - \omega_R * \psi'_{Rq} \tag{3.9}$$

$$v'_{Rq} = r'_R * i_{sq} + \frac{d\psi_{sq}}{dt} + \omega_R * \psi'_{Rd} \tag{3.10}$$

$$\underline{\psi}_s = L_s * \underline{i}_s + L_m * \underline{i}'_R \tag{3.11}$$

$$\underline{\psi}_R = L_m * \underline{i}_s + L_R * \underline{i}'_R \tag{3.12}$$

$$T_{el} = -\frac{3}{2} * p * Im\left\{\underline{\psi}_s * \underline{i}_s^*\right\} \tag{3.13}$$

The synchronous reference frame can be linked to the stator or rotor flux of the machine. However, a reference frame linked to the stator voltage space vector $\underline{v}_s$ is a convenient alternative because the $DFIG$ operates as a generator maintaining or being fed with constant stator voltage [29]. The slip of the induction generator is given as

$$s = \frac{\omega_s - \omega_{mech}}{\omega_s} = \frac{\omega_R}{\omega_s} \tag{3.14}$$

where s is the slip of the induction generator and a_{SR} is the voltage transform ratio between stator and rotor. The construction of doubly fed induction generator is mainly consisted of number of turns which are around 3 times more then that of stator.

Due to which the rotor voltage will be higher and current will be lower. This ratio is selected such that the voltage rating of the four-quadrant converter matches the stator voltage at maximum speed to avoid transformers in the rotor circuit [28]

$$V_R \approx s * a_{SR} * V_s \tag{3.15}$$

$$P_R = s * P_s \tag{3.16}$$

$$P_{mech} = (1 - s) * P_s \tag{3.17}$$

Equations (3.16) and (3.17) clearly shows the power flow in the $DFIG$ for above-synchronous and under-synchronous operation. Above synchronous speed, it operates as a generator and deliver active power to the grid. Below synchronous speed, the converter helps to circulates active power from the grid into the rotor circuit.

3.3 Hydro Power Plants

Hydro Power Plants were one of the first renewable source of energy used to generate electricity. The Hydro Power Plant has no harmful material consumption during production but has some environmental and ecological aspects to consider such as sedimentation, loss of wildlife, forest and biodiversity, emission of greenhouses gases from flooding of water, displacement of communities, loss of livelihood in fishing industry and less clean water supply for drinking purposes due to additional of harmful nitrates, sulphates. However the process itself makes the production of electricity environmentally friendly and once a Hydro Power Plant complex is constructed, the electricity generation produces no direct waste. In hydro power stations water falls down back to the river through pen stock and rotates the turbine with is connected to the generator. The water leaving the turbines is known as tail water, however this tail water still has the energy to produce electricity and can be pumped back to the reservoir during less demand of electricity.

A Hydro Power Plant is based on synchronous generators and its capacity can be in GW, therefore is has a very high inertia that is always connected to the system. Hydro Power Plant does not always require a large dam and a high altitude level to fall. Some hydro electric power plants just use a small canal or stream to transfer the river water through a turbine known as the *run-of-the-river* Hydro Power Plants. The energy carrier is the water and the power depends on most importantly on the incoming flow of water and the falling height.

$$P = g \times \eta \times Q \times H \tag{3.18}$$

Here, P is the electric power produced, when Q flow of water in m^3/h takes place at a height H, g is the gravitational acceleration equal to $9.8m/s^2$ and η is the efficiency of the Hydro Power Plant that is around 90% for the modern power plants.

3.3.1 Hydro Electricity Around the World

In 2015 Hydro Power generated 16.6% of the worlds total electricity and 70% of all renewable electricity and is expected to increase by about 3.1 percent each year for the next 25 years [32]. Hydro power is produced in 150 countries, with the Asia pacific region generating 33% of global Hydro Power in 2013. China is the largest Hydro Electricity producer with $920TWh$ of production in 2013, representing 20% of domestic electricity use in China [31]. The cost of hydroelectricity is relatively low, making it a competitive source of renewable electricity. The typical cost of electricity from a Hydro Plant with size above $10MW$ is $1-2$ cents per kWh in US [33].

3.4 Inertia of the Power System

Based on Wind Scenario 2040 and the scaling factors used in Figure 2.13, the demand of electricity in Sweden increases by *10%* to almost *182 TWh*. To supply electricity, based on Figure 3.1 almost *68 TWh* will come from Hydro as well as adding inertia into the system. And as discussed in previous chapter, there is almost *100 TWh* of electricity generation potential from Wind in 2040 according to Swedish Energy Agency as shown in Figure 2.12, however based on the assumptions and scaling factors, only $60TWh$ will be generated from Wind. The remaining electricity production will come from the combination of Solar, CHP and Gas Turbines and imports. This would mean that a power system based heavily on wind turbine and phasing out of Nuclear Plants might have its pitfalls and disadvantages that needs to be investigated further. One of them is whether a power system based on large amount Wind has enough stability as wind turbines that in its basic form does not add any inertia into the system due to the fact that power electronics separating the the grid and wind turbine, even though the electricity generation is based on rotating mass. However, advanced control methods can help in mitigating the effect and can help support the frequency variations in the power grid [35].

Therefore, it is important to understand the concept of inertia and how a rotating mass adds inertia into the system. In future, the Swedish Electric Power System (EPS) can have a very good inertia due to a lot of Hydro Power Plants. And it is expected that Wind technology will be refined in future to support the system frequency during the transient conditions. The current power system in Sweden has a very high inertia due to large Hydro and Nuclear Plants. Both of these power production technologies are based on large synchronous generators with high rotating mass. Inertia H is defined as the rotating kinetic energy stored at rated angular velocity and at rated nominal power. H is typically defined in seconds (s) and in physical terms it means the time in seconds that the rotor takes to reach rated angular velocity at nominal power.

$$H = \frac{\text{Stored Kinetic Energy at Synchronous Speed}}{\text{Machine Apparent Rating in MVA}} = \frac{MJ}{MVA} \tag{3.19}$$

As long as the rotors of Hydro and Nuclear Plants are rotating, it generate a large equivalent inertia H_{eq}, that is the sum of all individual N rotating masses of all available synchronous generators.

$$H_{eq} = H_1 + H_2 + H_3 + H_4 + ... + H_N \tag{3.20}$$

The active power of the system is closely related to the frequency of the system. An power system with an electrical supply equal to the demand is defined by a nominal system frequency. For example in US, it is 60 Hz while in Europe and other parts of the world, that is 50 Hz. However most of the generators and frequency dependent loads are designed to operate normally even if the frequency drops or rise in the range of ± 2 %, based on IEC 60034-1 *Zone A* [36]. Outside this operating range the generators and frequency dependent loads needs to be disconnected from the system in order to avoid any physical damages to the magnetic core and the windings of the rotating machines. If the frequency drops significantly, then generators excitation current increases and can lead to saturation in the core that leads to high losses or damage to the windings. In case of motor loads, drop in frequency or the motor speed consequently also leads to a high power consumed by the load that can significantly reduce the lifetime of these machines if it is not disconnected from the system appropriately. The Equation 3.21 explains this behaviour of frequency dependent loads [34].

$$\Delta P_e = \Delta P_L + D\Delta\omega_r \tag{3.21}$$

where, ΔP_e is the change in electrical power and ΔP_L is the non-frequency-sensitive load change and $D\Delta\omega_r$ frequency dependent load change.

3.4.1 Swing Equation

A power system is a combination of many synchronous generators with rotating mass supplying the electrical power and other rotating machines acting as load, all rotating at some stable point speed and its sum effect is defined by system frequency. However the rotating machines are subject to transients phenomena such as variation in turbine mechanical output connected to generators, a short circuit either at the terminal of the machine or somewhere far away in the system or the disconnection of a tie line etc. These leads to an adjustment in the rotor speed and a new system frequency point is reached. This acceleration or deceleration of rotor is defined as the *Swing Equation* defined in Equation 3.22.

$$\frac{2H}{\omega_r}\frac{d^2\delta}{dt^2} = P_m - P_e \tag{3.22}$$

where, δ is relative angle between stator and rotor field or commonly called as the rotor angle. ω_r is rotor speed in electrical *rad/s* and P_m and P_e is the mechanical output of turbine and electrical output of the synchronous generator, respectively.

3.4.2 Frequency Response at Different Inertia Value

As long as the supply is equal to demand, the system frequency remains constant but as soon as there is a mismatch between the supply and demand during a steady state or a transient phenomenon, the system frequency rise or drops accordingly. If the supply is more than demand, system frequency rise and vice versa. However, if the power system contains a large amount of rotating mass, then it adds inertia in the system. Inertia of power system (H) is defined as the property of the power system to remain at a synchronous frequency of the rotating mass. A high inertia adds inertia into the system thus avoiding sudden frequency drop and rise. In the Figure 3.9, two different cases are shown with $H=3$ *s* and $H=2$ *s* when a certain disturbance is initiated in the power system.

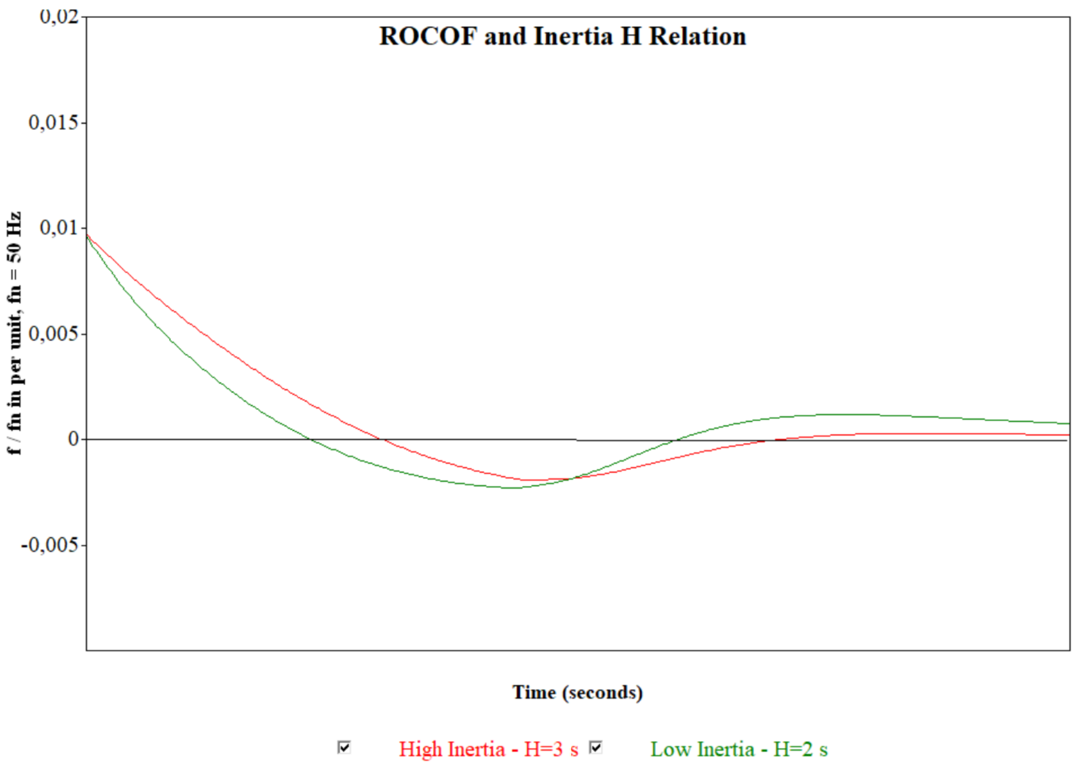

Figure 3.9: System Frequency Response for Different Values of Inertia H, higher the value of H, higher the synchronous generators in the system

It can be concluded that a power system having a high number of synchronous generation with rotating masses has a high value of inertia and is slow to react to disturbance originated in the grid and has less df/dt, the rate of change of frequency, while a power system with a low inertia is prone to a less stable grid with a higher df/dt as well as has a deeper frequency *nadir*, i.e. the lowest value of under-frequency. In many cases, these under-frequency dips can lead to the saturation of the magnetic core for the generators leading to high losses and ultimate physical damage to the property and the facilities.

3.5 Power Flow Analysis

In a power system the variables such as voltage, current, active and reactive power are not fixed quantity but always changing as there is always some variation in the load, switching actions, faults in the power system and other transients with respect to time. But the analysis of the power system can be done in simpler way using steady state techniques based on steady state *phasors*. For example, during the faults such as a three phase fault, transient state current can be determined through the steady state fault current and by applying mathematical techniques it is possible to calculate the transient currents. The steady state condition acts as the boundary condition for transient state calculations. It is essential to determine the currents and voltages of power system for a reliable and controllable power system. In every system a constant monitoring of these quantities is also important to prepare the system for any loss of a power component or mitigate occurrences such as voltage collapse or underfrequency operations.

In a power flow studies, all the voltages at the nodes should be known and to use them to calculate all the other unknown variables and interlinked parameters. A power system has some known quantities such as voltage, active and reactive power at the generating bus, transmission line impedence and charging, active and reactive power consumption at loads, transformer and tap ratios etc. and the quantities which are desired to be calculated are voltage magnitude and phase at every bus, excluding generating bus where voltage is a known quantity, active and reactive power flow in each transmission line and transformers are some of the unknown desired parameters.

$$I_n = Y_{nn} \times V_n \tag{3.23}$$

where,

- I_n is vector of positive-sequence currents flowing into the network buses
- V_n is vector of positive-sequence voltages at the network buses
- Y_{nn} is network admittance matrix of the complete system

If either I_n or V_n is known, the power flow calculation is straightforward. But in practice, I_n or V_n is an unknown quantity and the computer program such as PSS/E uses iterative techniques for both I_n or V_n such that they satisfy Equation 3.23 and all the load and generation conditions specified in the problem. After V_n has been determined, all individual transmission line active and reactive power and transformer flows can be obtained directly from the individual component equations [37]. In PSS/E, *Newton-Raphson* iteration technique is used to satisfy the Equation 3.23 and the underlying conditions of the power system in study.

3.5.1 Newton-Raphson Method

In load flow studies, two common techniques, namely *Newton-Raphson and Gauss-Seidel*, are used to calculate the voltages at all the buses, which is done by solving number of equations involving both the active power and reactive power. *Newton-Raphson* method is mostly used rather then the Gauss- Seidel method. *Gauss-Seidel* method is used for very large power distribution systems involving various numbers of transformers but the problem with this method is that it has slow convergences. *Newton-Raphson* method involves set of equations to be solved using iterative techniques to calculate the voltages at the buses. Some of the iterative steps involved in this method is described below.

• Calculating the admittance matrix Y_{nn}

• Initializing all the bus voltages at *k=0* iteration , i.e first iteration

$$V_i^{(k)} = 1\angle 0^\circ \quad \text{for } i = 2, 3, ..., n$$

• Calculating the *Jacobian Matrix* J^k at *k=0* iteration

$$\begin{bmatrix} \Delta P^k \\ \Delta Q^k \end{bmatrix} = \begin{bmatrix} J_1^k & J_2^k \\ J_3^k & J_4^k \end{bmatrix} \begin{bmatrix} \Delta \delta^k \\ \Delta |V|^k \end{bmatrix}$$

• Calculating the active and reactive power at the buses at *k=0* iteration

$$P_i^k = \sum_{j=1}^{n} |V_i^k||V_j^k||Y_{ij}| cos(\Theta + \delta_j^k - \delta_i^k)$$

$$Q_i^k = -\sum_{j=1}^{n} |V_i^k||V_j^k||Y_{ij}| sin(\Theta + \delta_j^k - \delta_i^k)$$

• Calculating mismatch of nodal active and reactive injection at *k=0* iteration

$$\Delta P_i^k = P_i - P_i^k$$

$$\Delta Q_i^k = Q_i - Q_i^k$$

• Calculating voltage magnitude and angle at *k=0* iteration using *Jacobian Matrix*

$$\begin{bmatrix} \Delta \delta^k \\ \Delta |V|^k \end{bmatrix} = \begin{bmatrix} J_1^k & J_2^k \\ J_3^k & J_4^k \end{bmatrix}^{-1} \begin{bmatrix} \Delta P^k \\ \Delta Q^k \end{bmatrix}$$

• Updating the system voltage magnitude and angle for next iteration

$$\delta^{(k+1)} = \delta^k + \Delta\delta^k$$

$$|V|^{(k+1)} = |V|^{(k)} + \Delta|V|^{(k)}$$

• Repeating all the above steps until k=n and mismatch is below tolerated error

$$max(\Delta P_1^k, ..., \Delta P_n^k)) \leq \epsilon$$

$$max(\Delta Q_1^k, ..., \Delta Q_n^k)) \leq \epsilon$$

3.5.2 PSS/E Approach to Solve Load Flow Studies

The steps to perform load flow has been discussed above. But each program uses a different approach to perform the mathematical calculation. PSS/E divides the problem into smaller well-defined parts. The load flow study is based on a number of buses, with each bus having a power system component connected to it. For each of these components, only certain values are known. In PSS/E, the buses are defined as either (1) Slack Bus, (2) PV Bus or (3) PQ Bus. Certain inputs are associated with these bus, that is either a known value or an unknown value. In a PQ bus, active and reactive power production or consumption is known and it is mostly where loads such as motors load, shunt capacitor or synchronous condensers are connected which draw or produce certain active or reactive power. In a PV bus, mostly generators are connected, for which mostly the active power and voltage is controlled to be at rated values.

• Bus Voltage (V)
• Bus Angle (δ)
• Active Power (P)
• Reactive Power(Q)

Bus Types	**P**	**Q**	**V**	δ
PQ Bus	*known*	*known*	*unknown*	*unknown*
PV Bus	*known*	*unknown*	*known*	*unknown*
Slack Bus	*unknown*	*unknown*	*known*	*known*

3.5.3 Slack Bus

A slack bus is commonly used to balance the active (P) and reactive power (Q) in a electrical power system therefore load flow studies cannot take place without at least one slack bus in computer programs like PSS/E. Generators connected to slack bus provide the active/ reactive power by absorbing or emitting the power to the electrical system, therefore before the load flow study, its values are not defined and adjusts according to the needs of the power system. In a power flow studies, the maximum and minimum P and Q is defined to be infinite and thus not limited by production and generates as much as needed to balance the power system and the equations discussed in *Newton-Raphson Method*. It provides for all the power losses produced in the transformers and transmission lines. However, during the dynamic simulation, steady state P and Q values for generators connected to swing bus are used as *boundary conditions* for transient studies, and therefore its important to define its transient properties to solve differential equations. The swing bus always defined as bus voltage at 1 p.u and angle at 0° making it a reference bus thus allowing all other angles to be calculated related to this voltage (V) and angle (δ).

3.6 Python Based Solution of Wind Scenario 2040

In the default form of calculation using PSS/E, a certain power system model is first defined with all different types of generators, loads, transmission line, transformers, circuit breaker, shunt elements etc. and the parameter values for each of these components are passed in PSS/E. These parameters are related to its steady state as well as transient response behaviour. For example, in defining a synchronous generator where its steady state power factor (PF) is defined, its *subtransient reactances* are also defined. Similarly when a load is defined in PSS/E, not only its steady state active and reactive powers are defined but also its *in-rush* and frequency change dependent behaviours are also defined and so on. Due to this, as the components are defined in more depth and more details, the results gets more accurate. After everything is defined such as total generation and total load, then to run a dynamic simulation following steps in PSS/E are taken to get the results.

- Applying Newton-Raphson for Steady State Results ($FNSL$)
- Converting Generator and Load to Current Source ($CONG$)
- Ordering of Buses to Maintain Sparsity of *Jacobian Matrix* ($ORDR$)
- Factorising Network Admittance Matrix ($FACT$)
- Solving the Network for Boundary Conditions ($TYSL$)
- Solving for User Defined Transient Conditions, e.g $L - L$ Faults

However, to simulate the condition where the generation and load consumption is changing in time as in year-long hourly data of generation and load consumption taken from *Svenska Kraftnät SvK* needs another approach. To simulate for the system voltage and frequency variation based on generation and load consumption for *Wind Scenario 2040*, it means running the above mentioned steps 8760 times using PSS/E. This becomes too much time consuming and not efficient. But using Python, it is possible to automate the whole process of reading the hourly data from a file and then indirectly run all the steps individually for each hour and iterate throughout 8760 hours and save the time for manually running each step. To run each individual step mentioned above, the application program interface (API) are used that connects *Python* and PSS/E software and runs PSS/E steps using *functions* defined for collaboration of two separate programs to run them simultaneously and in unison. The Figure 3.10 shows process in form of flowchart.

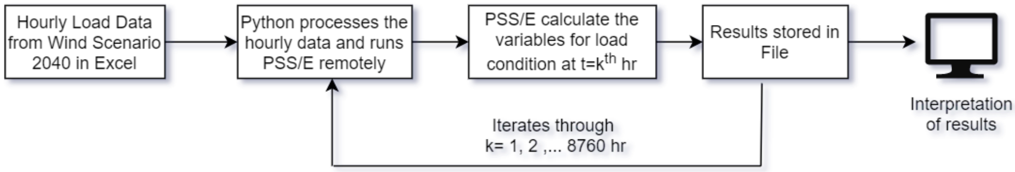

Figure 3.10: Python Based PSS/E Approach

3.6.1 Generation and Load Variation Approach

In *Wind Scenario 2040*, Hydro and Wind are the main source of electricity production. Hydro Power Plants are modeled as synchronous generators and Wind Turbines are modeled as Doubly-Fed Induction Generator ($DFIG$). As the data from *SvK* is in hourly basis. Therefore the information for change of parameters for a synchronous generator such as voltage, magnetic flux, active and reactive power is missing in between the *1-hour interval.* For example, after an hour, the generation from *SvK* data shows a sudden jumps from a high to low value and *vice-versa* which is theoretically not possible in a synchronous generator due to its relatively slow dynamic response defined by armature time constants T_a or along *d-axis* T_d, T_d', T_d'' [38]. Hence the hourly generation of Hydro will not be read by *Python.* Instead electricity production from of Hydro will be taken initially equal to its total expected installed capacity in *Wind Scenario 2040* equal to 17GW and will be used as *boundary-conditions* during transients such as its change in terminal voltage, active and reactive power etc. during the load variations.

Similarly for the case of Wind Turbines, the hourly data for electricity generation will not be read by *Python.* This is due to the fact that it is out of scope for this thesis. As the thesis is based on the effect of load variation on the system voltage and frequency when the generation from Hydro Power Plant and Wind Turbine are in steady-state and in stable operation, rather the reverse. In case of electricity generation from Wind, it is fluctuating and creates variation in system voltage and frequency. Instead electricity production from Wind will be taken initially equal to its total expected installed capacity in *Wind Scenario 2040* equal to 27GW and will also be used as *boundary-conditions* during transients such as its change in terminal voltage, active and reactive power etc. during the load variations.

Only the hourly data for load consumption from SvK will be read by *Python* and its effect on synchronous generators and $DFIG$ will be simulated. The results for system voltage and frequency stability will be discussed such as $ROCOF$, 'zenith' or 'nadir' for system frequency. Also the terminal voltage stability during *sudden load rise/drop* on hourly basis for each type of generation will be discussed in detail to predict the power system voltage and frequency stability for *Wind Scenario 2040.*

4

Methods

For this thesis work, an imaginary 5-bus power system is defined, which consists of three generation units i.e. two of them based on Hydro Power Plant and other based on Wind Turbines and a load connected to a bus drawing an real and imaginary power, as shown in Figure 4.1.

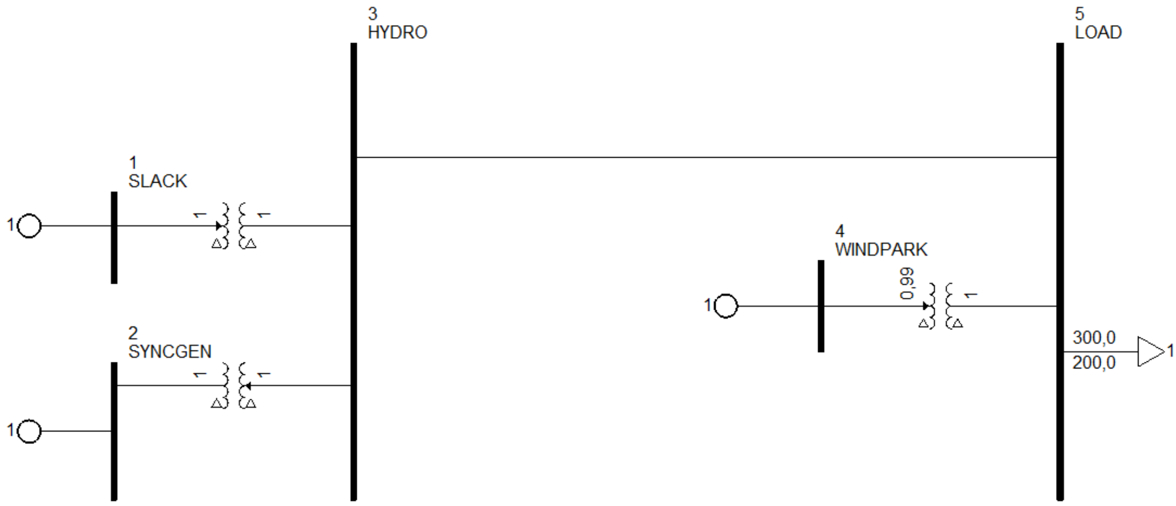

Figure 4.1: Model of the Power System in PSS/E

In order to model a system such as based on *Wind Scenario 2040* expected to dominate the Swedish Grid in the future, certain assumptions have been made for this thesis work. It is assumed that the Swedish power system in the future will be mainly based heavily on Hydro Power Plants and Wind Turbines. Hydro Power Plants will supply electricity as well as inertia as it is based on rotating mass that is always connected to the system physically. Therefore it helps the power system to have better stability during disturbances as explained in the section *Theory of Renewable Power Grid*. It is also assumed that in future the Swedish Grid will have Wind Turbines providing highest supply of electricity based on intermittent nature of wind. We assume that the installed capacity of Wind Turbines will be almost 4 times higher than installed capacity of Hydro Power Plants. For these above mentioned reason, a system solely based on Hydro and Wind Turbine is defined.

Different component of the power system is defined in the Table below.

Power System	
Component	Connection Point
Synchronous Generator (SLACK)	BUS1
Synchronous Generator (SYNCGEN)	BUS2
Wind Turbine (WINDPARK)	BUS4
Transformers T1	BUS1-BUS3
Transformers T2	BUS2-BUS3
Transmission Line 33 kV	BUS3-BUS4
Load	BUS5

4.1 Steady Sate Modeling of Power System

In PSS/E, a power system is solved first for steady state conditions before solving for dynamic conditions, as steady state solution provide the *boundary-conditions* for the dynamic simulations. For the steady state solution, below initial conditions for the power system are selected in per unit system *p.u* shown in Figure 4.2 - 4.5

Bus	Bus	VSched	In	PGen	PMax	PMin	QGen	QMax	QMin	Mbase	X Source	Grounding Z	Wind machine	Wind Machine
1	SLACK	1,0000	☑	-6,6454	9999,0010	0,0000	60,9225	9999,0010	0,0000	360,00	1,000000	P.U. (Per Unit)	Not a wind machine	1,000
2	SYNCGEN	1,0000	☑	55,0000	50,0000	0,0000	30,0000	30,0000	0,0000	360,00	1,000000	P.U. (Per Unit)	Not a wind machine	1,000
4	WINDPARK	1,0000	☑	252,0000	252,0000	11,2000	122,0492	122,0492	-122,0492	360,00	9999,000000	P.U. (Per Unit)	+, - Q limits based on WP	0,900

Figure 4.2: P and Q Injection at different buses

Bus	Bus	Base kV	Area	Zone	Voltage	Normal	Emergency	Emergency
1	SLACK	13,8	1	1	1,0000	1,1000	1,1000	0,9000
2	SYNCGEN	13,8	1	1	0,9886	1,1000	1,1000	0,9000
3	HYDRO	33,0	1	1	0,9777	1,1000	1,1000	0,9000
4	WINDPARK	3,3	1	1	0,9116	1,1000	1,1000	0,9000
5	LOAD	33,0	1	1	0,9165	1,1000	1,1000	0,9000

Figure 4.3: Voltages and Angles at different buses

From Bus	To Bus	Name	Controlled	Tap Positions	Control Mo	Auto	Winding	Specified R	Specified X	Wnd 1 Ratio	Rmax	Rmin	Connection
SLACK	HYDRO		3	33	Voltage	☑Yes	Turns ratio (pu on bus base kV)	0,000100	0,110000	1,0000	,10000	,99000	4 - No series or ground paths
SYNCGEN	HYDRO		3	33	Voltage	☑Yes	Turns ratio (pu on bus base kV)	0,000100	0,110000	1,0000	,10000	,90000	4 - No series or ground paths
WINDPARK	LOAD		5	33	Voltage	☑Yes	Turns ratio (pu on bus base kV)	0,000000	0,010000	0,9900	,10000	,99000	4 - No series or ground paths

Figure 4.4: Transformer Parameters

From B	To Bus	Line R	Line X	Charging B	In	Metered
HYDRO	LOAD	0,010000	0,001000	0,200000	☑	☑From

Figure 4.5: Transmission Line Parameters

Using these initial conditions for the power system, the steady state as well as dynamic state solution can be calculated using PSS/E. When it comes to dynamic simulations, additional information regarding the transformers, load machines electrical and mechanical parameters as well as information about the voltage regulators, excitation system and power system stabilizes etc are required to do the dynamic simulation, which will be dealt with in coming sections.

4.1.1 Steady State Result of Power System

Using Newton-Raphson method as explained in the *Theory of Renewable Power Grid*, a steady state solution is arrived at. As can be seen in the Figure 4.6, both generation unit combine to provide for the required electricity demand at the *Load Bus*.

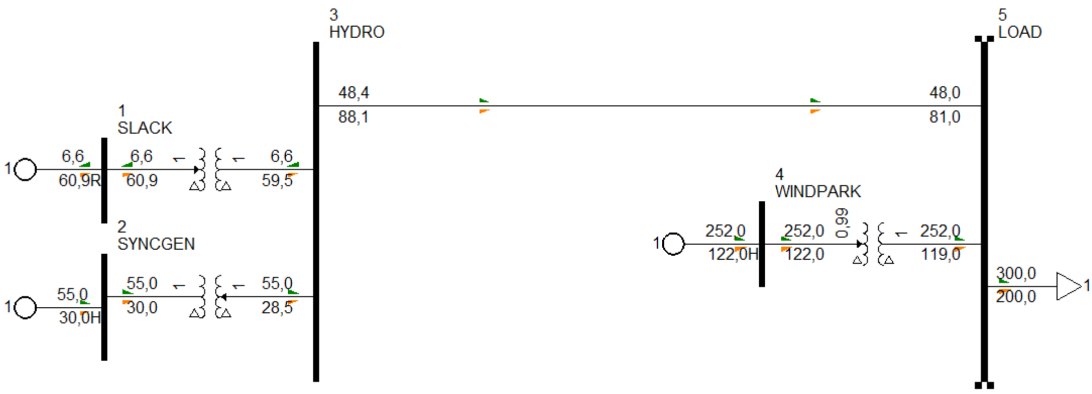

Figure 4.6: Steady State Solution of Power System

Also it can be noted that for a load consumption of $300MW$ and $200MVAR$, the Wind Turbines provides almost 80% of it as it has 4 times more installed capacity than the Hydro Power Plants as expected in the future for Swedish power system. The *SLACK* bus, being a swing bus, keep the bus voltage at 1 p.u and angle at $0°$ and all the other angles for different buses are calculated relative to this angle. Due to the transformers T1 and T2 and transmission line having a resistive and reactive component, the power flows through them are calculated accordingly. The green arrow on Figure 4.6 shows the direction of active power flow and the orange arrow shows the direction of reactive power flow. It can be seen that the transformer absorbs the reactive power.

4.2 Dynamic State Modeling of Power System

In order to analyze the power system behaviour such as active and reactive power, voltage, frequency, speed of the machine and rotor angle variations, dynamic simulations are used. The methods that PSS/E uses has been discussed earlier in chapter *Theory of Renewable Power Grid*. In order to perform the dynamic simulation of the power system, certain in-built models are defined in the PSS/E for each component of the power system. It is entirely up to the user to choose which model to use based on the complexity. In most cases, a more complex and a thorough model with many differential equations explains the behaviour of the system with accurate results.

As the power system that is defined in the thesis has two different type of generation; one based on synchronous generator and other as doubly fed induction generator ($DFIG$), so the constant, variables and differential equations used for the dynamic simulations are shown in detail in Appendix A and shown briefly below in the table.

4.2.1 Modeling of $SYNCGEN$ and $SLACK$

Both $SYNCGEN$ and $SLACK$ generation units are based on synchronous generator. Following types of models are used for these two generation units. The detail of each model is shown in Appendix. $GENSAL$ is a salient pole synchronous generator model that has mechanical power as input coming from the $HYGOV$ based turbine model and field voltage as input from the $SEXS$ excitation system model. The output of $GENSAL$ comprises of source current, voltage, speed and angle as the output. This source current is used in the *Norton-Equivalent Model* during the dynamic simulations. The input to the excitation system mainly comes from the output of $IEEEVC$ based *automatic voltage regulator* (AVR) and the output of $STAB2A$ based *power sensitive stabilizer*.

Model	Type
$GENSAL$	*Generator Model*
$SEXS$	*Exciter Model*
$HYGOV$	*Turbine Model*
$STAB2A$	*Stabilizer Model*
$IEEEVC$	*Compensator Model*

4.2.2 Modeling of $WINDPARK$

A wind turbine in its simplest form is a drive-train consisting of a shaft that rotates based on the wind energy and is then connected to the generator through a gearbox and the electrical power is produced at the stator of the generator that is then connected to the grid directly or indirectly. In the case of $WINDPARK$, these different component of the wind turbine are defined by the models in the table below.

Model	Type
$WT3G1$	*Generator Model*
$WT3E1$	*Electrical Model*
$WT3T1$	*Turbine Model*
$WT3P1$	*Pitch Model*

In this thesis work, $WT3G1$ based on General Electric (GE) $3.6MW$ Wind Turbine is used for the generator model, It is based on Doubly-Fed Induction Generator and takes E_q and I_q as inputs from the converter control based on $WT3E1$. The output of $WT3G1$ consists of a active and reactive power injection as well as real and imaginary component of terminal voltage. As can be noted, P_{rated} is $3.6MW$, which is the value for rated active power for one wind turbine.

In in order to model wind park, many wind turbines rated for $3.6MW$ each can be connected in series. In this thesis work 70 such wind turbines is connected to generate a total of $252MW$. When it comes to modeling, it is assumed that all these wind turbines behaves similarly.

Parameter	Value
Rating	*4 MVA*
P_{max}	*3.6 MW*
P_{min}	*0.16 MW*
Q_{max}	*2.08 MVAR*
Q_{min}	*-1.55 MVAR*
$V_{terminal}$	*3.3 kV*
$Z_{transformer}$	*7 %*

4.3 Dynamic State Result of Power System

The dynamic simulation is started at $t = 0$ and run until $t = 55s$. At $t = 15s$, a bus fault is created at Load Bus and applied for total of $200ms$ and fault is cleared at $t = 15.2s$. The fault properties are defined as

Constant	Value
Voltage	0 V
Resistance	0 Ω
Reactance	$-2 \times 10^9 \Omega$

Below are the plots shown in Figures 4.7 - 4.12, that is expected for a power system having a high penetration of wind and less hydro electricity production. The terminal voltages, rotational speed, active and reactive powers of the generators and the overall system frequency seen at the *Bus No 5* are simulated until $t = 55s$

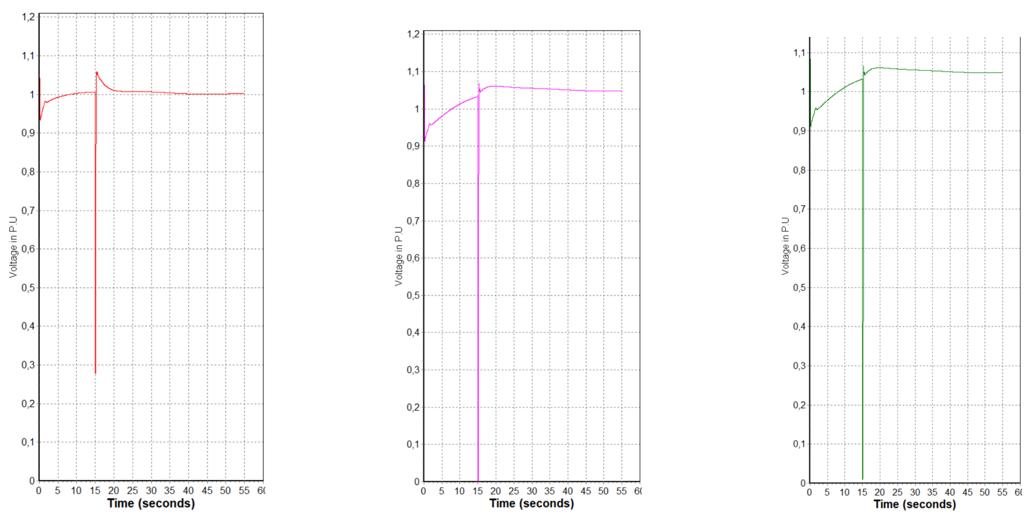

Figure 4.7: Left (Bus Voltage at HYDRO) – Middle (Bus Voltage at LOAD) – Right (Bus Voltage at WINDPARK)

Due to the bus voltage at the *Load Bus* drops to zero, the bus located close to it i.e $WINDPARK$, its terminal voltage also drops close to zero as well. But as the $HYDRO$ is lies far from the fault and is separated by a transmission line with almost $100 - km$ in length, therefore the voltage at $HYDRO$ is not as severe and only drops to around *0.3 p.u.* As soon as the fault is cleared at $t = 15.2s$ all bus voltage rises to its pre-fault nominal voltages in $2s - 3s$.

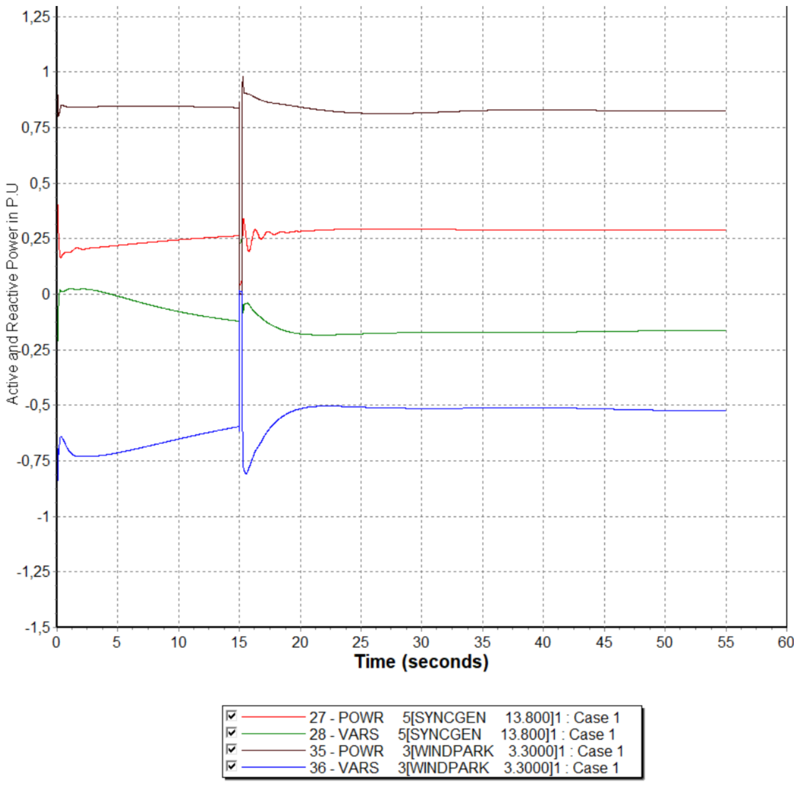

Figure 4.8: Active and Reactive Power of Generators

As it can be noted in Figure 4.8, during the fault the active power for both type of generation i.e $WINDPARK$ and $HYDRO$ starts decreasing towards zero as the load $P_{load} = 0$. Due to this, the reactive power increases and starts to feed the fault with reactive current and continues to increase until the fault is cleared. When the fault is cleared the active power starts increasing while reactive power starts decreasing and becomes stable after the transients. It is worth mentioning that the stable points for $SYNCGEN$ and $WINDPARK$ is reached at different time based on the models and its parameters defined in the Appendix. It is however interesting to see the behaviour of a wind turbine based on $DFIG$ technology. During the fault the active power injection towards the power system becomes zero but wind blades is still rotating due to wind and still produces unwanted kinetic energy that can be controlled using pitch control technique.

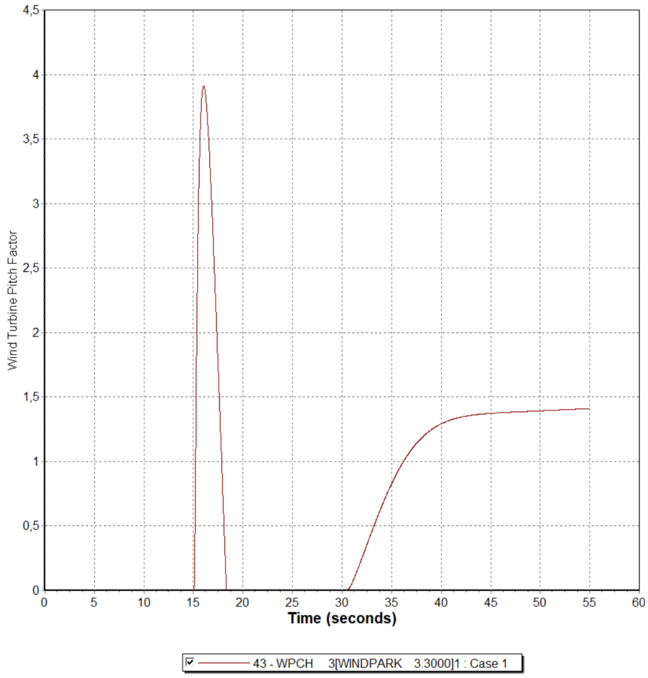

Figure 4.9: Pitch Angle of Wind Turbine

At the moment when the active power requirement of $WINDPARK$ becomes zero, the pitch control takes effect as shown in Figure 4.9 and starts positioning the angle of blades against the wind impact in such a way so as to reduce the kinetic energy produced at the shaft of the generator. Due to this, the mechanical power generated at the shaft of the wind turbine starts reducing until the fault is cleared at 15.2s as shown in Figure 4.10.

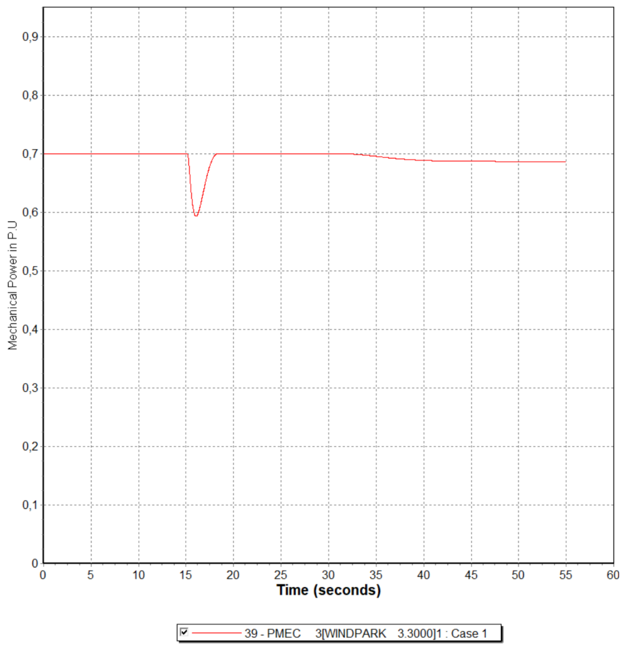

Figure 4.10: Input Mechanical Power for DFIG Generator

The speed variation for $SYNCGEN$ and $WINDPARK$ is shown in Figure 4.11. The speed variation is explained earlier in *Theory of Renewable Power Grid* using the *Swing Equation*.

$$\frac{2H}{\omega_r}\frac{d^2\delta}{dt^2} = P_m - P_e \tag{4.1}$$

When the mechanical power is higher than the electrical power, the rotor speed increase and vice versa. In this case during the fault between 15s until 15.2s, the electrical power injection of $WINDPARK$, becomes zero due to the terminal voltage on the $WINDPARK$ becoming zero as shown in Figure 4.7 and 4.8. But as shown in Figure 4.10, the mechanical power still remains positive during the fault condition. Due to this mismatch of higher mechanical and almost zero electrical power, the rotor speed starts to increase until the fault is cleared and the mechanical and electrical power equalizes after certain time. At this instant $\frac{d^2\delta}{dt^2}$ becomes zero and the $DFIG$ generator is said to be in a steady-state operation.

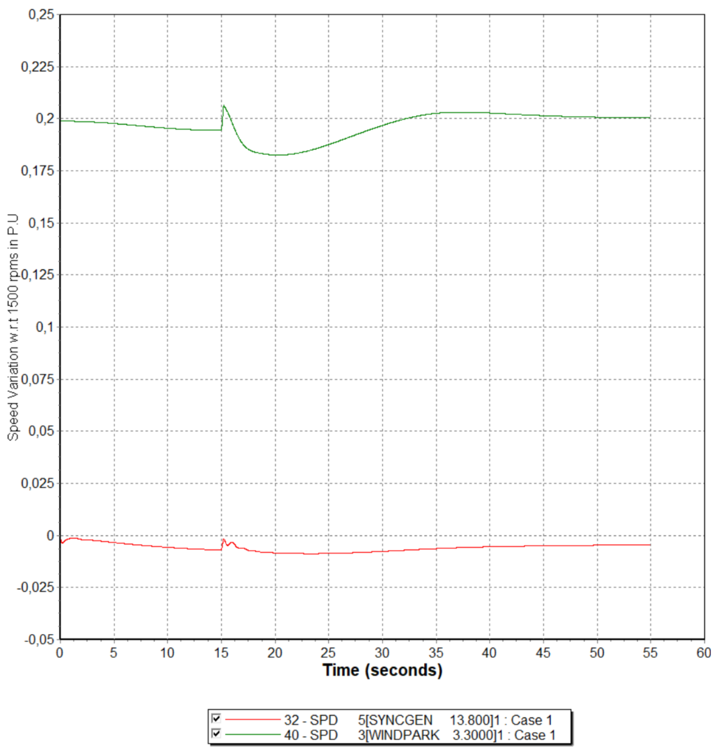

Figure 4.11: Speed Variation of Generators

The system frequency variation can be explained by the active power mismatch between generation and load. When the bus fault is applied at the *Load Bus*, then suddenly terminal voltage becomes zero and $P_{load} = 0$. When the requirement for the active power reduces, the synchronous and $DFIG$ generators quickly reduces its active power injection as well to follow the load demand.

During these instants in time, the active power generation is still higher than the active power consumption due to which the system frequency rises until the bus fault is cleared. At the instant when the bus fault at *Load Bus* is suddenly cleared, the active power from the synchronous and $DFIG$ generators is lower than the total load consumption due to which the system frequency starts to drop. The generators then again starts to produce more power as it sees a higher requirement to inject power. Due to this the system frequency again starts to rise and eventually come back to its stable *pre-fault* nominal level of around *50 Hz* as shown in Figure 4.12.

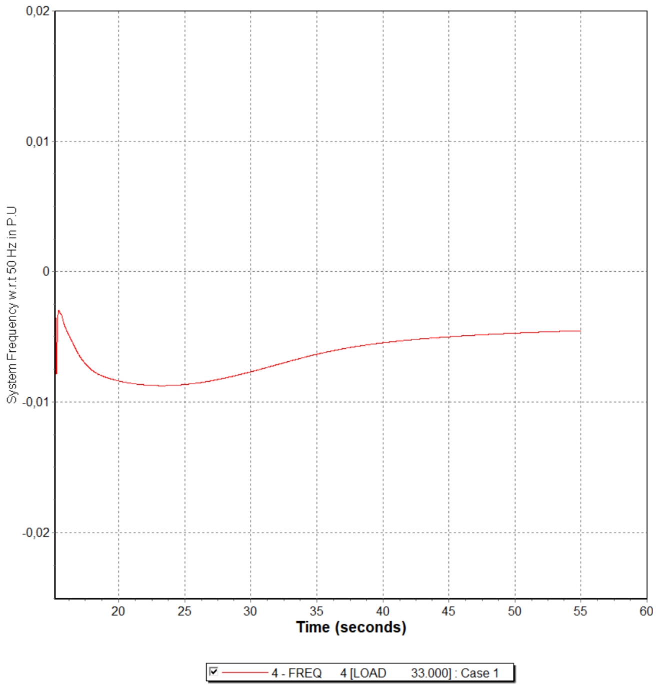

Figure 4.12: System Frequency of Power System

4.3.1 System Frequency and Addition of Inertia

As the wind penetration increases in the future, the system frequency will becomes prone to a lot of over-frequency and under-frequency occasions that can be a cause of damage to the power plants and also to the consumers. Due to this, different techniques are being studied such as using energy storage batteries based *ancillary services* that produce active power to support frequency dips [39]. Also other techniques are studied such as adding *Synchronous Condensers* which are able to provide voltage stability and frequency stability due to its rotating mass by increasing the equivalent inertia H_{eq} of system. In the following simulation, two cases are studied. *Case 1* is the system frequency based on earlier simulations without any addition of extra inertia, while *Case 2* is the system frequency with the addition of inertia from *Synchronous Condensors*. It is assumed that in *Case 2*, the H_{eq} increases twice. The results are shown in Figure 4.13

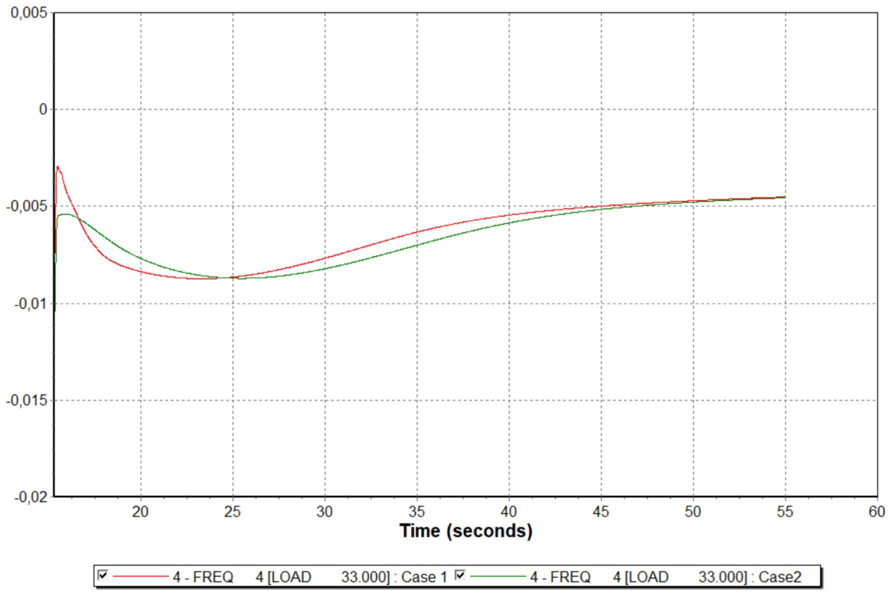

Figure 4.13: System Frequency
Case 1 (Red): Normal Condition
Case 2 (Green): Addition of Extra Inertia

As it can be noted that when the H_{eq} is increased, the system frequency has reduction in over-frequency at fault condition and also has less df/dt after the fault is removed. Although for both cases, there is no improvement in the *nadir* of the system frequency as well as the time to arrive at $df/dt \approx 0$. However other techniques have been studied that uses control algorithms to improve the slope of frequency variation and time to arrive at $df/dt \approx 0$ such as *Fast Frequency Response FFR* technique [40], that uses five different algorithm phases for the system frequency inertial support defined below.

- Activation phase decides when to disconnect *Maximum Power Point Tracking* MPPT controller of wind turbine to ensure the requirement of power is fulfilled even if the wind speed changes

- Support phase provides the kinetic energy from turbine to the power system based on the aerodynamic efficiency variation

- Transition phase decides when to move to the next phase of recovery phase

- Recovery phase helps to recover to the pre-disturbance rotor speed. Depending on the need of the system to withstand additional power imbalances, this can be prolonged or shortened

- Reconnection phase helps to switch back to *Maximum Power Point Tracking* MPPT in a controlled manner

4.4 Voltage and Freq. for Year 2040 using Python

In order to analyze how the yearly load variations will affect the power system voltage and frequency stability, it is possible to run the dynamic simulation for a large number of load variations (total $8760 - hrs$) using Python. In the simulation performed earlier, the nominal steady-state load was taken to be $P_{load} = 300MW$ and during fault condition for $200ms$ it was changed to $P_{load} = 0$ with a step-change and the results for voltage, frequency, active and reactive power, mechanical power, rotor speed and pitch angle were plotted.

A similar approach can be used for the network simulation with a large number of load variations. As explained in the Section 3.6, *Wind Scenario 2040* load variation data for $8760 - hrs$ is taken as input. As the load variation data for *Wind Scenario 2040* is in the range of $10,000 - 15,000MW$, therefore the network defined in the above simulation is also scaled by $50 : 1$. This means all ratings of lines, transformers, active and reactive power generations are increased by fifty times to fulfil a higher load demand. The excel file used as an input to *Python-PSS/E* combination has load variation data after every hour. So it will be assumed that load variation act as a step-change after every hour and remains constant in $1 - hour$ time interval between load variation data. Figure 4.14 and 4.15 shows the results for voltage and frequency variation for *Wind Scenario 2040*, respectively.

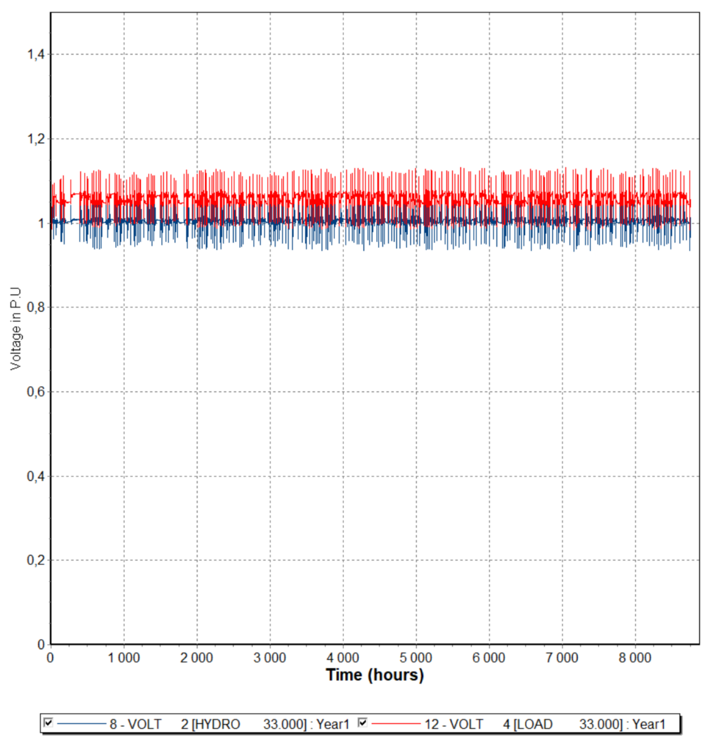

Figure 4.14: Expected Voltages at Different Buses for Wind Scenario 2040

As it can be noted in the Figure 4.14 that the voltage level is on average around 1.0-1.05 p.u. with instantaneous voltage rise and drop during load variation of around 1.15 p.u. and 0.95 p.u. at sudden load rejection and application, respectively. It can be clearly noticed that during the load variation for the network defined with *4 times* higher electricity generation from wind compared to electricity generation from hydro, the power system defined by models and parameters will be able to maintain the voltage stability during load variations.

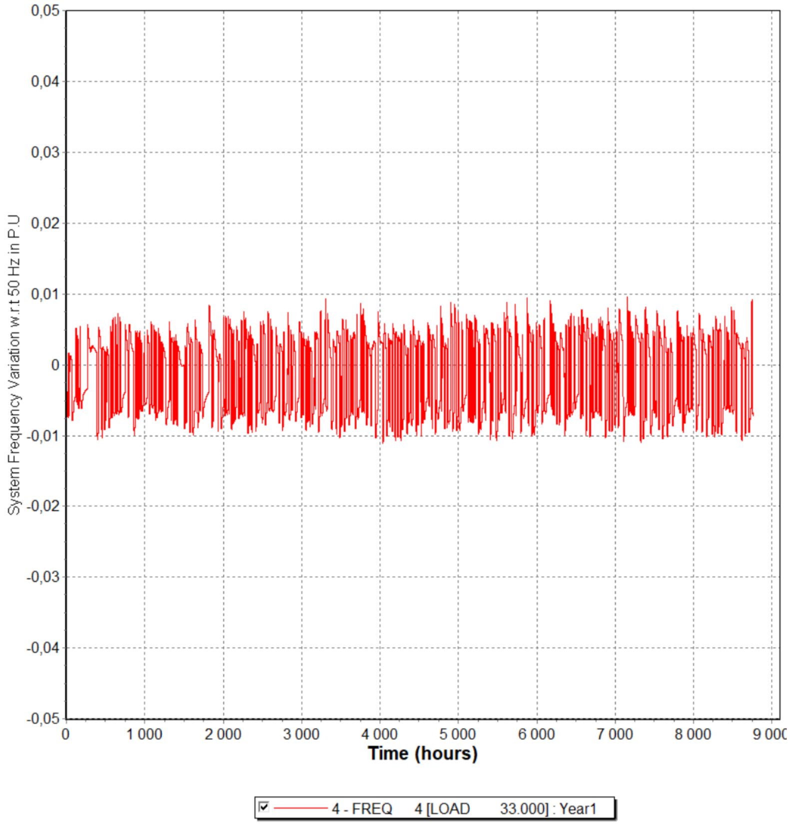

Figure 4.15: Expected System Frequency for Wind Scenario 2040

Similarly it can be noticed in Figure 4.15 that with less synchronous generators in power system and high penetration of wind turbines, the frequency swing of system is in range of ±1% for the hourly load variations. Therefore for the future Swedish power system, it is expected that the frequency tolerance (*deadband*) for activation of primary frequency control will have to be increased from the current ±0.2% i.e. between (49.9 - 50.1 Hz) to ±1% i.e. between (49.5 - 50.5 Hz) during normal hourly load variations [41]. This can affect the designs of the power system components in the future such as the design of generators, transformers to operate with higher voltage and frequency variation under normal operating conditions as well higher voltage and frequency variations for short-time transients such as the requirements recently outlined in *VDE German Grid Code* for Synchronous and Wind Turbine Generators [42].

5
Conclusion and Future Recommendation

5.1 Conclusion

At present, the Swedish Electric Power System (EPS) has a balanced combination of conventional and non-conventional generation technologies in the energy mix. Nuclear and Hydro has strong inertia support due to rotating mass physically connected to the power system while non-conventional generation technologies have either reduced inertia support or fully absent as in the case of Wind and Solar technologies, respectively. Due to presence of Nuclear Energy supplying a stable source of electricity to the base load throughout the year and Hydro Power Plant acting as load-follower, any additional electricity generated from intermittent source of energy − such as wind or solar − makes the total electricity production in the power system higher than total load and produces excess electricity in the power system, which is then exported and traded with other countries.

Due to this, in 2019 almost $24TWh$ was exported to other countries and only $2TWh$ imported. But this high export is not seen for the *Wind Scenario 2040* when scaling factors as in Figure 2.13 is used that involves *phasing-out* of Nuclear Energy and high increase of wind penetration. Based on the results, $60TWh$ of electricity will be produced due to threefold increase in installed capacity of wind turbines in 2040. To further increase the electricity generated from wind turbines close to the $100TWh$ range as predicted by Swedish Wind Energy, new installations can be done in those area which receive more wind throughout the year and wind turbines can also be made more energy efficient. It is expected that if Wind Scenario 2040 is implemented, the available electricity to export in 2040 will be reduced to $10TWh$ and a considerable increase in import of around $16TWh$ will be required. To reduce the import, heavy investments in other technologies such as Solar is necessary to have an improved energy balance. Due to a higher mismatch between supply and demand, the system voltage and frequency stability will be compromised, unless frequency support control algorithms and back-up power based on energy storage batteries etc. are not implemented to support the power system during the short-lived load variations or longer disturbances in the power system.

The transport sector in Sweden having combustion engine based drive-train currently consumes around $70TWh$ of energy. However if the all vehicles that are based on combustion engines are replaced by Electric Vehicles (EVs), then consumption of energy will be reduced to $15-20TWh$ due to $70-80\%$ more efficient drive-train in the Electric Vehicles (EVs). In this thesis, it was indicated that additional $10TWh$ that is generated due to high wind penetration can be used as available capacity to integrate additional Electric Vehicle (EVs) load demand of $3100MW$ every hour for $3227-hrs$.

It is concluded that if *Wind Scenario 2040* is implemented, then available electricity will not be enough to supply almost $19TWh$ of Electric Vehicle (EVs) charging demand and investments in more Wind or Solar will be required to improve energy balance. Other ways that can be used in the future to improve the energy balance is based on *Demand Side Management* techniques. Among others, only one technique was briefly touched in this thesis that uses the charging the Electric Vehicles (Evs) at certain instants with peak generations. In this thesis work, the FFT analysis on the generation of electricity from Wind was studied. It indicated that the peak generation of electricity arrives after every three days period and $24-hrs$ and $12-hrs$ interval. Therefore Electric Vehicles (EVs) can be charged *in-phase* with peak generation from Wind to improve energy balance and reduce the burden on the future Swedish Electric Power System (EPS).

5.2 Future Recommendation

- In this thesis work, for the calculation of energy balance of future Swedish Electric Power System (EPS), only one scenario was studied that is based on a high penetration of Wind, equivalent to about 300% increase in the current installed capacity. It was also based on *phasing-out* of Nuclear Energy and other generation technologies capacity change based on Figure 2.12 and 2.13. However, it is only one scenario among many that can happen in the future. Therefore it is recommended that future studies can use different scenario and different scaling factors to arrive at the conclusions of energy balance and hourly electricity trade shown in Figure 2.14 and Figure 2.16, respectively. Due to hourly electricity trade results for different scenarios, the possible Electric Vehicle (EVs) load integration will also be different for different scenarios that can be investigate in future.

- The Fast Fourier Transform analysis is based on combined hourly electricity generation data. However, to get accurate results, the sampling rate for electricity production can be increased by increasing resolution in time to minutes instead of hours to increase accuracy of results. During the analysis it was assumed that all wind turbines in Sweden are located close to each other due to which all the wind turbine experience same wind parameters such as pressure of air or its direction. However the Wind Turbine in reality will be spread at different locations in Sweden and will experience different wind parameters.

Therefore it is recommended to analyse for each generation areas in Sweden such as $SE1$, $SE2$, $SE3$ and $SE4$ [43] to analyze if there is a difference in number of days and hours when the peaks arrive for different generation areas in Sweden.

- The PSS/E and Python based simulation is performed on an imaginary 5-bus power system with a detailed modeling of generation technologies Hydro and Wind but a very basic modeling for transmission lines and transformers. It is recommended to increase the complexity of the network to make it look more close to the reality with addition of components such as circuit breakers, shunt reactors and capacitors etc and their modeling to analyze the system voltage and frequency during short-lived load variations and large disturbances in the power system. To achieve this, it is recommended to use *CIGRE Nordic 32-Bus System* and modeling of each individual component to perform the simulations and arrive at more accurate results for expected system voltage and frequency variations for future Swedish Electric Power System (EPS) based heavily on Renewable Energy Sources (RES).

6

Appendix

6.1 Hydro Power Plant Modeling

6.1.1 Generator Model

1.21 GENSAL

Salient Pole Generator Model (Quadratic Saturation on d-Axis)

This model is located at system bus	#_____	IBUS,
Machine identifier	#_____	ID,
This model uses CONs starting with	#_____	J,
and STATEs starting with	#_____	K.

The machine MVA is _________ for each of units = _________ MBASE.

ZSORCE for this machine is _________ + j _________ on the above MBASE.

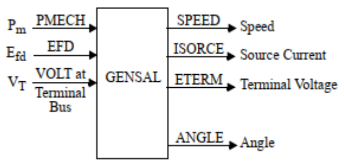

CONs	#	Value	Description
J			T'_{do} (>0) (sec)
J+1			T''_{do} (>0) (sec)
J+2			T''_{qo} (>0) (sec)
J+3			H, Inertia
J+4			D, Speed damping
J+5			X_d
J+6			X_q
J+7			X'_d
J+8			$X''_d = X''_q$
J+9			X_l
J+10			S(1.0)
J+11			S(1.2)

Note: X_d, X_q, X'_d, X''_d, X''_q, X_l, H, and D are in pu, machine MVA base.

X''_q must be equal to X''_d.

STATEs	#	Description
K		E'_q
K+1		ψkd
K+2		ψ''q
K+3		Δ speed (pu)
K+4		Angle (radians)

IBUS, 'GENSAL', ID, CON(J) to CON(J+11) /

Figure 6.1: GENSAL Model

	Con Value	Con Description
1	5,0000	T'do (> 0)
2	0,0500	T''do (> 0)
3	0,1000	T''qo (> 0)
4	3,0000	Inertia H
5	5,0000	Speed Damping D
6	1,1000	Xd
7	0,7000	Xq
8	0,2500	X'd
9	0,2000	X''d = X''q
10	0,1500	X1
11	0,1000	S(1.0)
12	0,3000	S(1.2)

Figure 6.2: GENSAL Parameters

6.1.2 Exciter Model

6.58 SEXS

Simplified Excitation System

This model is located at system bus	#_____	IBUS,
Machine identifier	#_____	ID,
This model uses CONs starting with	#_____	J,
and STATEs starting with	#_____	K.

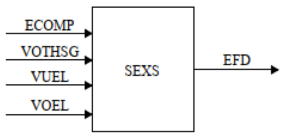

CONs	#	Value	Description
J			T_A/T_B
J+1			T_B (>0) (sec)
J+2			K
J+3			T_E (sec)
J+4			E_{MIN} (pu on EFD base)
J+5			E_{MAX} (pu on EFD base)

STATEs	#	Description
K		First integrator
K+1		Second integrator

IBUS, 'SEXS', ID, CON(J) to CON(J+5) /

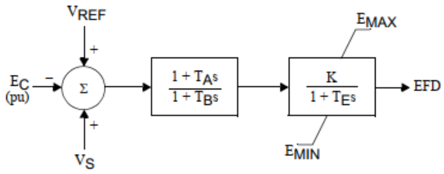

V_S = VOTHSG + VUEL + VOEL

Figure 6.3: SEXS Model

	Con Value	Con Description
1	0,2000	TA/TB
2	20,0000	TB (> 0)
3	50,0000	K
4	0,1000	TE
5	0,0000	EMIN
6	4,0000	EMAX

Figure 6.4: SEXS Parameters

6.1.3 Turbine Model

7.9 HYGOV

Hydro Turbine-Governor

This model is located at system bus	#_____	IBUS,
Machine identifier	#_____	ID,
This model uses CONs starting with	#_____	J,
and STATEs starting with	#_____	K,
and VARs starting with	#_____	L.

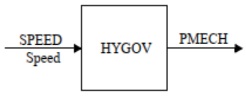

CONs	#	Value	Description
J			R, permanent droop
J+1			r, temporary droop
J+2			T_r (>0) governor time constant
J+3			T_f (>0) filter time constant
J+4			T_g (>0) servo time constant
J+5			± VELM, gate velocity limit
J+6			G_{MAX}, maximum gate limit
J+7			G_{MIN}, minimum gate limit
J+8			T_W (>0) water time constant
J+9			A_t, turbine gain
J+10			D_{turb}, turbine damping
J+11			q_{NL}, no power flow

STATEs	#	Description
K		e, filter output
K+1		c, desired gate
K+2		g, gate opening
K+3		q, turbine flow

VARs	#	Description
L		Speed reference
L+1		h, turbine head

R, r, and D_{turb} are in pu on generator MVA base.

IBUS, 'HYGOV', ID, CON(J) to CON(J+11) /

All material contained in this documentation is proprietary to Siemens Industry, Inc., Siemens Power Technologies International.

7-25

Figure 6.5: HYGOV Model

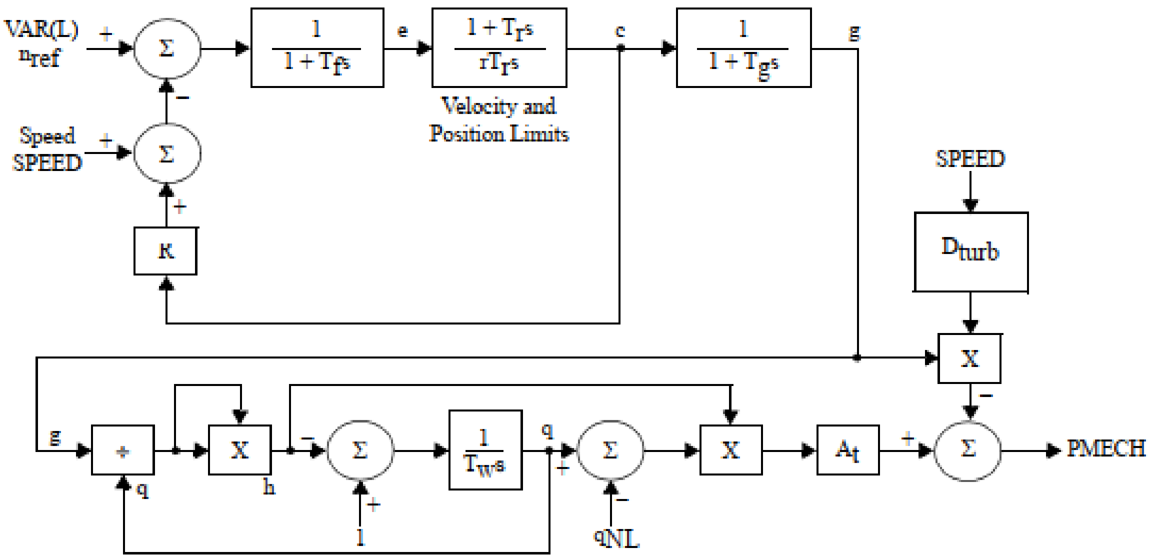

Figure 6.6: HYGOV Model

	Con Value	Con Description
1	0,0400	R, Permanent Droop
2	0,8000	r, Temporary Droop
3	5,0000	Tr (> 0) Governor Time Constant
4	0,0500	Tf (> 0) Filter Time Constant
5	0,1000	Tg (> 0) Servo Time Constant
6	0,1000	VELM, Gate Velocity Limit
7	0,9500	GMAX, Maximum Gate Limit
8	0,0000	GMIN, Minimum Gate Limit
9	1,0000	TW (> 0) Water Time Constant
10	1,0000	At, Turbine Gain
11	0,0000	Dturb, Turbine Damping
12	0,0000	qNL, No Load Flow

Figure 6.7: HYGOV Parameters

6.1.4 Stabilizer Model

3.16 STAB2A

Power Sensitive Stabilizing Unit (ASEA)

This model is located at system bus #_______ IBUS,
Machine identifier #_______ ID,
This model uses CONs starting with #_______ J,
and STATEs starting with #_______ K.

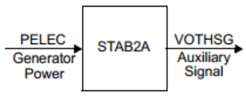

CONs	#	Value	Description
J			K_2
J+1			T_2 (sec) (>0)
J+2			K_3
J+3			T_3 (sec) (>0)
J+4			K_4
J+5			K_5
J+6			T_5 (sec) (>0)
J+7			H_{LIM}

STATEs	#	Description
K		Implicit
K+1		Integration
K+2		State
K+3		Variables

IBUS, 'STAB2A', ID, CON(J) to CON(J+7) /

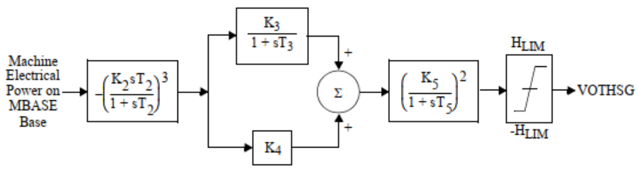

All material contained in this documentation is proprietary to Siemens Industry, Inc., Siemens Power Technologies International.

Figure 6.8: STAB2A Model

	Con Value	Con Description
1	1,0000	K2
2	4,0000	T2 (> 0)
3	1,0000	K3
4	2,0000	T3 (> 0)
5	0,3000	K4
6	1,0000	K5
7	0,0500	T5 (> 0)
8	0,0500	HLIM

Figure 6.9: STAB2A Parameters

6.2 Wind Turbine Modeling

6.2.1 Generator Model

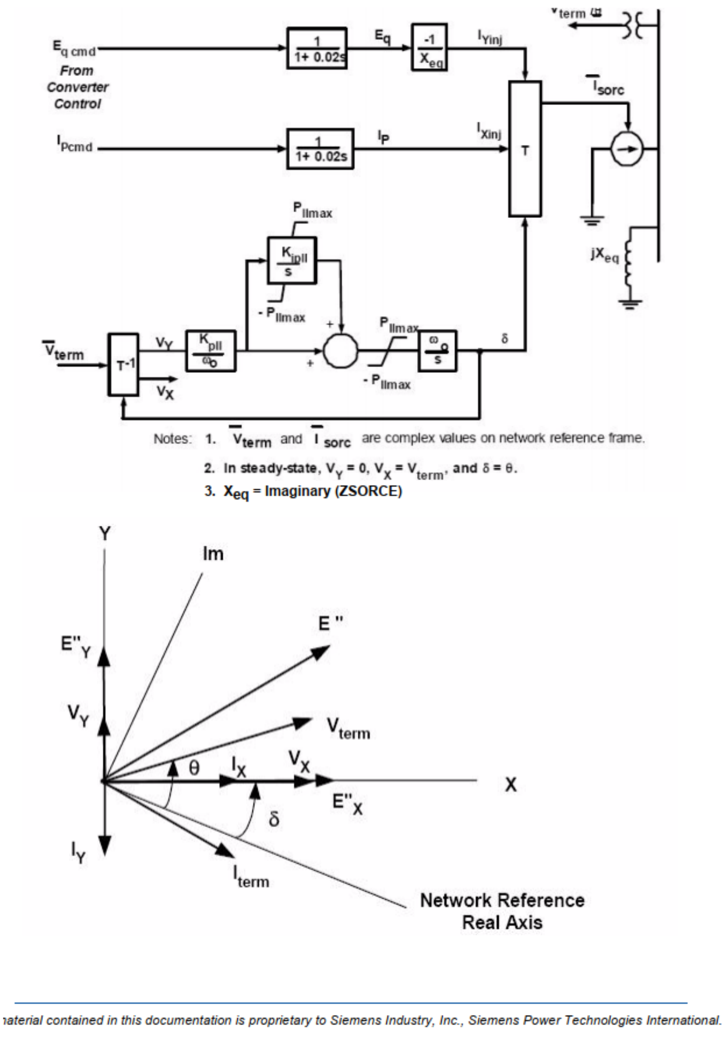

Figure 6.10: WT3G1 Model

The model is run for different values of lumped wind turbines. One General Electric WT3G1 Wind Turbine is $3.6MW$ each and to get a wind park made of $90MW$, a total of 25 lumped elements are used in the model. This is in $ICON$ section of model.

ICON	#	Description
M		Number of lumped wind turbines

Figure 6.11: WT3G1 Parameters

	Con Value	Con Description
1	0,8000	Xeq- equivalent reactance for current inj
2	30,0000	PLL gain
3	0,0000	PLL integrator gain
4	0,1000	PLL maximum limit
5	3,6000	Turbine MW rating

Figure 6.12: WT3G1 Parameters

6.2.2 Electrical Model

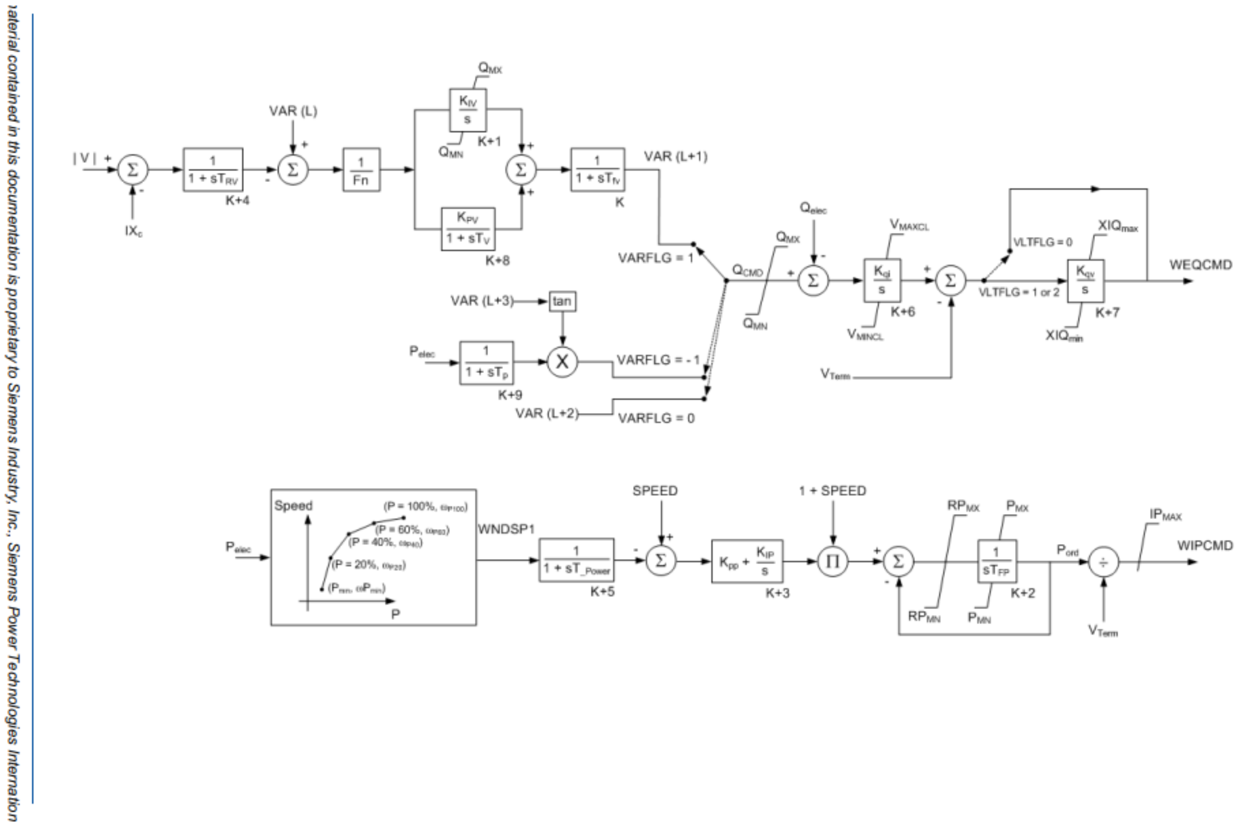

Figure 6.13: WT3E1 Model

	Con Value	Con Description
1	0,1500	Tfv - V-regulator filter
2	18,0000	Kpv - V-regulator proportional gain
3	5,0000	Kiv - V-regulator integrator gain
4	0,0000	Xc - line drop compensation reactance
5	0,0500	Tfp - T-regulator filter, seconds (>0)
6	3,0000	Kpp - T-regulator proportional gain
7	0,6000	Kip - T-regulator integrator gain
8	1,1200	PMX - T-regulator max limit
9	0,1000	PMN - T-regulator min limit
10	0,2960	QMX - V-regulator max limit
11	-0,4360	QMN - V-regulator min limit
12	1,1000	IPMAX - Max active current limit
13	0,0500	TRV - V-sensor
14	0,4500	RPMX - maximum Pordr derivative
15	-0,4500	RPMN - minimum Pordr derivative
16	5,0000	T_POWER - Power filter time constant,
17	0,0500	KQi - MVAR/Volt gain
18	0,9000	VMINCL
19	1,2000	VMAXCL
20	40,0000	Kqv - Volt/MVAR gain
21	-0,5000	XIQmin - min. limit (see documentation
22	0,4000	XIQmax - max. limit (see documentatio
23	0,0500	Tv - Lag time constant in WindVar cont

Figure 6.14: WT3E1 Parameters

23	0,0500	Tv - Lag time constant in WindVar cont
24	0,0500	Tp - Pelec filter in fast PF controller
25	1,0000	Fn - A portion of on-line wind turbines
26	0,6900	Wpmin, Shaft speed at Pmin, pu
27	0,7800	Wp20, Shaft speed at 20% rated powe
28	0,9800	Wp40, Shaft speed at 40% rated powe
29	1,1200	Wp60, Shaft speed at 60% rated powe
30	0,7400	Pwp, Minimum power at Wp100 speed,
31	1,2000	Wp100, Shaft speed at 100% rated po

Figure 6.15: WT3E1 Parameters

	Icon Value	Icon Description
1	4	Remote bus #
2	1	VARFLG: =0 Const. Q ctrl, =1 reactive
3	1	0 - bypass terminal voltage control, else
4	3	From bus - interconnection transformer
5	4	To bus - interconnection transformer
6	'1'	Id - interconnection transformer

Figure 6.16: WT3E1 Parameters

6.2.3 Mechanical Model

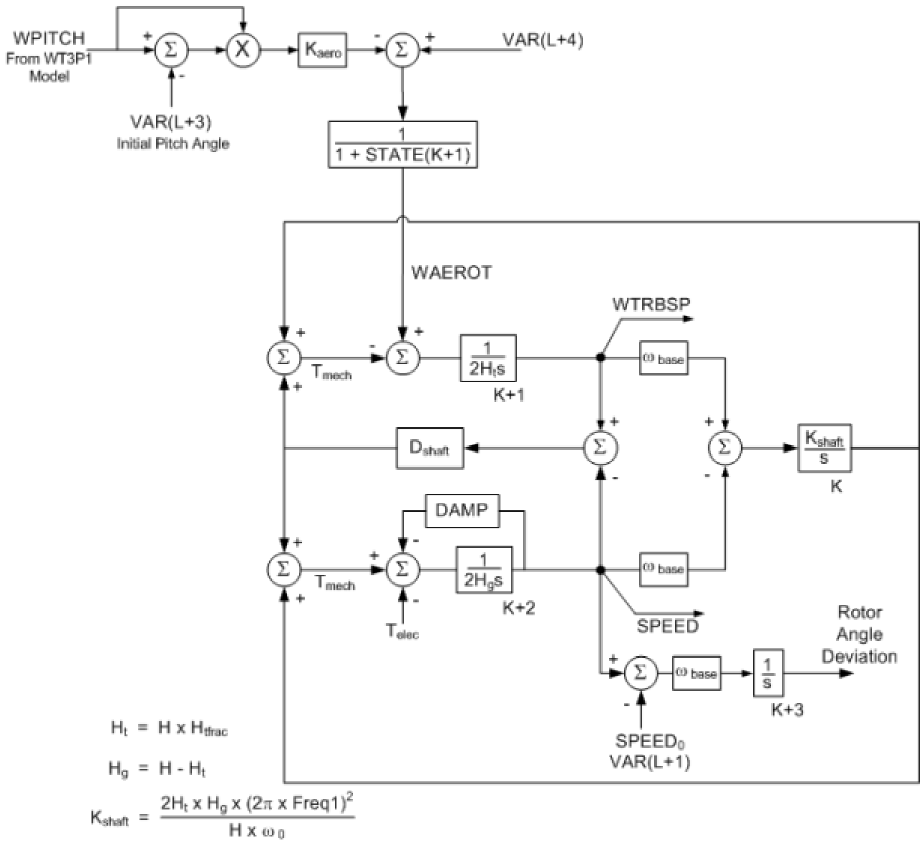

Figure 6.17: WT3T1 Model

	Con Value	Con Description
1	1,2500	Vw - Initial wind speed, pu of rated wind
2	4,9500	H - Total inertia constant, MW*sec/MVA
3	0,0000	DAMP - Machine damping factor, pu P/
4	0,0070	Kaero - Aerodynamic gain factor
5	21,9800	Theta2 - Blade pitch at twice rated wind
6	0,0000	Htfac-Turbine inertia fraction; 0 for 1 ma
7	1,8000	Freq1 - First shaft torsional resonant fre
8	1,5000	DSHAFT - Shaft Damping factor, pu P/

Figure 6.18: WT3T1 Parameters

6.2.4 Pitch Model

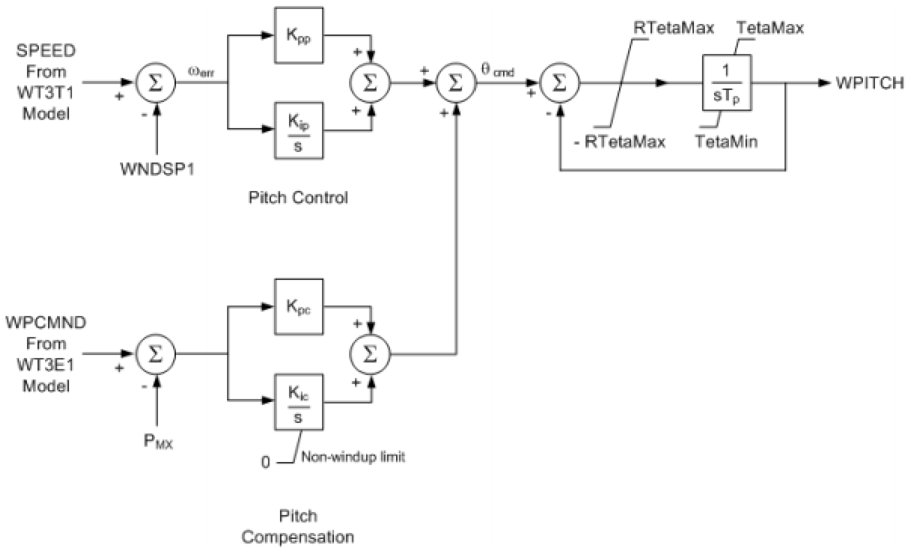

Figure 6.19: WT3P1 Model

	Con Value	Con Description
1	0,3000	Tp - Time constant of the output lag (se
2	150,0000	Kpp - Proportional gain of PI regulator(
3	25,0000	Kip - Integrator gain of PI regulator (pu)
4	3,0000	Kpc - Proportional gain of the compens
5	30,0000	Kic - Integrator gain of the compensator
6	0,0000	TetaMin - Lower pitch angle limit (degre
7	27,0000	TetaMax - Upper pitch angle limit (degr
8	10,0000	RTetaMax - Upper pitch angle rate limit
9	1,0000	PMX - Power reference (pu)

Figure 6.20: WT3P1 Parameters

6.3 Python Code for PSS/E Implementation

```
import os,sys
import math

##################################
##Declare PSSE and CASE location##
##################################

#Locations of PSSE and CASE, SEE ALL CHANGE LOCATIONS NOTES TO CHANGE THE FILE PATHS
#PSSE_LOCATION = r"C:\Program Files (x86)\PTI\PSSEUniversity33\PSSBIN" ####Change Location##########################################################################
PSSE_LOCATION = r"C:\Program Files (x86)\PTI\PSSEXplore33\PSSBIN"
sys.path.append(PSSE_LOCATION)
os.environ['PATH'] = os.environ['PATH'] + ';' + PSSE_LOCATION


import csv
import random
import psspy
import dyntools
import redirect
#import excelpy

CASE = r"C:\Users\abuba\Documents\Abubakar Data\Chalmers\Master Thesis\Simulation\Small Grid Model\Base300\more_wind\python-ran\Network_morewind_5 - Year.sav" ####

redirect.psse2py() #Redirect output from PSSE to Python

###############
#Initiate case#
###############
psspy.psseinit(8000)
psspy.case(CASE)

########################
#Run initial power flow#
########################
# Modify original loads


if __name__ == '__main__':
      psspy.fnsl(
        options1=1, # disable tap stepping adjustment.
        options5=1, # disable switched shunt adjustment.
        options6=1, # Flat start.
        )
pspy.save(r"C:\Users\abuba\Documents\Abubakar Data\Chalmers\Master Thesis\Simulation\Small Grid Model\Base300\more_wind\python-ran\Network_morewind_5 - Year.sav")
```

Figure 6.21: Python Code (1/3)

```
###############
#Convert Loads#
###############
psspy.conl(-1,1,1)
psspy.conl(-1,1,2,[0,0],[50,50,50,50])
psspy.conl(-1,1,3)

####################
#Convert Generators#
####################
psspy.cong()

####################
#Solve for dynamics#
####################
psspy.ordr()
psspy.fact()
psspy.tysl(1)

########################
#Save converted network#
########################
psspy.save(r"C:\Users\abuba\Documents\Abubakar Data\Chalmers\Master Thesis\Simulation\Base300\more_wind\python-ran\Network_morewind_5 - Year_C.sav")

##################
#Add dynamic data#
##################
###psspy.addmodellibrary(r"Z:\Master Thesis\Thesis files\System protection model\SYSPROTMODEL.dll") ################### CHANGE Location ###################
psspy.dyre_new(dyrefile=r"C:\Users\abuba\Documents\Abubakar Data\Chalmers\Master Thesis\Simulation\Base300\more_wind\python-ran\Network_morewind.dyr")

##############
#Add Channels#
##############

import channelimport
```

```
############
#Initialize#
############
timestep = 1
time_run=0
i=0
psspy.strt(outfile=r"C:\Users\abuba\Documents\Abubakar Data\Chalmers\Master Thesis\Simulation\Small Grid Model\Base300\more_wind\python-ran\Year1.out") ####Change Lo
with open(r'C:\Users\abuba\Documents\Abubakar Data\Chalmers\Master Thesis\Simulation\Small Grid Model\Base300\more_wind\python-ran\load_data.csv', 'r') as file:
 my_reader = csv.reader(file, delimiter=',')
 j=1 #this is just a counter
 for row in my_reader:
      if (i <=758):
            i = i + 1
      if (i==759):
            psspy.run(tpause=10*j,nprt=0,nplt=timestep)
            #print(str(i)+' YES IT WORKED. 1st!')
            #print(str(j)+' YES IT WORKED. 1st!')
            i=i+1
            j=j+1
      if (i==1635):
            print(str(j)+' YES IT WORKED. Last one!')
            break;
      if (i>759):
            psspy.run(tpause=10*j,nprt=0,nplt=timestep)
            j=j+1

            x=row[1].replace(",",".")

            x=float(x)

            rando=random.randint(0,1)
            if(rando==0):

                  ierr=psspy.load_data_4(i=4,id='1', realar3=151+(0.004*float(x)))


            if(rando==1):

                  ierr=psspy.load_data_4(i=4,id='1', realar3=151-(0.001*float(x)))
##            aList = str(151+(0.004*float(x)))
##            dataFile = open('writetest.txt', 'w')
##            for eachitem in aList:
##             dataFile.write(str(eachitem)+'\d')

            i=i+1
            #psspy.conl(-1,1,1)
            #psspy.conl(-1,1,2,[0,0],[100,0,100,0])
            #psspy.conl(-1,1,3)
            #psspy.ordr()
            #psspy.fact()
            #psspy.tysl(1)
            print(str(i)+' YES IT WORKED!')
```

Figure 6.23: Python Code (3/3)

Bibliography

[1] https://www.eia.gov/todayinenergy/detail.php?id=12251

[2] https://unfccc.int/process-and-meetings/the-paris-agreement/the-paris-agreement

[3] https://www.iea.org/reports/global-ev-outlook-2019

[4] https://www.statista.com/statistics/696187/electric-and-hybrid-cars-number-in-norway/

[5] https://www.researchgate.net/publication/258399637

[6] https://ourworldindata.org/energy

[7] https://ourworldindata.org/co2-and-other-greenhouse-gas-emissions

[8] https://www.harbortaxgroup.com

[9] https://www.iea.org

[10] https://www.renewableenergyworld.com/types-of-renewable-energy

[11] https://www.iea.org/reports/world-energy-outlook-2019

[12] https://www.energimyndigheten.se/nyhetsarkiv/2020/2019-rekordar-for-svensk-elproduktion/

[13] Energy in Sweden 2019, A Report by Energimyndigheten, Swedish Energy Agency

[14] Power Plant Cycling Costs, April 2012, N. Kumar, P. Besuner, S. Lefton, D. Agan and D. Hilleman, Intertek APTECH, Sunnyvale, California, NREL Technical Monitor: Debra Lew

[15] https://weather-and-climate.com/average-monthly-precipitation-Rainfall,mariefred-sodermanland-se,Sweden

[16] https://www.energimyndigheten.se/statistik/den-officiella-statistiken/

[17] https://svenskvindenergi.org/statistik/2017-3

[18] 100 percent renewable electricity by 2040, A report by Svensk Vindenergi Accessed at: https://swedishwindenergy.com

[19] Swedish Future Electricity Production, Report by IVA Accessed at: https://www.iva.se/globalassets/rapporter/vagval-el/201705-iva-vagvalel-framtidens-elproduktion-english-c.pdf

[20] https://www.iea.org/reports/global-ev-outlook-2019

[21] https://new.abb.com/news/detail/55577/abb-and-volvo-to-electrify-gothenburgs-city-streets

[22] Impact on the Distribution System due to Plug-In Electric Vehicles and Changes in Electricity Usage, David Steen, Chalmers University of Technology

[23] Design and Assessment of Battery Electric Vehicle Powertrain, with Respect to Performance, Energy Consumption and Electric Motor Thermal Capability, Emma Arfa Grunditz, Doctoral Thesis, CHALMERS UNIVERSITY OF TECHNOLOGY

[24] Comparison between Battery Electric Vehicles and Internal Combustion Engine Vehicles fueled by Electrofuels, Master Thesis, CHALMERS UNIVERSITY OF TECHNOLOGY, TOBIAS GUSTAFSSON ANDERS JOHANSSON

[25] A method based on the Van der Hoven spectrum for performance evaluation in prediction of wind speed, Elif KAYA, Burak BARUTÇU1, Şükran Sibel MENTEŞ2

[26] https://www.eia.gov/energyexplained/us-energy-facts/

[27] Control of a wind turbine equipped with a variable rotor resistance, Master Thesis, HÉCTOR A. LÓPEZ CARBALLIDO, Department of Computer Science and Engineering, CHALMERS UNIVERSITY OF TECHNOLOGY, May 2009

[28] Doubly Fed Induction Generators for Wind Turbines by S. MÜLLER, M. DEICKE RIK DE DONCKER

[29] T. Jahns and R.W. De Doncker, "Control of generators," inThe Control Handbook, W. Levins, Ed. Boca Raton, FL: CRC, 1996

[30] N. Elmouhi, A. Essadki, H. Elaimani and R. Chakib, "Evaluation of the Inertial Response of Variable Speed Wind Turbines Based on DFIG using Backstepping for a Frequency Control," 2019 International Conference on

Wireless Technologies, Embedded and Intelligent Systems (WITS), Fez, Morocco

[31] https://www.hydropower.org/country-profiles/china

[32] https://web.archive.org/web/20140924062448/

[33] http://www.wvic.com/

[34] Power System Stability and Control, Prabha Kundur, ISBN: 9780070359581

[35] N. Elmouhi, A. Essadki, H. Elaimani and R. Chakib, "Evaluation of the Inertial Response of Variable Speed Wind Turbines Based on DFIG using Backstepping for a Frequency Control

[36] https://webstore.iec.ch/publication/28145

[37] https://www.scribd.com/document/241950119/POM-PSSE33-pdf

[38] EVALUATION OF REACTANCES AND TIME CONSTANTS OF SYNCHRONOUS GENERATOR, Shaheena Khanum, K.L Ratnakar, Ramesh K., Ravi

[39] Design of a Battery Storage Based Ancillary Service for Frequency Support in the Nordic Power System, Juárez Moreno, Omar, epartment of Electrical Engineering, CHALMERS UNIVERSITY OF TECHNOLOGY Gothenburg, Sweden

[40] Frequency Response by Wind Farms in Power Systems with High Wind Power Penetration, MATTIAS PERSSON, PhD Thesis, Department of Electrical Engineering, CHALMERS UNIVERSITY OF TECHNOLOGY Gothenburg, Sweden, 2017

[41] https://www.svk.se/en/national-grid/the-control-room/

[42] https://www.vde.com/en/fnn/topics/european-network-codes/rfg

[43] https://www.nordpoolgroup.com/the-power-market/Bidding-areas/